

Journal of Information Technology and Applications (BANJA LUKA)

JITA

Exchange of Information
and Knowledge in Research

APEIRON
ЖУРНАЛ



THE AIM AND SCOPE

The aim and scope of the Journal of Information Technology and Applications (JITA) is:

- to provide international dissemination of contributions in field of Information Technology,
- to promote exchange of information and knowledge in research work and
- to explore the new developments and inventions related to the use of Information Technology towards the structuring of an Information Society.

JITA provides a medium for exchanging research results and achievements accomplished by the scientific community from academia and industry.

By the decision of the Ministry of Education and Culture of the Republic of Srpska, no.: 07.030-053-160-4/10 from 3/3/2010, the journal „Journal of Information Technology and Applications“ Banja Luka is registered in the Registry of public organs under the number 591. Printed by Markos, Banja Luka in 300 copies two times a year.

Indexed in: LICENSE AGREEMENT, 3.22.12. **EBSCO** Publishing Inc., Current Abstracts

 ebscobase.com	 crossref.org
 indexcopernicus.com	 road.issn.org
 citefactor.org/contact	
 scholar.google.com	
 doisrpska.nub.rs	

Printed on acid-free paper

Full-text available free of charge at <http://www.jita-au.com>

CONTENTS

EDITORIAL	4
SIMULATION OF PROCESSES IN TRACTION ELECTRIC ACTUATORS OF AUTONOMOUS VEHICLES	5
<i>Yu. M. INKOV, E. V. SACHKOVA, YA. A. KOROBANOVA, T.N. FADEIKIN</i>	
AUTOMATIC TEMPERATURE REGULATION SYSTEM OF LOCOMOTIVE TRACTION INDUCTION MOTORS WITH POWER LOSSES MINIMIZATION	13
<i>A.S. KOSMODAMIANSKIY, VI. VOROBIEV, A.A. PUGACHEV</i>	
A NEW APPROACH TO COMPUTER ANALYSIS OF QUEUING SYSTEMS WITHOUT PROGRAMMING	25
<i>ZORAN Ž. AVRAMOVIĆ, RADOMIR Z. RADOJIĆIĆ, SAŠA D. MIRKOVIĆ</i>	
THE PERSPECTIVE OF HIGH-TEMPERATURE SUPERCONDUCTIVITY ELECTRICAL EQUIPMENT APPLICATION FOR TRACTION POWER SUPPLY AND THE PROBLEMS OF ELECTROMAGNETIC COMPATIBILITY	33
<i>M.P. BADJOR, Yu. M. INKOV</i>	
SAFETY AND RISK MANAGEMENT	42
<i>V.M. LISENKOV, P.F. BESTEMYANOV</i>	
WATER TREEING IN EXTRUDED CABLE INSULATION AS REHBINDER ELECTRICAL EFFECT	55
<i>Iz. B. PESHKOV, M. YU. SHUVALOV, V.L. OVSIENKO</i>	
CONTROL SYSTEMS FOR AUTOMATED VESSEL PILOTING THROUGH LOCAL STATIONARY OBSTACLES	61
<i>DOVGORBOD GEORGY MOISEEVICH, KLYACHKO LEV MIKHAYLOVICH</i>	
PROSPECTS OF HIGH TECHNOLOGIES IN THE REMOTE DIAGNOSIS OF THE TRACK	65
<i>LIEVIN, BORIS A., NEDORCHUK, BORIS L.</i>	
INSTRUCTIONS FOR AUTHORS	72

EDITORS:



**GORDANA
RADIĆ, PhD**
EDITOR-IN-CHIEF



**ZORAN
AVRAMOVIĆ, PhD**



**DUŠAN
STARČEVIĆ, PhD**



Dear Readers,

According to the signed Agreement on the scientific cooperation between PanEuropean University Apeiron and Moscow State University of Railway Engineering (MIIT), the JITA Editorial Board made a decision that academician **Inkov Yuri M.** will be guest editor for this issue.

Inkov Yuri M., Doctor of Sciences Habil., Professor, Honoured Scientist of Russian Federation, Honorary Worker of Higher Professional Education of the Russian Federation, Honorary Railwayman, Honorary Worker of Transport of Russia, member of International Academy of Electrotechnical Sciences, Russian Engineering Academy, Serbian Academy of Engineering, IEEE, Chief Scientific Secretary of the Academy of Electrotechnical Sciences of the Russian Federation, professor of the Moscow State University of Railway Engineering (MIIT).

Inkov Yuri M. published more than 200 scientific papers, more than 120 patents for inventions, 15 monographs, textbooks and manuals for students of higher educational institutions. He is a research consultant and an author of over 30 articles of the Great Soviet Encyclopaedia (3rd edition), a member of the Editorial Board, the author of the articles and scientific supervisor of sections “Power and Information Electronics” and “Electrical Transport Systems and Space Equipment”. He is a co-author of the “Encyclopaedia of Electric Engineering”, a unique scientific -practical work in the field of electric engineering and electrical power engineering.

SIMULATION OF PROCESSES IN TRACTION ELECTRIC ACTUATORS OF AUTONOMOUS VEHICLES

Yu. M. Inkov¹, E.V. Sachkova², Ya. A. Korobanova³, T.N. Fadeikin⁴

¹*D. Sc. Habil., professor*

²*PhD, associated professor*

³*post-graduate student*

⁴*post-graduate student*

MSURE (MIIT)

Contribution to the state of the art

DOI: 10.7251/JIT1501005I

UDC: 629.424

Abstract: At the stage of construction of traction electric drives of electric power systems (EPS) the analysis of electromagnetic and energy processes in various operational and emergency modes is needed. The calculation of complex multi-electromechanical systems of modern vehicles is only possible by computer simulation. The programming of such complex systems by traditional methods is practically impossible, or is a time-consuming process. The use of universal modeling systems is the only possible way of modeling of multi-component systems. In this article we deal with the mathematical model of the synchronous generator of autonomous vehicle in computer-aided design (CAD) OrCAD 10.0 (Pspice). The software package OrCAD 10.0 (Pspice) is one of the most versatile in the field of simulation of electrical circuits with a large number of components. OrCAD libraries contain proven by the time mathematical models of practical application of electric power components and it is continuously ever-growing. At the end of the article the characteristics for different modes of operation of a synchronous generator are summarized.

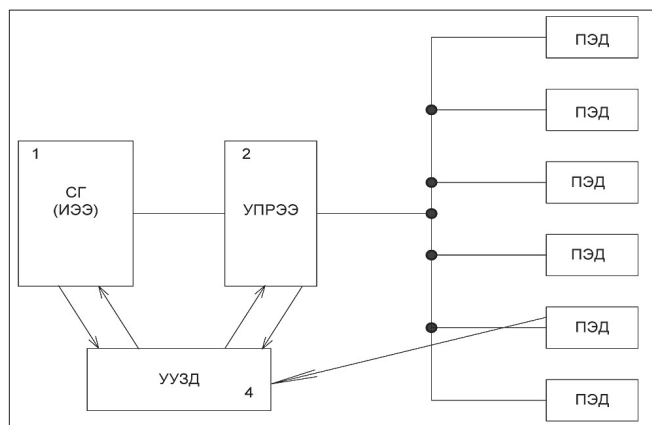
Keywords: traction electric drive, autonomous locomotive, marine engine, mathematical model, energy processes, electromechanical system, synchronous generator, the hysteresis loop.

In traction electric drives of modern vehicles, including autonomous locomotives of railways, ships and vessels regardless of the type of driving (traction) engine as a primary power source the synchronous generators are applied, which are geared by diesel engines or turbines.

The analysis of electromagnetic and energy processes in electric drives of such vehicles, including comparative analysis, is worth while carrying out on mathematical models of traction electric drives, which allows to enter in the analyzed system the parameters of its components with any required accuracy. These system parameters are: the source of power, converters and regulators of parameters of energy transmitted from the source to electric engines and the engine themselves.

The most suitable for the simulation of electromagnetic and energy processes in complex multi-electromechanical systems, which also include traction electric drives, is a software package OrCAD 10.0. This allows to perform multivariate calculations of electromagnetic and energy processes in such systems during reasonable time.

Using the specified software package the system under analysis is divided into interconnected individual modules that are managed by a specific algorithm.



СГ – synchronous generator (power source)
 ИЭЭ – power source
 УПРЭЭ – converting and electric energy regulating device
 ПЭД – drive motors
 УУЗД – control, protection, and diagnostics device

Figure 1. The power circuit structure of the of electric equipment of traction electric drive of autonomous vehicle: 1 – synchronous generator (power source); 2 - converting and electric energy regulating device; 3 - drive motors; 4 - control, protection, and diagnostics device.

In particular, the traction electric drive of the autonomous vehicle, as electromechanical system, can be represented by the structure, shown in Figure 1 and including four modules 1-4.

Mathematical models should be drawn up for each of the modules of the analyzed system, depending on the purpose of the analysis. The given algorithm defines the interaction of the mentioned models and allows obtaining of the required solution of the problem.

In this paper the mathematical model of the input module of the analyzed system - synchronous generator type SGDM - 5000 - 8 - OM4, used in traction motor drives of ship vehicles is regarded.

The building of the model of a synchronous generator is started with the creation of the model of the magnetic core.

The model of the magnetic core is based on the template created on the basis of the model Giles-Atherton [6, 7]. The initial data for the model are:

1. The size of the gap, Gap [centimeters];
2. the cross-section area of the core, Area [square centimeters];

3. the length of the median line of the core, Path [centimeters];
4. the duty factor of the core, Pack (dimensionless).

In addition, to construct a model of the core it is necessary to set the hysteresis loop for the core material (Figure 2).

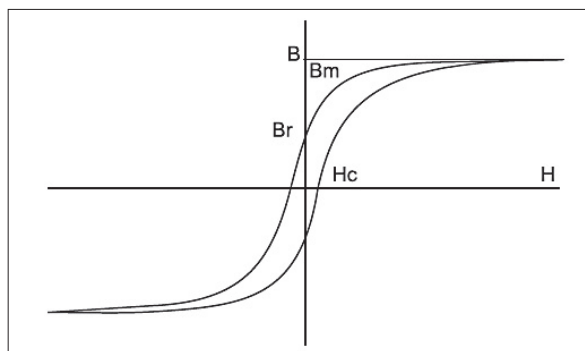


Figure 2. The hysteresis loop for the core material

For Figure 2 the following symbols are accepted:
 Hc [Oersted] - the electromagnetic field strength of the core when induction equals to zero;

- Br [Gauss] - induction in the core when the electromagnetic field strength equals to zero;
- Hm [Oersted] - the electromagnetic field strength of the core when induction equals to the saturation induction;
- Bm [Gauss] – the saturation induction.

In addition to that, the value of initial magnetization (Initial Perm) is set.

The initial information is entered in the Model Editor in table of Hysteresis Curve and Parameters. The information in the table of Hysteresis Curve is entered in the form of:

- (0, Br);
- (Hc, 0);
- (Hm, Bm).

The attempt to construct a more accurate hysteresis loop for more points does not give positive results, because only the first three pairs of numbers listed in the table are consider in the Model Editor.

In the version OrCAD 9.2 is used the 2nd level (LEVEL = 2) of core model, and in version OrCAD 10.0 - the 2nd (LEVEL = 2) or the 3rd (LEVEL = 3).

For the third level we introduce the following assumptions [7]:

1. the loop is static, its shape does not depend on the frequency variation of the electromagnetic field strength H;

2. the saturation induction B_m for the model of the magnetic core is defined as the asymptote of the hysteresis loop. The manufacturers of the magnetic core typically define saturation as point on the hysteresis loop, above which a decrease of penetrability in the core begins to limit its application. If the values B_m are taken directly from the reference tables of manufacturers cores, the core model will work with a low value of the value B_m . Taking into account the different definitions of the saturation induction, it is not recommended to use values of B_m from the reference data; instead of it, it is used the values B_m , which was defined directly on the hysteresis loop;

3. The model of the air gap may be incorrect at low operating frequencies (typically <100 Hz). Obtained in this case error is caused by the 0,001Ω resistor introduced in series with the inductor of core. To improve the accuracy of the modelling of air gap one of the following conditions should be met: winding resistance is greater than or equals to 0.1Ω; the inductive component of the impedance (ZL) is greater or equals to 0.1 Ω. The verification showed, that in this case these conditions are hold true.

The value of inductive impedance component is calculated by the formula as $|Z_L| = \omega L_{eq}$,

where $\omega = 2\pi f$ - angular frequency; L_{eq} - equivalent inductance.

When replacing the L_{eq} on an equivalent expression, we obtain:

$$|Z_L| = \frac{2\omega\mu An}{L},$$

where μ - magnetic permeability; A - area; n - number of windings; L - length;

The results of the calculation circuit, comprising a core, in which saturation induction B_m is greater than 10^6 G, may differ from the results of simulation of real cores [7].

In case of convergence problems appearing while modelling of core with very high saturation induction and very low coercive force the core should be replaced by the ideal core, which model provides the calculation of the saturation induction at infinite and zero coercive force.

In [5] we analyzed the problems of modification PSpice-model of the magnetic core for defining its parameters by reference characteristics; also we proposed modification PSpice-model to account the magnetic properties of materials.

MS - saturation magnetization (magnetization saturation) [ampere / meter] = 4,903,089.039498;

A - shape parameter of no hysteresis magnetization curve (thermal energy parameter) [ampere/meter] = 48.64212819596;

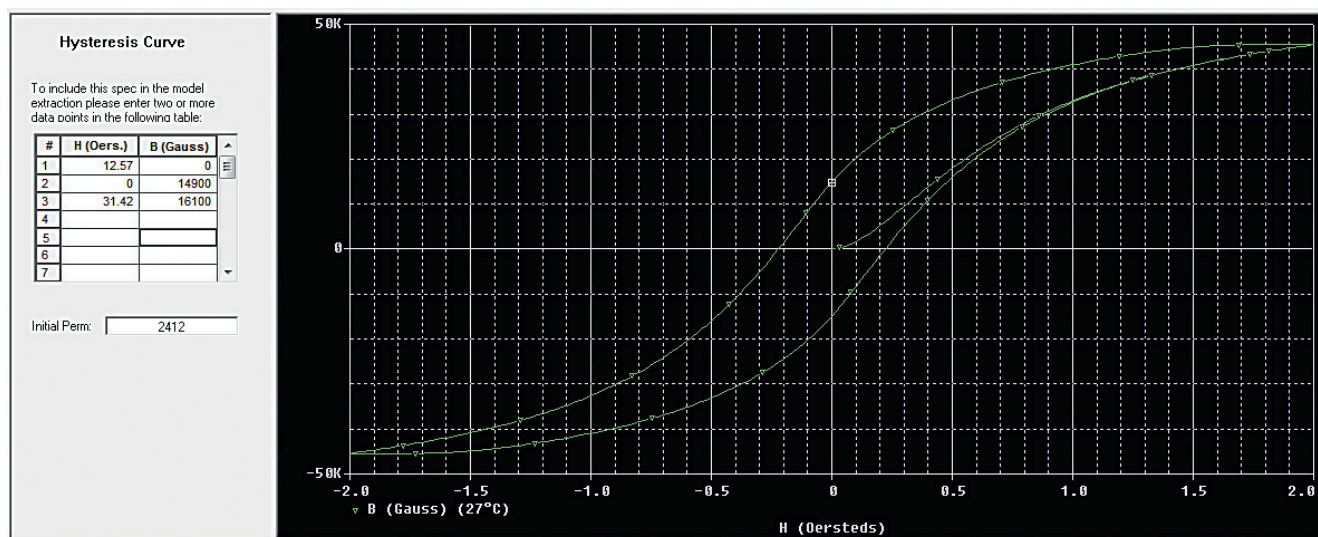


Figure 3. The hysteresis loop for the core model of the electrical plate steel of steel quality 2412.

C – the constant value of elastic displacement of domain edges (domain flexing parameter) = 0,01001;

K - the constant value of mobility of domain (domain anisotropy parameter) [amperes / meter] = 19.8446694766.

Hysteresis loop for the constructed model of the core is shown in Figure 3.

Now we develop a model of the specific magnetic core. Its parameters, according to the task: GAP = 0,968 cm, AREA = 143,184 cm², PATH = 101,9 cm, PACK = 1. As the core material the electrical plate steel of quality 2412 was used. The values of B_r , H_c , H_m and B_m are taken from the passport. So, $H_c = 12,57$ Oe, $B_r = 1,49 * 10^4$ G, $H_m = 31,42$ Oe, $B_m = 1,6 * 10^4$ G. According to these data we calculated the required characteristics of the model.

The next step will be the modelling of a synchronous generator operating in short circuit and idling modes. The electric diagram of such generator is shown in Figure 4.

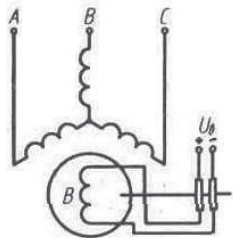


Figure 4. The electric diagram of a synchronous generator

The scheme of the developed model is shown in Figure 5.

The vehicles EPS are complex systems consisting of several diesel or turbo-generators and dozens or even hundreds of asynchronous motors, dozens of static loads. The most advisable way to carry out the study of such systems is by using models of synchronous generators in the phase coordinates. However, the presence of variable coefficients in the equations of these elements causes considerable computational difficulties which at solving of the given tasks by the traditional research methods are non-defined. Currently the objectives of the study of transients in EPS are solved by using the models of synchronous generators written in the axes d, q . The presentation of

synchronous generators mathematical models in this form in case of applying the program PSpice a/d is decisive. The program PSpice a/d generates the communication equations between the electric machines models recorded in this way, and they are compiled automatically, without the researcher intervention. Moreover, generated in this way models easily integrate into the available in libraries DesignLab components.

The type of the differential equations of AC electrical machines is different depending on the choice of the voltage vector direction, the flux linkages, the initial mode (generator or motor). The transients study method by using the PSpice program is suitable for any form of differential equations.

The three-phase synchronous generator with salient-pole rotor is analysed. The generator has a symmetrical three-phase winding on the stator. The field coil and the damper winding are located on the rotor. The damper winding is intended primarily for damping of the rotor fluctuations, the improvement of the conditions of pulling into synchronism and prevention from overvoltage in the stator windings under unbalanced load conditions. The system of differential equations describing electromagnetic and electromechanical transient processes in a synchronous generator includes the equation of the equilibrium voltage of all electrical circuits in the stator and rotor and the equation of rotor operation.

$$\left\{ \begin{array}{l}
 \psi_d = x_s i_d - E_{\delta q}; \\
 \psi_q = x_s i_q + E_{\delta d}; \\
 \psi_r = \frac{x_{ad}}{x_r} E_{\delta q} + \frac{x_{sr}}{x_r} E_q; \\
 \psi_{r di} = \frac{x_{ad}}{x_{r di}} E_{\delta q} + \frac{x_{sr di}}{x_{r di}} E_{r qi}; \\
 \psi_{r q k} = -\frac{x_{aq}}{x_{r q k}} E_{\delta d} - \frac{x_{sr q k}}{x_{r di}} E_{r dk}; \\
 \frac{d\psi_r}{dt} = \frac{1}{T_r} (E_r - E_q); \\
 \frac{d\psi_{r di}}{dt} = -\frac{1}{T_{r di}} E_{r qi}; \\
 \frac{d\psi_{r q k}}{dt} = -\frac{1}{T_{r q k}} E_{r dk}; \\
 \frac{ds}{dt} = \frac{1}{T_j} (M_T - M_E); \\
 \frac{d\delta}{dt} = \omega_s (s - s_v); \\
 E_{\delta q} = \vartheta_d \left(x_{ad} i_d + E_q + \sum_{i=1}^{n_d} E_{r qi} \right); \\
 \frac{1}{\omega_s} \frac{d\psi_d}{dt} + (1+s)\psi_q + r i_d = -u_d; \\
 (1+s)\psi_d + \frac{1}{\omega_s} \frac{d\psi_q}{dt} - r i_q = u_q.
 \end{array} \right.$$

· where ψ_d, ψ_q, i_q, i_d are the flux linkage and current of the equivalent damping windings under longitudinal and transverse axes, respectively;

· x_s - reactive impedance of the stator leakage;

· $E_{\delta d}, E_{\delta q}$ - longitudinal and transverse component of the EMF;
 x_{ad}, x_{aq} - reactive impedance of the stator (armature) reaction in the longitudinal and transverse axes;

· r - reactive impedance of the stator winding;

· $x_r = x_{ad} + x_{sr}, \quad x_{r di} = x_{ad} + x_{sr di},$
 $x_{r q k} = x_{aq} + x_{sr q k}$ - reactive

impedance of the excitation winding, longitudinal and transverse damping circuits;

· $E_q = \frac{\omega_s M_{ad} i_r}{\omega_s M_{ad} i_{\delta r}}, \quad E_{r dk} = \frac{\omega_s M_{ad} i_{r di}}{\omega_s M_{ad} i_{\delta r d}},$
 $E_{r qi} = -\frac{\omega_s M_{aq} i_{r q k}}{\omega_s M_{aq} i_{\delta r q}}$ Is the EMF induced in the

stator by the magnetic field of the currents of the rotor contours during the synchronous rotor speed;

· $x_{sr}, x_{sr di}, x_{sr q k}$ - reactive impedance of the leakage of the excitation winding, longitudinal and transverse damping circuits;

· $\psi_r, \psi_{r di}, \psi_{r q k}$ - flux linkage of excitation winding of i - longitudinal and k - transverse equivalent damping circuits;

· $T_r = \frac{x_r}{\omega_s r_r}$ - the time constant of the excitation winding when other circuits are open, with;

· E_r - excitation voltage;

· S - slide;

· M_T - torque of the generator drive motor;

· M_E - generator electromagnetic torque;

· ω_s - synchronous angular velocity;

· ϑ_d - the saturation parameter along the longitudinal axis;

· $T_j = J \frac{\omega_s^2}{S \delta p^2}$ - inertial constant of the generating unit.

Using the above system of the synchronous generator differential equations with variable coefficients all the main processes of the synchronous generator can be modelled.

In this diagram a three-phase network is modelled by the sinusoidal voltage sources U1, U2, U3. The voltage amplitude is 3642 V, the magnitude of the DC component equals to 0, and the frequency is 50 Hz. The shift between the phases is by 120 electrical degrees. The inductors L1, L2, L3 simulate the filters protecting against the interference in the network. The wire resistance is modelled by using resistors r1, r2, r3, r4, r5. The resistor r6 simulates the idle mode, and the resistor r7 simulates the short circuit mode. The inductors L4, L5, L6, L7, L8 simulate the actual

generator operation. The number of windings is taken from the passport data of the synchronous generator SGDM - 5000 - 8 - OM4 type. Element K2 simulates the core operation which model is described above.

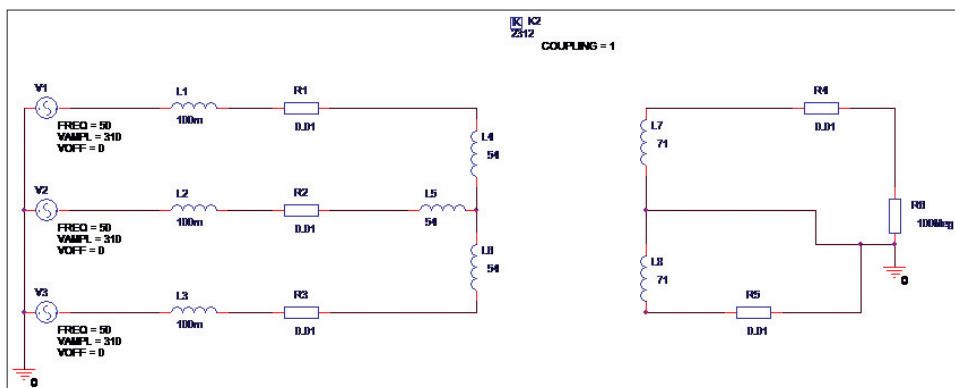


Figure 5. The diagram of model a synchronous generator

Figure 6 shows the power in the idle mode, and Figure 7 shows the power in the short circuit mode.

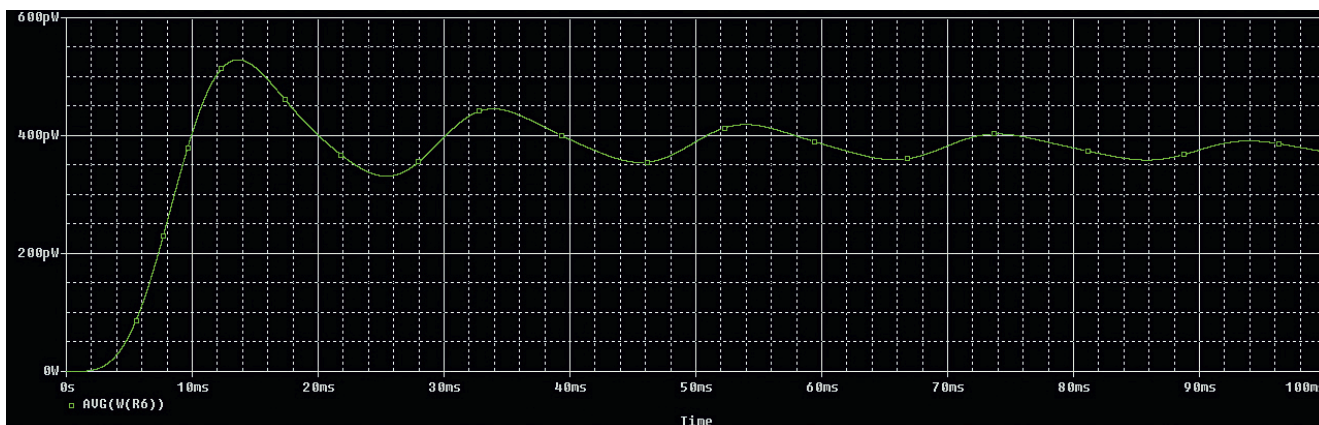


Figure 6. Power in the idle mode

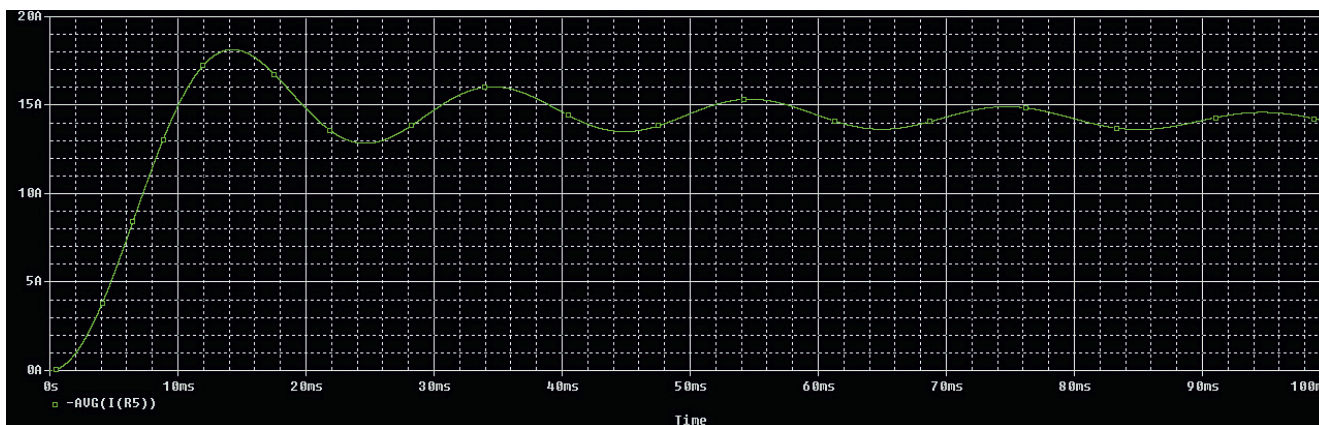


Figure 7. Power in the short circuit mode

The oscillograph records demonstrate clearly that in the idle mode the energy is not released. This fact confirms the adequacy of the model. It also proves that the regulation quality is at a high level.

Finally, the last stage of the simulation is the analysis the synchronous generator processes in the real load mode. According to the calculations, the load is simulated by the current source I1. The complete diagram of a synchronous generator model is shown in Figure 8.

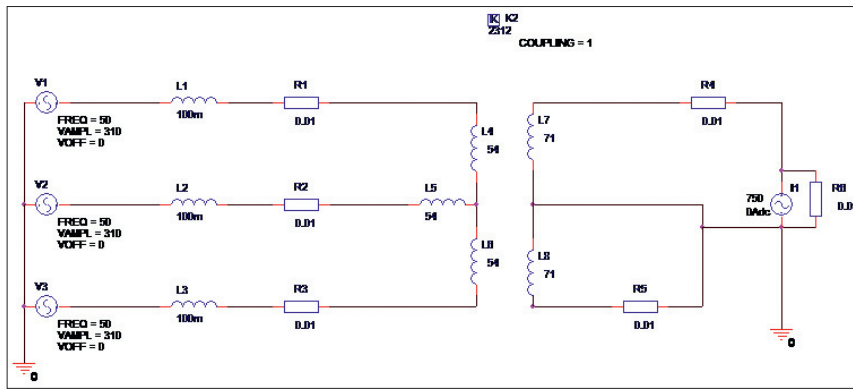


Figure 8. The diagram of a synchronous generator model operating in load mode

Figure 9 shows the load current oscillograph record, and Figure 10 shows the load voltage.

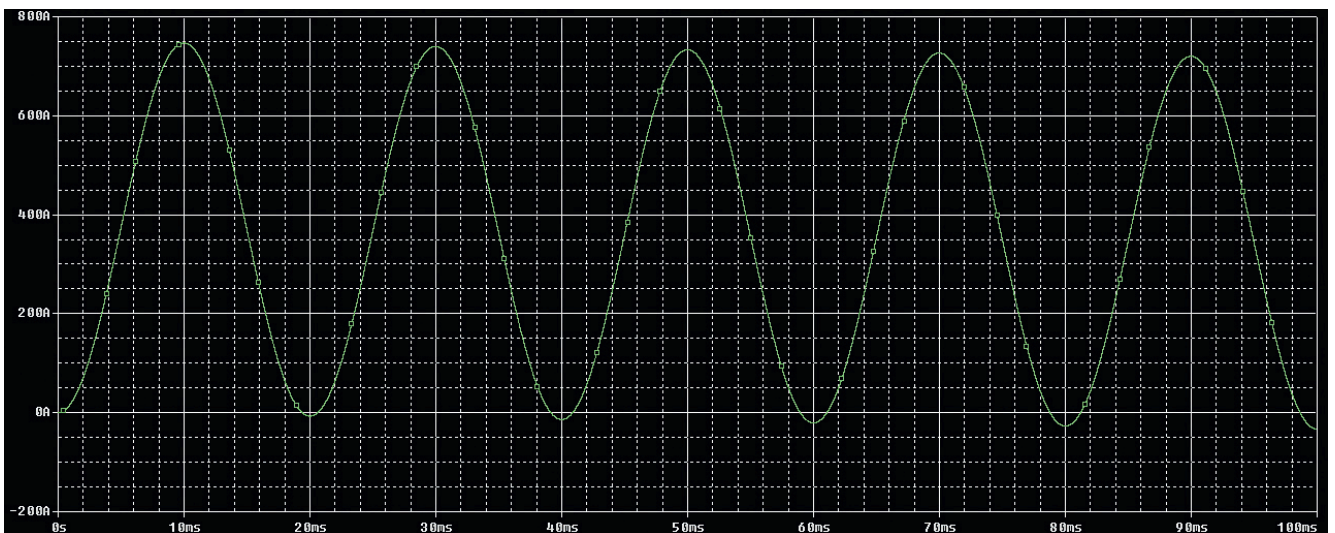


Figure 9. The load current oscillograph record

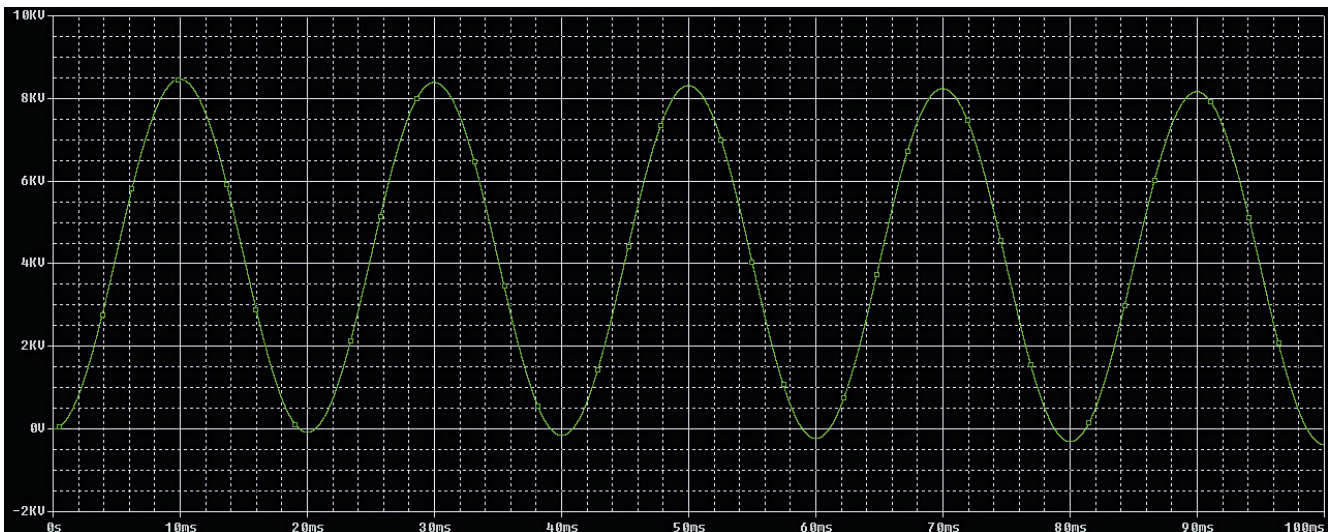


Figure 10. The load voltage oscillograph record.

The proposed model of a synchronous generator for autonomous locomotive takes into account the actual characteristics of electrical steel of core and allows to obtain the necessary characteristics of the generator in a wide range of loads. The model can be used for analyze of electromechanical processes in autonomous traction electric locomotives and determining of the energy efficiency of electric drives.

BIBLIOGRAPHY

- [1] Boskobovich, V.Yu., Koroleva, T.N., Pavlova, V.A. (2001). *Electric power installation and vehicle power electronics*. SPb.: Elmore.
- [2] Boskobovich, V.Yu. (2008). *Modeling of the electric propulsion devices with the use of OrCAD systems*. SPb.: Litera.
- [3] Kopylov, I.P. (2006). *Electric machines*. M.: Higher school.
- [4] Merkuryev, G.V., Shargin, Yu. M. (2006). *Stability of power systems. Calculations*: SPb.: NOU. "The training centre of power engineering".
- [5] Nedoluzhko, I., Kayukov, D. (2005). *The Modification of the PSpice Magnetic Core Model*. Power Electronics. № 1. SPb.: Finestreet, pp. 116-119.
- [6] PSpice Reference Guide, Product version 9.2., Cadence Design System, Inc. 360 p.
- [7] PSpice A/D Reference Guide, Product version 10.0, Cadence Design System Inc. 426 p.
- [8] Tokarev, L.N., Komarov, V.M., Vasin, I.M., Popel, G.V. (2010). *Marine power systems*. SPb.: VMII.
- [9] Tokarev, L.N. (2006). *Marine electrical engineering and electrical mechanics*. SPb.: Beresta.
- [10] Vasin, I.M., Tokarev, L.N., (2008). *Physical processes in electrical machines and systems*. Mathematical description and calculation. SPb.: Litera.

Submitted: April 30, 2015.

Accepted: May 8, 2015.

AUTOMATIC TEMPERATURE REGULATION SYSTEM OF LOCOMOTIVE TRACTION INDUCTION MOTORS WITH POWER LOSSES MINIMIZATION

A.S. Kosmodamianskiy¹, V.I. Vorobiev², A.A. Pugachev²

*¹Russian Open Transport Academy (MSUT branch), ²Bryansk State Technical University
alexander-pugachev@rambler.ru*

Contribution to the state of the art

DOI: 10.7251/JIT1501013K

UDC: 629.424:621.313.333

Abstract: The air cooling systems are shown to be used to provide required temperature condition of traction induction motors on locomotives. The automatic temperature regulation system is developed for its using to solve such a task. Results of experimental investigation showed that the AO63-4 induction motor stator end winding on the side opposite to air supply is the most heated part of the induction motor. Based on the results of the research, it was used an aperiodic second-order transfer function for approximation of the thermal transient curves. The design of an induction motor control system maintaining operating mode with minimum of the stator current are considered. It is shown that the modes of minimum of the stator current and minimum of power losses are quite close to each other. The MatLab simulation results taking typical nonlinearities and iron power losses in an induction motor and conduction and commutation power losses in semiconductors of frequency converter into account are presented. It is shown that as a result of application of the suggested system the power losses reduction may be led up to 20 % relatively to classical scalar control.

Key words: induction motor, locomotive, automatic system, equivalent circuit, power losses minimization.

INTRODUCTION

Application of induction motors as traction and auxiliary means of rolling stock has become popular due to their relative simplicity, high reliability, efficiency, satisfactory design, compactness and performance characteristics. However, the induction motor quality indicators for rated operating conditions do not coincide with those of real operation in response to the variety of factors.

Analyzing the results of researches [6] one can conclude that many failures and malfunctions are directly or indirectly related to or caused by extensive heating of the different motor parts involved in machine operation. That is why the accurate track of motor thermal state and adequate response of the motor control system to abnormal situations are very important.

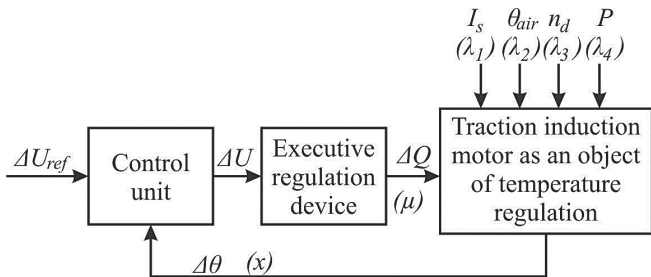
Except causing failures and damages, the temperature of induction motor windings is known to affect the operating modes of the electric drive, particularly static mechanical characteristics and it also violates the settings of optimal control systems on any quality indicator [4]. This is particularly critical in traction electric drives, where except meeting strict requirements on the energy and mass and dimensions, the drive must provide a prescribed driving force to ensure the required quality of the transition process.

It follows from the survey carried out that for implementation of traction forces of the electric drive with power losses minimization it is necessary to consider fully a temperature condition of the traction induction motor and take measures to prevent it from extreme or often overheating.

To provide the required temperature condition of traction motors on locomotives air cooling systems are used. In [7], in particular, it is noted that cooling regulation of traction electric motors allows reducing the cooling air flow through the drive motor by 25% when outdoor temperature is below 18 °C. The greatest effect in solving the problem of increasing efficiency of cooling systems can be achieved if cooling systems of traction motors will be equipped with a controlled drive fans, allowing continuous and automatic change of cooling air flow depending on the temperature of the heated parts of the equipment, its current load and temperature of cooling air.

AUTOMATIC TEMPERATURE REGULATION SYSTEM OF LOCOMOTIVE TRACTION INDUCTION MOTORS

The static and dynamic characteristics of object of regulation, the executive regulation device and the control unit which can be implemented in various mathematical models have to be known for creation of automatic regulation system. The scheme of automatic temperature regulation system of traction induction motors, feasible for using on a locomotives, is given in Fig. 1.



μ – regulatory reference, x – regulated parameter, λ_i – disturbances; $\Delta\vartheta$ – change of temperature of a traction induction motor, ΔU_{ref} – change of reference, ω – change of speed of fan shaft, ΔQ – change of the air flow, I_s – stator current of a traction induction motor, ϑ_{air} – temperature of the air, n_d – frequency of rotation of the diesel-generator, P – power of the diesel-generator

Figure 1. Scheme of automatic temperature regulation system

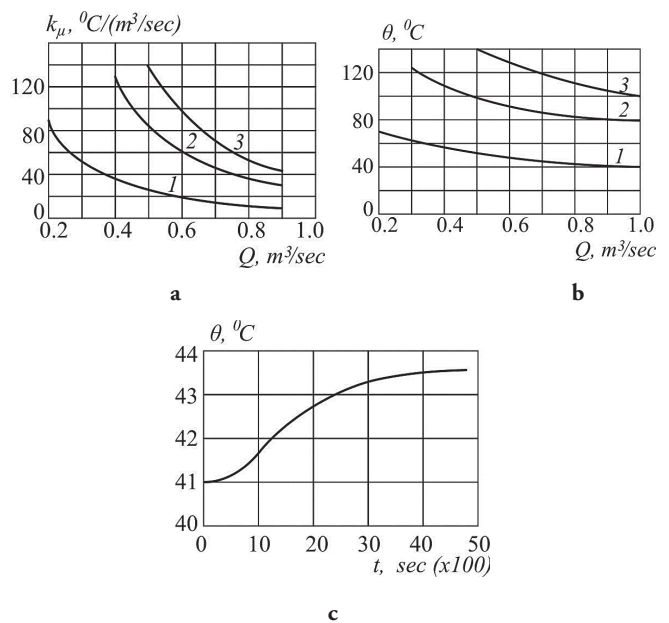
It is necessary to analyse properties of each of functional units of scheme (Fig. 1) for designing up the whole block diagram of automatic temperature regulation system. In this investigation the authors considered the possibility of implementation of automatic system using the centrifugal fan driven by induction motor drive with frequency converter as the executive regulation device.

TRACTION INDUCTION MOTOR AS AN OBJECT OF TEMPERATURE REGULATION

As a result of experimental research [11] it was found that the greatest overheating occurred in the stator end winding on the side opposite the air supply. In this regard, the stator end winding was chosen as the element limiting in heating of the AO63-4. Hereafter, the experimental results related to the stator end winding are discussed.

Results of experimental research of static and transient modes are shown in Fig. 2. The ambient temperature is 18...25 °C.

As it can be seen from Fig. 2, the experimental curves of the stator winding temperature and static characteristics of the cooling system $\theta(Q)$ are non-linear in the whole range of the cooling air flow, that indicates significant non-linearity of the induction motor as an object of regulation of temperature. The values of the transfer coefficients k_μ vary within wide limits (10 times or more) depending on Q and I_s . k_μ increases with increasing of the I_s stator current. The smaller values of Q correspond to higher values of k_μ .



1 – $I_{s*} = 0,5$, 2 – $I_{s*} = 0,8$, 3 – $I_{s*} = 1,0$, $I_{s*} = I_s / I_{s, rat}$

Figure 2. Experimental results of transfer coefficient depending on the air flow (a), temperature of the stator end winding depending on the air flow (b) and on the time (c)

It is shown in [7] that the design of the automatic regulation system needs just determination of the dynamic characteristics and parameters of the cooling system of the traction electric motors only on the regulatory reference with all possible changes of disturbances. For the design of regulation system it requires an experimental curves presented in the form of mathematical functions, written as a transfer functions.

Based on the results of the research, for approximating the thermal transient it was decided to use the following type of transfer function:

$$W(p) = \frac{k_{\mu}}{(T_1 p + 1)(T_2 p + 1)}, \tag{1}$$

where k_{μ} determined by Fig. 2,a, T_1, T_2 denote the time constants.

To determine time constants Oldenberg and Sartorius methods and Orman interpolation method have been used. Parameter values of the transfer functions (1) are summarized in Table 1.

Table 1. Parameters of transfer function (1)

Baseline	T_1 , sec	T_2 , sec	k_{μ} , °C/ ($\frac{m^3}{sec}$)
$Q = 0,91 \text{ m}^3/\text{sec}, l = 1, u_{s^*} = 1, f_{s^*} = 1$	958	169	42
$Q = 0,91 \text{ m}^3/\text{sec}, l = 0.5, u_{s^*} = 1, f_{s^*} = 1$	821	152	12
$Q = 0,51 \text{ m}^3/\text{sec}, l = 1, u_{s^*} = 1, f_{s^*} = 1$	969	271	130
$Q = 0,51 \text{ m}^3/\text{sec}, l = 0.5, u_{s^*} = 1, f_{s^*} = 1$	659	101	25
$Q = 0,51 \text{ m}^3/\text{sec}, l = 0.5, u_{s^*} = 0.23, f_{s^*} = 0.35$	659	101	25
$Q = 0,51 \text{ m}^3/\text{sec}, l = 1, u_{s^*} = 0.23, f_{s^*} = 0.35$	969	271	130

Here subscript * denotes the relative value of some parameter, i.e. $u_{s^*} = u_s / u_{s \text{ rat}}, f_{s^*} = f_s / f_{s \text{ rat}}$, where u_s denotes the stator voltage, f_s denotes frequency of the stator current, subscript rat denotes the rated value of some parameter

Analysis of the results comparison of the transients curves obtained during the experiment with the curves obtained in the simulation of the transfer function (1) (parameters of transfer function defined in Table 1) showed high results convergence.

Centrifugal fan as an executive device of automatic temperature regulation system

The important condition for correct design of system control of cooling fan electric drive is precise identification of fan parameters as a mechanical load for electric motor. The main parameter of fan, in terms of electric drive, is relation between T_L load torque and the ω rotor speed: $T_L = f(\omega)$ called a mechanical characteristic. The kind of this function as well a relation between the T motor torque and the rotor speed determine the initial energy efficiency of electric drive.

The mechanical characteristic of the fan can be written as follow:

$$T_L = T_{L0} + \frac{C_H H_s + \omega^2}{\omega \eta(\omega, H_s)} \sqrt{\omega^2 - \frac{H_s}{H_0}}, \tag{2}$$

where T_{L0} is an idling load, H_0 is a static air pressure, H_s is an air pressure under closed latch, i.e. air flow $Q = 0$, C_H is a empirical coefficient, $\eta(\omega, H_s)$ is a fan efficiency.

Relation between the H air pressure and the ω rotor speed can be described as follow:

$$H = H_0 \left(\frac{\omega}{\omega_{rat}} \right)^2 - c Q^2, \tag{3}$$

where c is an empirical coefficient.

Equations (2), (3) contain the main parameters of fan, including efficiency change, and allow to take it into account in the further researches as a load torque for induction motor.

Induction motor drive as a regulation device of automatic temperature regulation system

The correct mathematical model of the induction motor taking all possible losses, and also nonlinearity caused by features of work in various modes into account is necessary for synthesis of control system of electric drive of automatic temperature regulation system. It is obvious that the greatest difficulties are presented by the accounting of losses in iron [1, 10]. The equivalent circuit for induction motor with stator and rotor iron losses is shown in Fig. 3.

In Fig. 3 and further in the article R_s, R_r denote the stator and the rotor resistances; R_{μ} denotes the

resistance equivalent to iron losses caused by eddy current and hysteresis; $L_{\sigma s}$, $L_{\sigma r}$, L_{μ} denote the stator and rotor leakage inductances and magnetizing inductance, respectively; ω_k denotes the electrical angular frequency (or speed) of reference frame; u_s , i_s , i_r , i_{μ} , i_i denote the voltage and currents in a corresponding branches of the circuit.

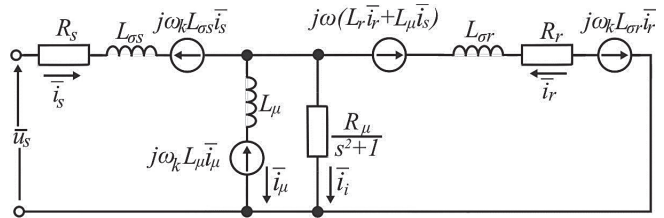


Figure 3. Equivalent circuit for induction motor

A problem with the loss model is the complexity caused by additional contour formed by iron losses and magnetizing branches.. A good way to simplify

the mathematical model is based on the fact that the magnetizing current i_{μ} is much larger than the iron loss current i_i .

$$|\bar{i}_{\mu}| \gg |\bar{i}_i|. \tag{4}$$

Then it follows from circuit (Fig. 3) that i_{μ} is approximated so that:

$$\bar{i}_{\mu} \cong \bar{i}_s + \bar{i}_r. \tag{5}$$

The stator and rotor voltage equations in the synchronous frame written with taking (5) into account for circuit (Fig. 3):

$$\bar{u}_s = R_s \bar{i}_s + L_{\sigma s} \frac{d\bar{i}_s}{dt} + j\omega_k L_{\sigma s} \bar{i}_s + L_{\mu} \frac{d(\bar{i}_s + \bar{i}_r)}{dt} + jL_{\mu} \omega_k (\bar{i}_s + \bar{i}_r), \tag{6}$$

$$0 = R_r \bar{i}_r + L_{\sigma r} \frac{d\bar{i}_r}{dt} - j\omega_k (L_r \bar{i}_r + L_{\mu} \bar{i}_s) + j\omega_k L_{\sigma r} \bar{i}_r + L_{\mu} \frac{d(\bar{i}_s + \bar{i}_r)}{dt} + jL_{\mu} \omega_k (\bar{i}_s + \bar{i}_r), \tag{7}$$

$$\bar{i}_s + \bar{i}_r = \frac{s^2 + 1}{R_c} \left(L_{\mu} \frac{d(\bar{i}_s + \bar{i}_r)}{dt} + jL_{\mu} \omega_k (\bar{i}_s + \bar{i}_r) \right) + \bar{i}_{\mu}. \tag{8}$$

The electromagnetic torque of the induction motor is given by:

$$T = \frac{3p_n}{2L_{\sigma r}} [(L_{\sigma r} i_{ru} + L_{\mu} i_{\mu u}) L_{\mu} i_{\mu v} + (L_{\sigma r} i_{rv} + L_{\mu} i_{\mu v}) L_{\mu} i_{\mu u}]. \tag{9}$$

The mechanical move is described by:

$$T - T_L = J \frac{d\omega}{dt}. \tag{10}$$

The effect of saturation on main magnetic path is taken into account by:

$$L_{\mu*} = -0,002I_{\mu*}^6 + 0,037I_{\mu*}^5 - 0,261I_{\mu*}^4 + 0,87I_{\mu*}^3 - 1,278I_{\mu*}^2 + 0,214I_{\mu*} + 1,413. \tag{11}$$

The nonlinear function linking the resistance equivalent to the iron losses and frequency is presented by:

$$R_{\mu} = \begin{cases} 88,3135 + 5,646f_s + 0,0534f_s^2, & f_s \leq 50\text{Hz}, \\ 1261,3 - \frac{37868}{f_s}, & f_s > 50\text{Hz}. \end{cases} \tag{12}$$

For evaluating of efficiency the next expressions are used.

Mechanical power on the motor shaft:

$$P_{mech} = T\omega. \tag{18}$$

Active electric power:

$$P_s = \frac{3}{2} (i_{su} u_{su} + i_{sv} u_{sv}). \tag{19}$$

Reactive electric power:

$$Q_s = \frac{3}{2} (i_{sv} u_{su} - i_{su} u_{sv}). \tag{20}$$

The copper power losses in the stator winding:

$$\Delta P_{sc} = \frac{3}{2} I_s^2 R_s = \frac{3}{2} (i_{su}^2 + i_{sv}^2) R_s. \tag{21}$$

The copper power losses in the rotor winding:

$$\Delta P_{rc} = \frac{3}{2} I_r^2 R_r = \frac{3}{2} (i_{ru}^2 + i_{rv}^2) R_r. \tag{22}$$

The iron power losses in the stator and rotor core:

$$\Delta P_i = \frac{3 u_{12}^2}{2 R_\mu}, \tag{23}$$

where u_{12} voltage can be taken according to Fig. 3:

$$\bar{u}_{12} = L_\mu \frac{d(\bar{i}_s + \bar{i}_r)}{dt} + j L_\mu \omega_k (\bar{i}_s + \bar{i}_r). \tag{24}$$

The module of u_{12} voltage in the steady state can be written as follow:

$$u_{12} = u_{12u}^2 + u_{12v}^2 = \left(\omega_k L_\mu (i_{su} + i_{ru}) \right)^2 + \left(\omega_k L_\mu (i_{sv} + i_{rv}) \right)^2. \tag{25}$$

The power balance may be written as follow:

$$P_s = \Delta P_{sc} + \Delta P_{rc} + \Delta P_i + P_{mech}. \tag{26}$$

Control system of induction motor drive

The most common features of electric drives of cooling fans for locomotives traction electric equipments and motors are highlighted from the survey of operation modes of the auxiliary drives and machines. It can be listed as follows:

- shifting of speed to its lower values causes considerable reducing of load torque and mechanical power on the motor shaft;
- the long period of time of operation mode with permanent speed and load torque;
- the absence of reverse mode;
- the restricted range of speed change;
- the absence of overloads, the value of overload may be determined in advance;
- the start-up time is not limited, the start is preferred to have a small start-up time for restricting dynamic overloads.

For all these reasons, the strict requires in transient modes to closed-loop system control of cooling fan electric drive are not applied. For restricting the dynamic overloads it is wisely to put not a steplike reference signal but a ramped one.

It is obvious that the scalar control system thor-

oughly satisfies all features mentioned above. The scalar control system of induction motor are shown in Fig. 4.

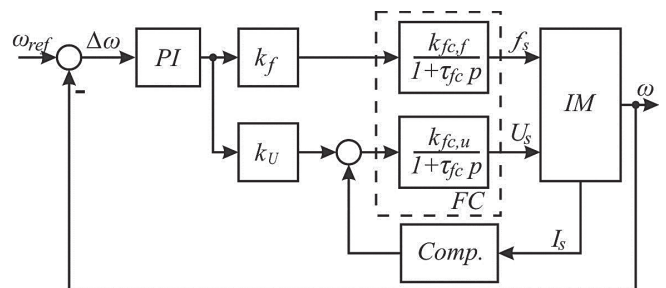


Figure 4. The scalar control system of induction motor

The voltage source inverter of frequency converter is presented as the next transfer functions of frequency and voltage:

$$W_f(p) = \frac{k_{fc,f}}{1 + \tau_{fc} p}, \tag{27}$$

$$W_u(p) = \frac{k_{fc,u}}{1 + \tau_{fc} p}, \tag{28}$$

where k_{fc} is the gain and τ_{fc} is the time constant.

k_f and k_u coefficients provide the proportional relationship between f_s frequency of stator current and U_s stator voltage.

The equation of the speed PI-controller:

$$W_{sp}(p) = k_{sp} + \frac{1}{\tau_{sp}p}, \tag{29}$$

where k_{sp} is the gain and τ_{sp} is the time constant.

The unit in Fig. 4 named *Comp* takes a function of compensation of voltage drop over the stator resistance. Two cases of such compensation are applied: *IR*-compensation and *IZ*-compensation.

Expression for voltage augment in case of *IR*-compensation:

$$U_{aug} = U_{s,rat}f_{s*} + I_{s,rat}R_s(1 - f_{s*}). \tag{30}$$

Expression for voltage augment in case of *IZ*-compensation:

$$U_{aug} = U_{s,rat}f_{s*} + I_{s,rat}\sqrt{R_s^2 + X_s^2}(1 - f_{s*}). \tag{31}$$

Controller of temperature as a control unit

Controller of temperature working on a signal of mismatch of the reference and feedback is used as a control unit of automatic temperature regulation system. The type and parameters of the controller influence on a steady state and transient mode. It needs to find a correct point where transient time, error of regulation, variability, etc. have a satisfying values. In this work P- and PI-controller of temperature are presented and discussed:

$$W_{CU}(p) = k_{CU}, \tag{32}$$

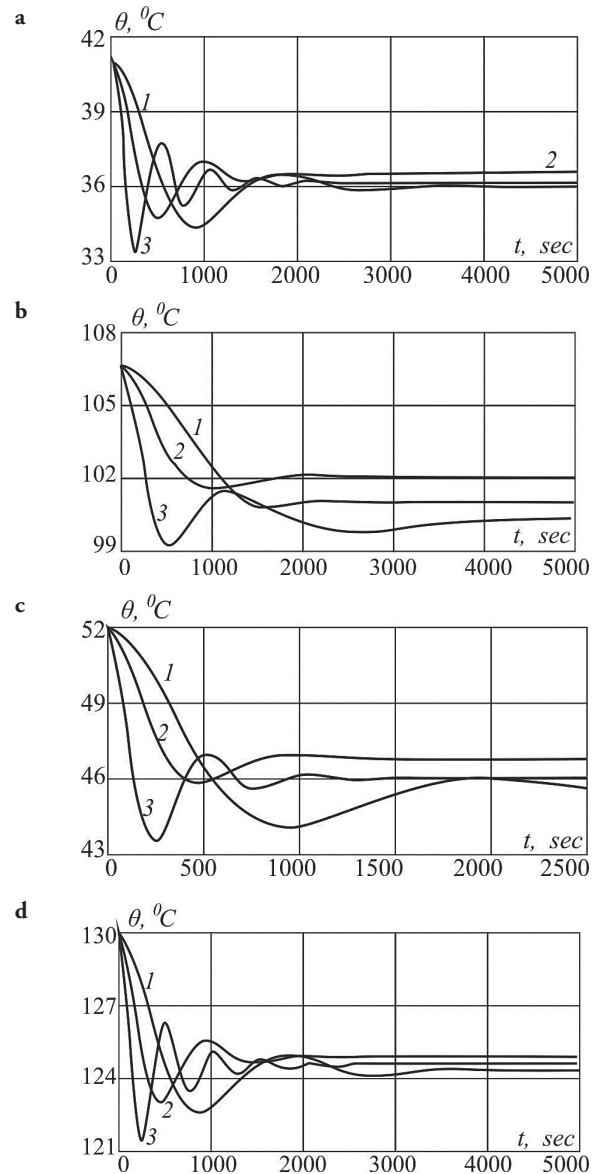
$$W_{CU}(p) = k_{CU} + \frac{1}{\tau_{CU}p}. \tag{33}$$

Simulation of automatic temperature regulation system

Simulation of automatic temperature regulation system was carried out by using of Matlab Simulink. The object of temperature regulation was simulated by transfer function (1) with parameters presented in Table 1. The centrifugal fan was described by (2), (3). The induction motor was presented in accordance to (6) – (10), the nonlinearity are implemented by (11) – (17). The energy equations of an induction motor are included by (18) – (26). The scalar control system was implemented by (27) – (31). The equations

of (32), (33) were used to simulate the control unit in various configurations of automatic temperature regulation system.

The results of simulation of transient modes of automatic temperature regulation system are shown in Fig. 5.



1 – $W_{CU}(p) = 3$, 2 – $W_{CU}(p) = 10$, 3 – $W_{CU}(p) = (p+0.0008)/p$.
 a – $I_s = 1.0$, $Q = 0.91 \text{ m}^3/\text{sec}$, $u_s = 1$, $f_s = 1$,
 b – $I_s = 0.5$, $Q = 0.91 \text{ m}^3/\text{sec}$, $u_s = 1$, $f_s = 1$,
 c – $I_s = 1.0$, $Q = 0.51 \text{ m}^3/\text{sec}$, $u_s = 0.23$, $f_s = 0.35$,
 d – $I_s = 0.5$, $Q = 0.51 \text{ m}^3/\text{sec}$, $u_s = 0.23$, $f_s = 0.35$

Figure 5. The temperature change of the stator winding of the traction induction motor

The analysis of results of simulation let us make some conclusions. The value of transient time changes over a wide range depending on the cooling air flow and the stator current. The value of transient time decreases as the value of stator current increase. At the same time, the value of transient time increases while the value of the air flow increase too.

The increase of value of controller gain is an effective way to reduce error of regulation but it leads to decreasing of stocks of stability and deteriorating of quality indicators. It includes the increase of variability, overshooting and transient time. More expedient way in relation to increasing in value of controller gain is implementation of PI-controller. It leads not to the increase of variability and transient time but to eliminating of error of regulation in steady state.

The gain and time constant of PI-controller is expedient to change at any change of regulation values and reference for providing constant stocks of stability of system and rational values of quality indicators. It can be explained by Table 1 and equations (1) – (26) and peculiarity of the scalar control system as the static and dynamic parameters of transfer functions of regulation system are variables. It is possible to implement it in systems with microprocessor automatic controllers due to continuous change of values of parameters by software.

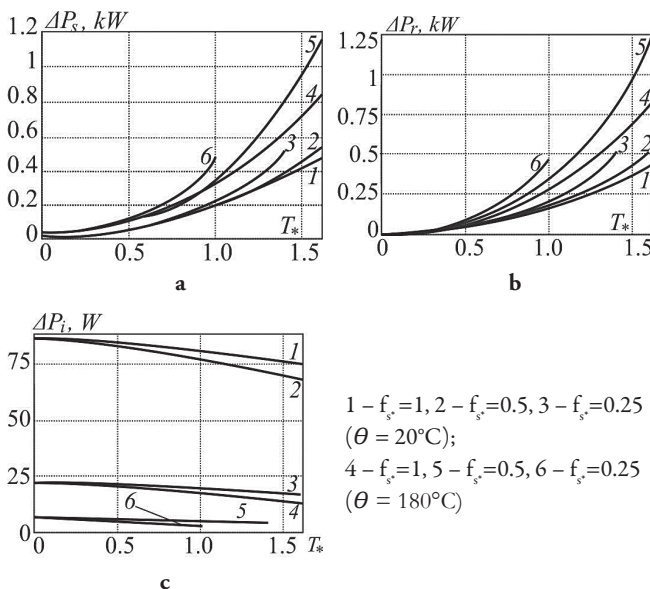


Figure 6. Power losses in copper of the stator (a), copper of the rotor (b) and iron of the core (c) depending on the relative torque under the scalar control with $u_s/f_s=const$

The results of simulation of energy processes in 4A112M6U3 induction motor are shown in Fig. 6 and 7.

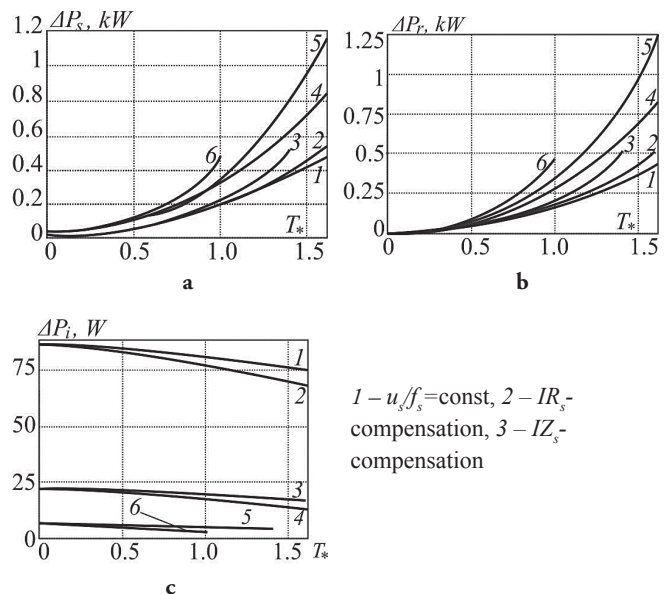


Figure 7. Power losses in copper of the stator (a), copper of the rotor (b) and iron of the core (c) depending on the relative torque under $\theta = 20^\circ C$ and $f_s^*=0.25$

The analysis of results of simulation shows that there is quite narrow range of change of the torques for each of the applied scalar control system where this scalar control system is appeared to be more energysaving than the others. It speaks about need of creation of the high-dynamic control systems allowing to minimize power losses in the wide range of change of the torque and speed.

INDUCTION MOTOR DRIVE WITH POWER LOSSES MINIMIZATION

Survey of efficiency optimization techniques

Optimum design of induction motor is a non-linear multi-dimension problem whereas optimal control is a single or two dimension problems. Numerous scientific papers on the problem of loss reduction in induction motor drive have been published in the last few decades. Although good results have been achieved, there is still no generally accepted technique for loss minimization. According to the proceedings and results of scientific researches, there are three main techniques for dealing with the problem of efficiency optimization of the induction motor drive [4,12]:

- simple state control;
- loss model control;
- search control.

The simple state control is based on the control of one of the variables in the drive [2]. This variable must be measured or estimated and its value is used in the feedback control of the drive, with the aim of running the motor by predefined reference. This technique is simple, but gives good results only for a narrow set of operation conditions. Also, it is sensitive to parameter changes in the drive due to temperature changes and magnetic circuit saturation.

The loss model control are fast because the optimal control is calculated directly from the loss model [13]. The main disadvantage of this technique is that the power loss simulation and calculation of the optimal operating conditions is very complex and it is also highly sensitive to parameter variations in the drive.

The search control uses the on-line procedure for efficiency optimization [8]. The on-line efficiency optimization control on the basis of search changes one of variables in steps until the measured input power settles down to the lowest value is very attractive. Search technique has an important advantage compared to other techniques. It is absolutely insensitive to parameter changes while effects of the parameter variations caused by temperature and saturation are very expressed in two other techniques. Also there is an significant drawback in its use: convergence of controlled variable to its optimal value sometimes can be

too slow, and it never reaches the value of minimal losses then in small steps oscillates around it.

There are some hybrid techniques that combine peculiarities and advantages of three techniques mentioned above [1, 9, 5], but, nevertheless, it can be classified by presented ones.

As a result of survey carried out and features of electric drives of cooling fans, it has been concluded that the search control with indirect power losses minimization is worth to be applied. The variable controlled to reach the optimization point is the stator voltage, the variable choosen to be minimized is the stator current. The next subsections is presented to prove proximity of minimum current and minimum losses modes.

Overall power losses model of induction motor drive

Besides the induction motor taken part in energy conversion, it is also voltage source inverter of frequency converter takes its place in electrical energy conversion. As a rule of thumb, it used to be eliminated from considering as a source of power losses due to a values of losses slightly compared to values of induction motor one. But now, since the computer technology made a huge step forward, it is not so onerous and tremendous to extract the equations of power losses in frequency converter.

The average power losses of frequency converter over switching period of time are determined by follow equations [9]:

- for transistor and diode conduction losses:

$$\Delta P_{c,VT} = \frac{1}{2\pi} \int_0^\pi u_{ce}(i_s, \theta_j) I_s \sin(2\pi f_s t) \frac{1 + \mu(t)}{2} d(2\pi f_s t), \tag{34}$$

$$\Delta P_{c,VD} = \frac{1}{2\pi} \int_\pi^{2\pi} u_{ce}(i_s, \theta_j) |I_s \sin(2\pi f_s t)| \frac{1 + \mu(t)}{2} d(2\pi f_s t), \tag{35}$$

- for transistor turn-on and turn-off commutation losses:

$$\Delta P_{sw,VT} = \frac{1}{2\pi} \int_0^\pi (E_{on}(i_s) + E_{off}(i_s)) \frac{U_{dc}}{U_{dc, rat}} \frac{1}{\tau} d(2\pi f_s t), \tag{36}$$

- for diode commutation losses due to reverse recovery:

$$\Delta P_{rr,VD} = \frac{1}{2\pi} \int_0^{2\pi} E_{rr}(i_s) \frac{U_{dc}}{U_{dc, rat}} \frac{1}{\tau} d(2\pi f_s t). \tag{37}$$

In (34) – (37) u_{ce} denotes the voltage drop over collector-emitter, E_{on} and E_{off} denote the transistor turn-on and turn-off energy, E_{rr} denotes the diode energy reverse recovery. $\mu(t)$ denotes the modulation index.

The modulation index $\mu(t)$ is determined by type of used modulation. In case of sinusoidal pulse width modulation the modulation index is a function of sinus, in case of space vector pulse width modulation the modulation index can be evaluated as follow [3]:

In (34) – (37) u_{ce} denotes the voltage drop over collector-emitter, E_{on} and E_{off} denote the transistor turn-on and turn-off energy, E_{rr} denotes the diode energy reverse recovery. $\mu(t)$ denotes the modulation index. The modulation index $\mu(t)$ is determined by type of used modulation. In case of sinusoidal pulse width modulation the modulation index is a function of sinus, in case of space vector pulse width modulation the modulation index can be evaluated as follow [3]:

$$\mu(t) = \mu_0 \sin(2\pi f_s t) + \frac{3\sqrt{3}}{8\pi} \sum_{k=0}^{\infty} \left(\frac{\sin(3(4k + 1)2\pi f_s t)}{18k^2 - 9k + 1} - \frac{\sin(3(4k + 1)2\pi f_s t)}{18k^2 + 27k + 10} \right), \quad (38)$$

where $k = 0, 1, 2, \dots$

The dependence of voltage drop over collector-emitter from current and temperature of junction can be written as follow:

$$u_{ce}(i_s, \theta_j) = 1,21 + 9,93 \cdot 10^{-3} i_s - 1,88 \cdot 10^{-3} \theta_j - 2,54 \cdot 10^{-5} i_s^2 + 3,22 \cdot 10^{-5} i_s \theta_j. \quad (39)$$

To simplify (34) – (37) it has to substitute losses over switching period of time by real-time losses calculation per component:

$$\Delta P_{c,VT} = u_{ce}(i_s, \theta_j) i_s \frac{\tau_{cond}}{\tau}, \quad (40)$$

$$\Delta P_{c,VD} = u_{ce}(i_s, \theta_j) i_s \frac{\tau_{cond}}{\tau}, \quad (41)$$

$$\Delta P_{sw,VT} = (E_{on}(i_s) + E_{off}(i_s)) \frac{U_{dc}}{U_{dc, rat}} \frac{1}{\tau}, \quad (42)$$

$$\Delta P_{rr,VD} = E_{rr}(i_s) \frac{U_{dc}}{U_{dc, rat}} \frac{1}{\tau}, \quad (43)$$

where τ denotes the switching period of time, τ_{cond} denotes time of conduction for this semiconductor.

The overall power losses of frequency converter:

$$\Delta P_{fc} = 6(\Delta P_{c,VT} + \Delta P_{c,VD} + \Delta P_{sw,VT} + \Delta P_{rec,VD}). \quad (44)$$

The overall power losses of electric drive taken (17) – (26) and (40) – (44) into account has to be written as follow:

$$\Delta P_{ed} = \Delta P_s + \Delta P_c + \Delta P_r + \Delta P_{fc}. \quad (45)$$

Comparison between minimum current and minimum losses modes

As it was undermined in subsection 2.3 the scalar control system has been chosen to utilize. To provide the minimum power losses it needs to implement a gauge of active power or calculate by mathematical model. But for locomotives the mounting of com-

plementary equipment is not such a widely used technique because of the strict limit of free space, sophistication in exploitation and maintenance. To implement the stator current sensor is much better way for reaching the aim. It leads to shift from point of minimum power losses inevitably and this shift has to be evaluated. It is obvious that analytical solv-

ing this problem is very complex task. The numerical methods has been utilized to get the relationship between power losses under the different modes. Mathematically, this task for the scalar control system can be written as follow:

$$\Delta P_{ed}(T, \omega, s) \rightarrow \min \Rightarrow s_{opt}, \tag{46}$$

where $s = \omega_0 - \omega$, s_{opt} denotes its optimal value in terms of losses minimization.

Table 2 contains the most important results of the numerical investigation for 4A112M6U3 induction motor. IGBT module of SKiiP 11HEB066V1 was used as a voltage source inverter.

The quantity comparison of overall power losses in electric drive between minimum current and minimum losses modes shows its almost thoroughly coincidence. So, the maximum mismatch in overall power losses under two considered modes for $0.2 \leq T_s \leq 1.5$ and $0.25 \leq \omega_s \leq 1.25$ equals to 8%.

Table 2. Comparison between minimum current and minimum losses modes

mode	ω_s	$\Delta P_{ed}, W$					
		$T_s=0.2$	$T_s=0.4$	$T_s=0.6$	$T_s=0.8$	$T_s=1.0$	$T_s=1.2$
minimum	1.25	138.1	243.1	361.6	499.3	653.4	839.5
	1	116.3	212.3	324.9	458.3	615	793.5
power	0.75	96.1	184.2	292.1	422.7	576.5	753
	0.5	77.2	159.2	263.5	491.5	543.2	718
losses	0.25	61.9	138.5	239.8	365.7	515.5	689.5
	1.25	146.2	246.3	362.3	499.1	659.5	841
minimum	1	120.1	213.2	324.4	459	616	796.5
	0.75	97.3	184.2	292.3	423.8	579	777.5
current	0.5	77.8	159.5	264.5	393.7	597	724
	0.25	62.1	139.4	241.8	369.1	521	691.2

Implementation of power losses minimization

The developed control system of induction motor are shown in Fig. 8, a. The control system may be divided into two subsystems: the common scalar control system having closed loop with speed feedback (Fig. 4) and the control system providing the minimum current mode.

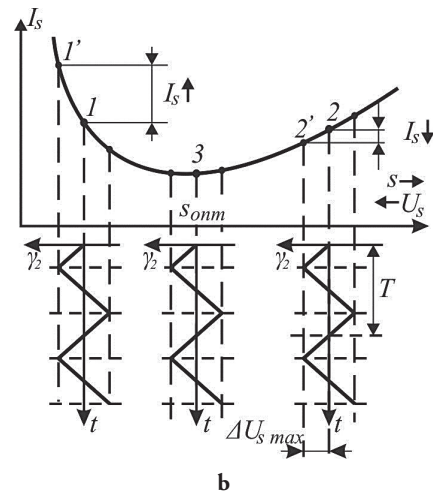
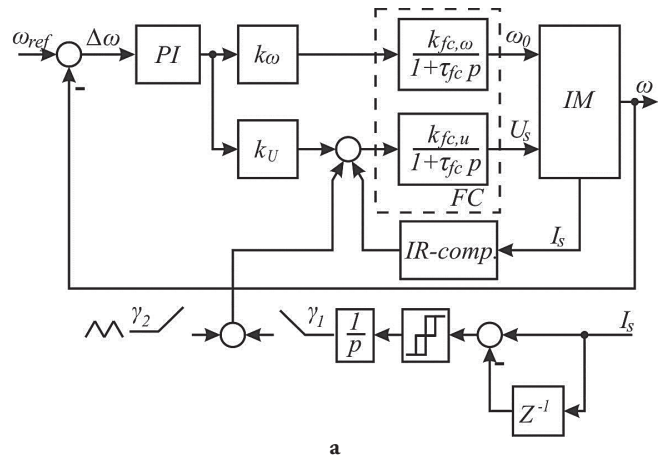


Figure 8. The scalar control system of induction motor with power losses minimization (a) and technique of searching for minimum of the stator current (b)

The essence of the control system providing the minimum current mode is the next. If a steady state of the operation can be found, the search control system is enabled, until the stator current reaches the minimum. It is used an external, periodical test signal, triangular shape wave, that determines the increases or the decreases of the additional voltage control signal. Once the minimum point was reached, the system operates in this new steady state, until a change in the stator current is detected.

The search technique uses as manipulated variable the γ_1 voltage and as test signal the γ_2 triangular voltage in order to change the stator voltage:

$$U_{s,tot} = U_s + \gamma_1 + \gamma_2. \tag{47}$$

It is applied that the γ_2 test signal has the amplitude $\Delta U_{s,max}$ and the τ_γ period then the position of the

current operating point (1, 2 or 3 in Fig. 8, b) relative to the minimum point can be determined by the variation of the ΔI_s stator current due to the $+\Delta U_{s,max}$ test signal in the first $\tau_\gamma/2$ half of period so that:

- if $\Delta I_s > 0$ then the slip is $s < s_{opt}$ (point 1);
- if $\Delta I_s < 0$ then the slip is $s > s_{opt}$ (point 2);
- if $\Delta I_s = 0$ then the slip is $s = s_{opt}$ (point 3).

In order to make the induction motor to operate close to minimum point it needs to choose the ramp sign of the manipulated variable ($\gamma_I = \varepsilon t$, where ε is an empirical coefficient) so that:

- if ΔI_s increases then γ_I has to decrease the stator voltage:

$$\Delta U_s = -\gamma_1 + \gamma_2 = -\varepsilon t + \gamma_2 = \gamma; \tag{48}$$

- if ΔI_s decreases then γ_I has to increase the stator voltage:

$$\Delta U_s = \gamma_1 + \gamma_2 = \varepsilon t + \gamma_2 = \gamma; \tag{49}$$

- if $\Delta I_s \approx 0$ then the signal is $\gamma \approx 0$.

Simulation of induction motor drive

Simulation of the drive was carried out in MatLab as follows. At the first interval of time the soft start of the induction motor to the referenced speed was carried out. The system of the stator current minimization is disconnected. After completion of transition processes the search control technique is added to classical system of scalar control and starts registering the direction of change of the stator current in the first half of period of a test signal. Depending on change of the stator current the system of its minimization begins developing the γ_I manipulated signal directed on reduction of the current. When change of the current becomes less than a hysteresis of the relay regulator (Fig. 8, a), the test signal is disconnected until owing to various reasons (change of the load torque, temperature of windings, etc.), not depending on change of a reference speed, slip will not deviate the optimum value that will cause the corresponding increase in the current and, consequently, in the power losses.

The results of simulation are shown in Fig. 9. The stator current are presented in synchronous frame so that its frequency in Fig. 9 is null.

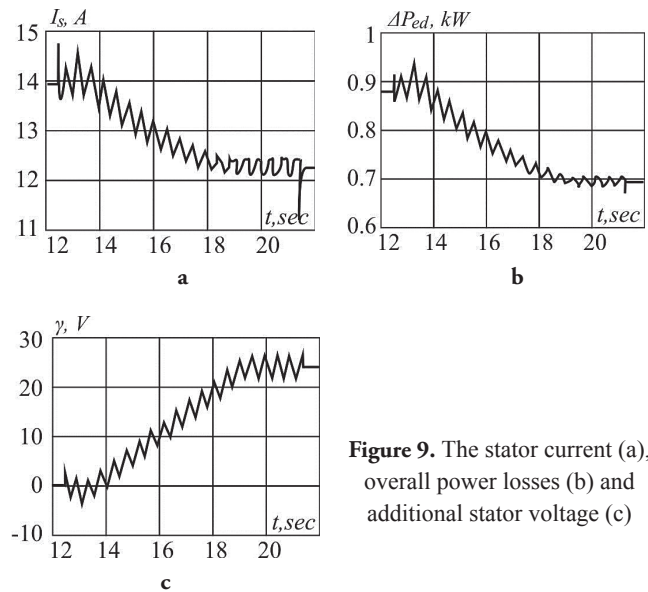


Figure 9. The stator current (a), overall power losses (b) and additional stator voltage (c)

The analysis of results shows operability of the developed control system. So, with speed twice reduced relative to the rated and load torque one and a half times exceeded relative to the rated, for ensuring the minimum stator current it is necessary to increase the stator voltage. It leads to a simultaneous reduction of power losses (about 20%). The stator current decreases approximately by 15...20%. Speed after shutdown of system of the current stator minimization comes back to the value before inclusion of the system. Oscillations of speed under the search control system are insignificant and do not exceed 0.5%.

CONCLUSIONS

The developed automatic temperature regulation system of traction induction motors consists of control unit implemented by P- or PI-controller, executive regulation device implemented by induction motor drive with the centrifugal fan. The developed and constructed physical model of both traction and auxiliary drive of locomotive allows to investigate the thermal and electromechanical and control processes. The developed control system of the induction motor with the stator current minimization provides also power losses minimization. The minimization mode is feasible under the steady state. The control system gives the greatest effect under lowered speed and/or the lowered or raised load torques due to regulation in necessary limits of the stator current by means of change of the stator voltage. Reduction of both power losses and the stator current can reach

20% of initial value depending on the providing speed and torque.

The reported study was supported by Russian Foundation for Basic Research (RFBR), research project No. 14-08-31274.

Acknowledgements

REFERENCES

- [1] Aissa, K., Eddine, K.D. (2009). *Vector control using series iron loss model of induction motors and power loss minimization*, World academy of science, engineering, and technology, 52,. – P. 142 – 148.
- [2] Benbouzid, M.E.H., Nait Said, N.S. (1998). *An efficiency optimization controller for induction motor drives*, IEEE Power Engineering Review, Vol. 18, Issue 5, pp. 63 –64.
- [3] Bierhoff, M.H. [et al.] (2004). *Semiconductor losses in voltage source and current source IGBT converters based on analytical derivation*, Power Electronics Specialists Conference,. PESC 04. 2004 IEEE 35th Annual, Volume 4, pp. 2636 – 2642.
- [4] Blamisa, B., Vukosavic, S.N. (2013). *Efficiency optimization of induction motor drive*, Naučno-stručni simpozijum Energetska efikasnost, ENEF 2013, Banja Luka, 22. – 23. Nov. 2013.
- [5] Blanuša, B., Marić, P., Dokić, B. (2010). *New hybrid model for efficiency optimization of induction motor drives*, in Proceedings of 52nd International Symposium ELMAR-2010, pp. 313–317.
- [6] Kosmodamianskiy, A.S., Vorobiev, V.I., Pugachev, A.A. (2011). *The temperature effect on the performance of a traction asynchronous motor*, Russian Electrical Engineering, 2011, Vol. 82, No. 8, pp. 443 – 448.
- [7] Kosmodamianskiy, A.S. (2002). *Theoretical bases and development of locomotives traction electric motors temperature control system*, thesis, doctor in engineering – Moscow, – 306 p.
- [8] Kosmodamianskiy, A.S., Vorobiev, V.I., Pugachev, A.A. (2012). *Induction motor drives with minimal power losses*, Russian Electrical Engineering, Vol. 83, No. 12, pp. 667 – 671.
- [9] Kosmodamianskiy, A.S., Klyachko, L.M., Vorobiev, V.I., Pugachev, A.A. (2014). *Control system of a tractive drive with temperature control of thermally loaded elements*, Russian Electrical Engineering, Vol. 85, No. 8, pp. 513 – 518.
- [10] Lim, S., Nam, K. (2004). *Loss-minimising control scheme for induction motors* IEEE Proc.-Electr. Power Appl. Vol. 151. No. 4, July 2004. – p. 386 – 397.
- [11] Pugachev, A., Fedyayeva, G. (2015). *Definition of the transfer function of asynchronous motor as an object of temperature control*, Applied Mechanics and Materials. 2015.–vol. 698. – pp. 124 – 130.
- [12] Thanga Raj, C., Srivastava, S. P., Pramod, A. (2009). *Energy efficient control of three-phase induction motor*, a review, International Journal of Computer and Electrical Engineering, Vol. 1, No. 1, April 2009. – pp. 61 – 70.
- [13] Vukosavic, S.N., Levi, E. (2003). *Robust DSP-based efficiency optimization of variable speed induction motor drive*, IEEE Transaction of Ind. Electronics, Vol. 50, No. 3, pp. 560-570, 2003.

Submitted: April 30, 2015.

Accepted: May 8, 2015.

A NEW APPROACH TO COMPUTER ANALYSIS OF QUEUING SYSTEMS WITHOUT PROGRAMMING

Zoran Ž. Avramović, Radomir Z. Radojičić, Saša D. Mirković

University of Belgrade, zoran.avramovic@sf.bg.ac.rs

Contribution to the state of the art

DOI: 10.7251/JIT1501025A

UDC: 662.62:519.245

Abstract. The paper presents original object oriented programming system *ARS* for modelling and simulation queuing systems. Programming system was developed in programming language C++. It establishes connection with intrinsic, but also with other Windows programming packages, in a simple way, through object oriented environment. Basic characteristics and possibilities of programming system, as well as comparative analysis of simulators: mathematical model (analytical solution) - GPSS/H - *ARS*, on the example of closed queuing network in the paper is given. The significant application for computer performance evaluation is reported.

Keywords: simulation, queuing system, programming system, computer performance evaluation.

INTRODUCTION

Since the invention of computer the growing importance is attached to virtual experiments on the computer. In view that the subject of attention in the research activities are more and more frequently the complex systems, where the mathematical or statistical analyses are either too complex or do not give results, the computer simulation has been obtaining a growing importance [6,7].

The methodological approach to modelling is directly related to the language choice for the system simulation. The experience in development of the theory and practice of simulation indicates that the most efficient means of the simulation models programming are the specialised simulation languages.

ARS is a simulation system which, in a simple way, by defined graphical models, creates the model (specifying a sequence of activities and precisioning the operations performed by their implementation over the attributes of the model objects).

The philosophy of the *ARS* programming system

is based on the object approach to the modelling and simulation process.

THE CONCEPT OF THE SYSTEM

The *ARS* has been conceived as a general programming system intended for stochastic modelling and to processes oriented discrete simulation. It has been accomplished on an object approach, establishing a close, natural relationship between the analysed system and the simulation model - alleviating the modelling and simulation process to the user.

The *ARS* programming system enables the modelling and simulation of single- and multiphase of queuing systems, either single- or multi-channel ones (with equivalent or non-equivalent servers). It is also possible to model and simulate both open and closed networks, but also the queuing networks with and without the feedback.

The motive for development and implementation of this system is the authors' wish to expand and improve the capabilities of modern simulation languages and simplify their use and application.

BASIC CHARACTERISTICS OF THE SYSTEM

The *ARS* programming system represents an object approach to the simulation modelling, which enables a simple modelling procedure, a high detail level of real processes, updating and use of the results in all steps of operation. It is enough to have a basic knowledge on the computer operation for its use. The users' requests to model the systems and laws of their functioning as truly as possible for the requirements of various investigations, are met by *ARS* through the flexible graphic environment available and a wide range of basic and derived "objects".

The basic elements present in modelling by the *ARS* programming system are static and dynamic objects (transactions). Any change in the object status results from the occurrence of an event, which may represent either starting or ending an activity.

The static objects direct, hold, update and partly control the dynamic objects, or change their parameters' values. One of the basic static objects in *ARS* is a server, representing the object by which the activity duration or delay is modelled.

The dynamic objects are created in input points of the model by the basic object for generation of objects, or defined by an initial state of the system. These objects are moved through the model bearing their characteristics - transaction parameters. As long as they are present in the model, the dynamic objects are in interaction with other objects in various forms.

During the simulation, it is possible to achieve the interaction and communication, in all variants, between static and dynamic objects (either directly or indirectly), with a possibility of using additional variables and functions from a wide range of the offered ones, as well as those derived there from.

The objects may be basic and derived. The basic objects are defined in advance and they cannot change their intended function, but their specified parameters can be changed.

The *ARS* programming system incorporates a capacity of modelling the queuing system by user through the application of offered or independently

designed objects. By designing of the own objects of an arbitrary complexity and through the definition of their parameters, it becomes possible for the user to better imitate the computer system functioning so that the desired level of detailing in an accessible way is obtained.

THE MODELLING AND SIMULATION

The model of the queuing system in *ARS* is a series of static objects through which the transactions pass during the simulation [8].

The simulation of queuing system operation in the *ARS* system is performed by a simple procedure: after creating a graphic model of the system and defining the work load and system resources parameters, the interactive simulation is activated and implemented [1,2]. During the simulation and on its completion, the user has at disposal (current and final) simulation results - statistic indicators of basic and derived performances of the queuing model.

The user has at disposal a large number of different probability distributions of arrivals of open network transactions, various distributions of service time and standard scheduling algorithms (FCFS, LCFS, PRI, RSS, and RR).

The modelling is implemented with the graphic editor's support, by simply creating a state-transition diagram, using the offered objects, and on the basis of already created models in the form of the derived objects. It would be possible to use either the mouse or develop a model by means of the keyboard.

The visual monitoring of the transactions flow in all stages of creation and modelling, as well as in the phase of simulation, represents an important innovation in relation to the program packets of similar nature.

The monitoring and analysis of the transient response and steady state are achieved by storing and erasing the selected statistic indicators, dynamic objects and their attributes. When detecting the steady state (by monitoring the steadiness of relevant, pre-selected indicators of system performances), it is possible to automatically stop the simulation.

By building a more detailed model and defining the derived objects based on the requirements, creating the own functions of distributions on the basis functions, by definition of users' functions to be used during the simulation, and based on the appearance of working environment, the adjustment of the system is made according to the users' requirements.

WORKING ENVIRONMENT

The *ARS* programming system communicates and uses, in a very flexible way, both internal and other Windows program packets having the required inter-relation with it. The system is furnished with the original program packet for a curve-fitting, representing an important supplementary characteristic. The use of a wide set of approximate functions and deriving of conclusions on the basis of numerical processing and graphical presentation of simulation results brings an advantage over the existing program packets of a similar application.

The user has in front of him a possibility of a dialogue with the computer in all steps of modelling and simulation.

The interactive simulation enables the experimenting during which, in randomly selected moments, or after the meeting of a particular condition, an arbitrary object in the system can be approached, watched and its current status monitored, the values of some variables can be changed, the status of the system also can be changed by introducing taking out or updating of the object parameters or even modify the initial diagram and continue the simulation thereafter.

A particular advantage of the interactive operation is shown in detecting, locating and correcting of errors.

The system comprises a standard HELP giving the required information in all steps of model elaboration and in all stages of simulation. There is also a possibility of a multi-media presentation of the programming system, with an animation and accompanying vocal presentations, supplementing the basic elements of the simulation system. Programming

system was developed in programming language C++ [9,12].

SIMPLE QUEUING MODEL OF THE CLOSED NETWORK (THE COMPARATIVE ANALYSIS)

The comparative analysis of queuing system (mathematical model - GPSS model - *ARS* model), has been made on a simple example of a closed network with central and three parallel connected servers with an exponential distribution of serving time (Figure 1). The results related to selected servers in relation to time and number of transactions in the system is presented, namely:

- mean serving time,
- mean utilisation of server, and
- mean turnaround time of transaction in the central server and its queue.

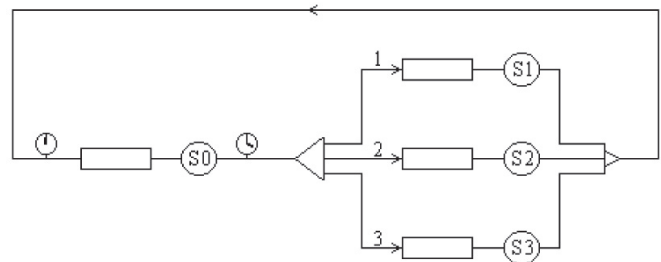


Figure 1. Queuing model of the closed network with the central and three parallel servers

Mathematical model - Analytical solution

As an indicator of performances of the analysed system, the server's utilisation has been observed. The analytical solution, through the application of Buzen's algorithm [5], gives following utilisation of the *j*-th server:

$$U_j = x_j \cdot G(n-1) / G(n), \quad j = 1, 2, \dots, k \tag{1}$$

where the «normalising denominator»

$$G(n) = g(n, k) \tag{2}$$

was derived as limes from a recurrent equation:

$$g(i, j) = g(i, j-1) + x_j \cdot g(i-1, j), \quad (i > 0, j > 0), \tag{3}$$

with boundary conditions:

$$g(i, 0) = 0, \quad i = 1, 2, \dots, n \tag{4}$$

$$g(0, j) = 1, \quad j = 1, 2, \dots, k \tag{5}$$

where:

n - number of transactions circulating through the system,

k - number of servers, and

x_j - normalised request for the j -th server.

Simulation model in GPSS/H language

The listing of the program implemented in the simulation language GPSS/H is elementary [3,4,11].

Simulation model in the ARS programming system

The queuing model of the implemented solution of the closed network, in the programming system ARS is shown in Figure 1. The basic static objects used in this network:





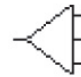
-  **Chronoscope** (Object for time measuring - punctual measuring of small time particles)
-  **Queue** (Object for waiting for serving; finite queue; n-queue capacity)
-  **Server** (Variable delay object for serving or processing)
-  **Collector** (Merging point. Object for putting the transactions together)
-  **Distributor** (Branching point. Object for probabilistic branching of transactions)

Table 1. The server's basic parameters

Server	Server's name	Mean serving time
S0	Central	5 ms
S1	First parallel	25 ms
S2	Second parallel	25 ms
S3	Third parallel	10 ms

Table 2. The probabilistic branching element's basic parameters

Channel	Probability of transfer
1	2/11
2	2/11
3	7/11

Review and analysis of the results

Figure 2 shows the mean serving time of serving by the first parallel server in relation to the number of transactions in the model. The comparison with the value from Table 1 shows that the ARS programming system gives a lower and more stable relative error of serving time dispersion. For the illustration, we should mention that the mean relative error in the concrete case is: for ARS 2.35%, and for GPSS/H 4.37%.

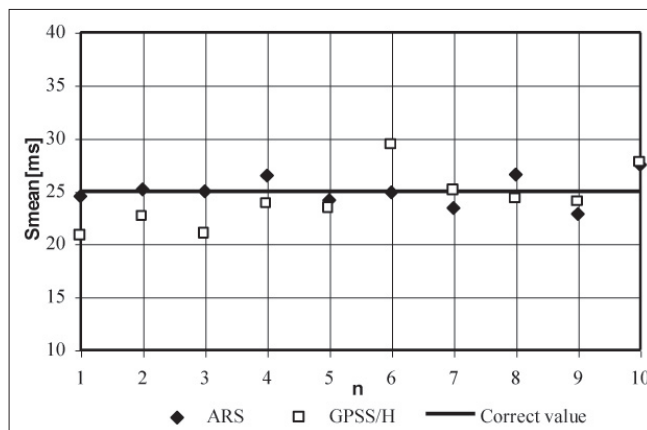


Figure 2. Mean serving time for the first parallel server in relation to the number of transactions in the model

The results showing the dependence of the central server's utilisation from the number of transactions in the model (Figure 3) indicate that the ARS programming system is significantly more convergent to results obtained by the analytical method from the mathematical model. In the case in question the relative error mean value for ARS is 3.28%, and for GPSS/H 5.91% (whereas their maximum values are 7.68% for ARS and 18.10% for GPSS/H).

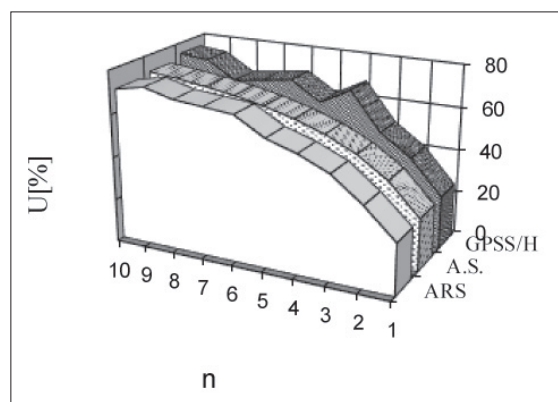


Figure 3. Utilisation of the central server in relation to the number of transactions in the model (A.S. - Analytical solution)

Of a particular interest are the results obtained by observation of the central server utilisation in relation to the simulation time. It is not difficult to notice in Figure 4 that utilisation offered by the *ARS* programming system, during the transient regime of simulation, has an unstable value which, as the simulation continues, converts into steady, close to the theoretical one. As the opposed to this, GPSS/H demonstrates, for the same parameter, a higher dispersion during the entire period under consideration. It has been found that during the whole period under consideration, the mean value of a relative error for the *ARS* programming system is 3.01%, and for GPSS/H 3.61%.

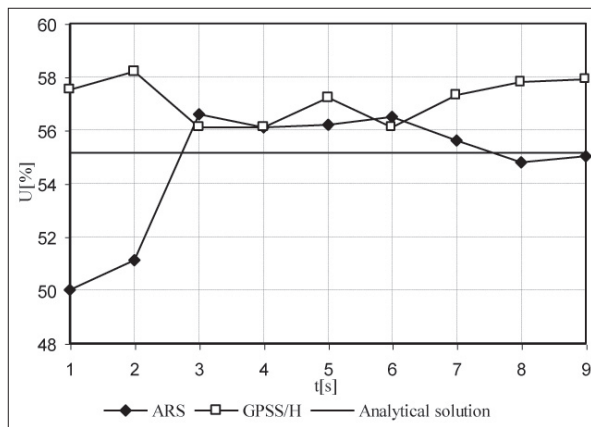


Figure 4. The simulator behavior in the transient time (on an example of the central server utilization) (for 4 transactions in the model)

The mean time of transactions' holding in the central server and its queue (Figure 5), and the mean time of transactions' queuing at the central server (Figure 6), in relation to the number of transactions in the model, for the programming system *ARS* and GPSS/H have approximately same law of change.

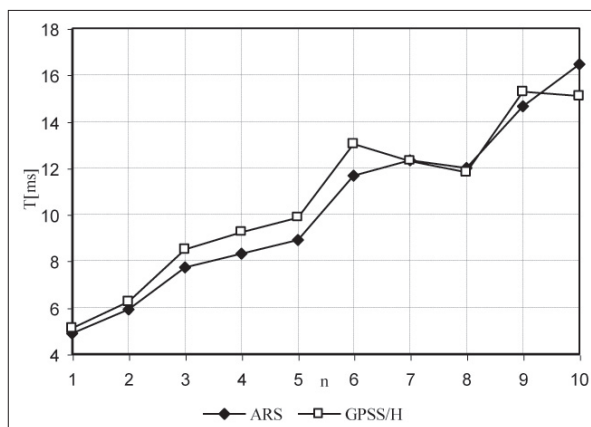


Figure 5. Turnaround time in the central server and its queue in relation to the number of transactions in the model

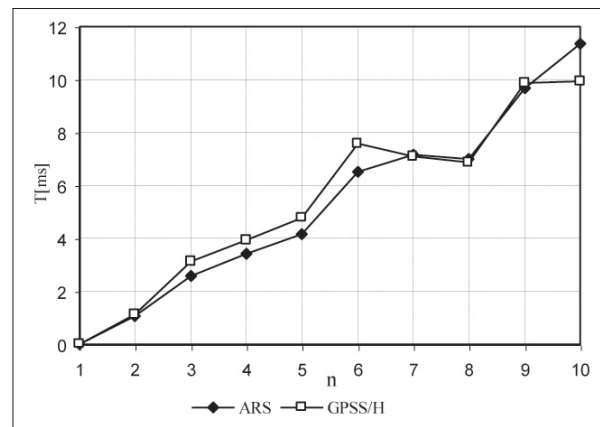


Figure 6. Turnaround time in the central server's queue in relation to the number of transactions in the model

The *ARS* programming system, using the own least-squares curve-fitting program, has established the approximate function for the mean time of transactions' queuing in relation to the number of transactions in the model:

$$T_q \text{ [ms]} = a \cdot \ln(1+n) + b / \ln(1+n) + c \cdot \sqrt{n} + d / \sqrt{n} + e / n + f, \quad n=1,2,\dots \tag{6}$$

Values of coefficients in equation are:

$$a = -341.63, b = -38541.22, c = 640.82, d = 1048.67, e = 38190.69, f = 18087.80. \tag{7}$$

For the found approximate dependence, the correlation coefficient is 0.991.

SIMULATION MODEL OF THE COMPUTER SYSTEM

The simulation analysis of the computer system model functioning has been made on the example of a closed multi-processor multi-processes network (Figure 7) with three processors, two disks, paging storage consisting of 512 pages, five priority queues for the processor, three priority queues for storage allocation and ten processes moving through the model, respecting the dependence of the processes activities (as shown in Figure 8). The attributes of all processes are presented in a tabular form (Table 3).

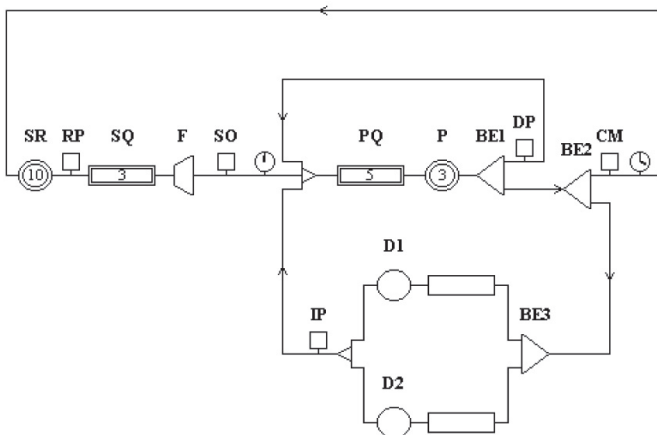


Figure 7. Queuing model of the multi-processor multi-processes computer system

Legend:

SR - State of rest (10)	P - Processors (3)
RP - Request for the processes	DP - Decreasing of priority
SQ - Storage queue (3)	IP - Increasing of priorities
F - Filter	CM - Clearing of memory
SO - Storage occupation	D - Disks (2)
PQ - Processor queue (5)	BE - Branching elements (3)

Table 3. Dynamic objects (processes) of the system with attributes and initial values

Process	A1	A2	A3	A4	A5	A6	A7	A8	A9	A10	A11
1	18	5	5	5	0.01	0	1000	1.00	10	2	0
2	32	4	3	4	0.02	0	2000	0.50	20	5	0
3	40	3	2	4	0.05	0	3000	0.00	20	8	0
4	46	3	2	4	0.05	0	4000	0.50	5	10	0
5	74	3	1	4	0.10	0	5000	0.50	10	50	0
6	88	3	1	4	0.10	0	6000	0.00	40	40	0
7	92	3	1	4	0.10	4	7000	0.30	50	60	0
8	144	3	1	4	0.20	2	8000	0.50	100	15	0
9	166	3	1	4	0.30	2	9000	1.00	200	17	0
10	200	3	1	4	0.40	3	10000	0.80	250	30	0

Legend: A1 - number of pages, A2 - current priority, A3 - the lowest priority, A4 - the highest priority, A5 - probability of transfer to the state of rest, A6 - request for process, A7 - mean turnaround time of the state of rest, A8 - probability of transfer to the first disk, A9 - mean time serving for disk, A10 - mean time of serving for the processor, A11 - remaining processing time (established after the interruption of the process due to the lapse of the processor time quantum)

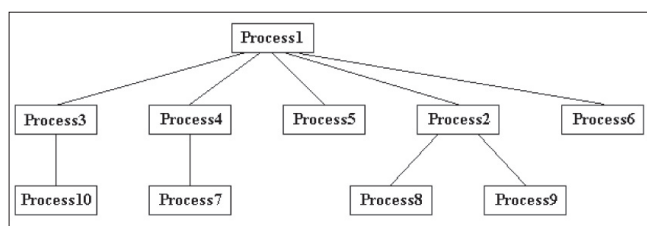


Figure 8. Tree presenting the dependence of processes by presence in the storage (when a process is active, all preceding ones must be stored)

The static objects in this network and their basic parameters are (serving times by all servers are the exponentially distributed):

SR: Multi-channel server (10 channels). It obtains the mean serving time through its attribute process (A7). While receiving the request from object RP, object SR releases the requested processes, in case they are served within it.

RP: The object for events generation and updating of variable systems, transaction attributes and object parameters. It generates the event to object SR for release to the first process and the process determined by attribute A6 of the current process.

SQ: A multiple queuing for storage. It consists of three queues. The highest priority queue comprises the processes with more than 100 pages, the medium priority - processes with the number of pages between 50 and 100 and the lowest priority - other processes.

F: The object letting in the transactions when the condition required is met. If the coming process requires more pages than available at the moment, it is on admitted until the required number of pages is available.

SO: By processing through this object, the value of the variable SR (the number of pages available in the storage, the global variable of the system) decreases by the number of pages of the current process.

PQ: Five queues accepting the processes by their priority attribute.

P: Multi-channel server with three processors. The mean serving time is obtained from the process attribute (A10). The upper limit of the serving time is specified - the processor time quantum. (The remaining serving time is recorded in attribute A11 of the process, and the process is released. If on the process occupation attribute A11 is other than zero, this value is added to the current serving time).

BE1: The process is forwarded to the first branch if attribute A11 is more than zero.

BE2: The branching is implemented according to the leaving probability (the first branch is approached with the probability given by attribute A5).

DP: It decreases the priority to the process by 1 (if it is higher than the minimum value for that process).

CM: The storage is clear. Variable SR increases by the number of required pages for the current process.

BE3: Divides the processes according to probabilities obtained from attribute A8 of the current process (disk D1 is approached with the probability given by attribute A8).

D1 and D2: Servers with mean serving time according to attribute A9 of the process.

IP: It increases the priority to the process (if it is lower than the maximum value for that process).

Computer model exploitation

The simulation starts from the state where all processes are inactive (meaning that the storage is quite clear). After the expiration of the phase of rest of the process, the storage begins to be fed, gradually. By watching the transient time up to the twentieth second (Figure 9); one can see that the storage utilisation grows up to the steady value of 80%, when all processes are active.

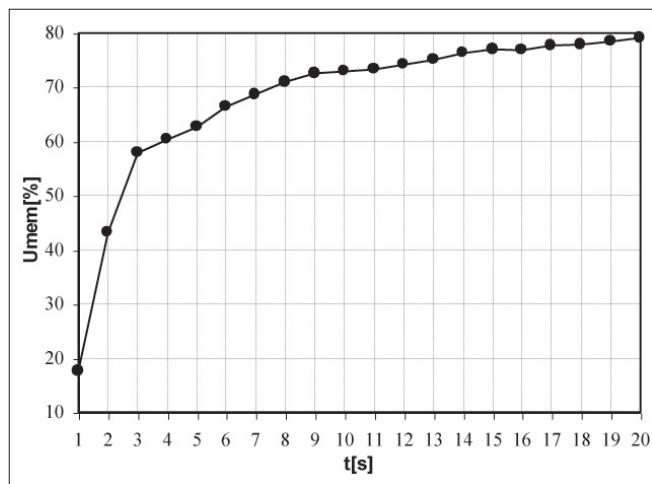


Figure 9. Storage utilisation in the transient time (for the processor time quantum $q = 9$ ms)

Using its own least-squares curve-fitting program, the **ARS** has established the approximate function for storage utilisation in relation to time:

$$U [\%] = a \cdot \ln (t) + b \cdot t^2 + c \cdot t + d\sqrt{t} + e, \quad (t > 0, t[s]). \tag{8}$$

The values of coefficients in equation are: $a = 105.97, b = -0.13, c = 17.44, d = -153.83, e = 154.04.$ (9)

For the obtained approximate dependence, the correlation coefficient is 0.998.

The particularly interesting results have been obtained for the total times of process staying in the subsystem (from occupation of storage to cessation of further activities and clearance of the occupied storage - between two chronoscopes) in relation to time (Figure 10). The first process is needed by all other processes (if any process is activated, then the first one must also be activated, Figure 8), so that it practically does not leave the subsystem. With the third process, the rectilinear dependence disappears, and the curve is more inclined to abscissa (since it is conditional for one process only - the tenth). With the tenth process the curve is much closer to abscissa (as expected, since that process is not conditional for any other one and its mean rest time is considerably longer).

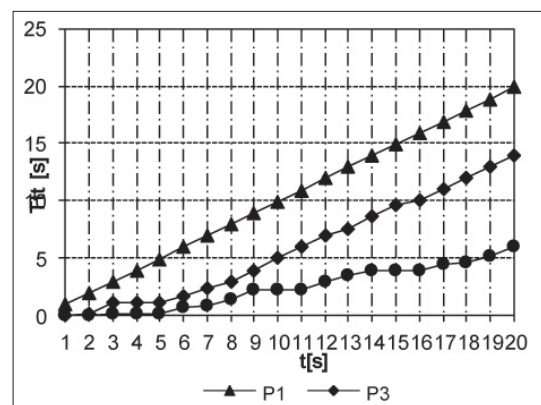


Figure 10. Turnaround time of the processes between two chronoscopes (for the processor time quantum $q = 9$ ms)

The process priority changes in relation to whether it addresses the disk (the priority increases), or interrupts due to the processor time quantum expired (the priority decreases). Since the priority change depends on the time quantum, hence the total turnaround time in the priority queues depends on quantum (as the quantum grows, the number of process interruptions decreases, and therefore the priority of the processes decreases less frequently - which results in higher priorities, so that the turnaround time in the higher pri-

ority queues is longer). Figure 11 shows that the total turnaround time in priority 4 queue is significantly longer than turnaround time in priority 1 queue with the longer quantum of the processor time.

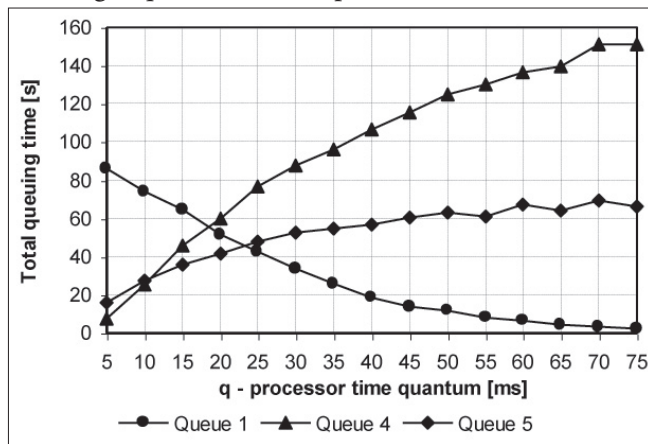


Figure 11. Total queuing times for the processor in relation to the processor time quantum

CONCLUSION

The paper presents the original programming system *ARS* for simulation of the queuing system. The

presented programming system is applicable for the simulation of open and closed queuing networks of an arbitrary complexity. It enables a simple modelling, interactive simulation, adequate presentation and numerical processing of results, arbitrary adjustment of working environment and system resources and other advantages, aiming at a more efficient designing.

The programming system offers to the user a possibility of introducing his own objects, enabling a more successful modelling of complex systems. The own system for numerical processing of the simulation results is an efficient tool for collecting the statistic indicators of the relevant system performances. The interactive simulation and a possibility of changing the structure of the analysed of queuing system makes a basis for a successful detection and removal of errors found during the modelling.

Considering the before specified properties of the *ARS* programming system, we are of the opinion that it represents an adequate tool in the field of modelling the discrete queuing systems.

REFERENCES

- [1] Avramović, Z.Ž., Radojičić, R.Z., "ARS - new programming system for computer performance analysis" (in Serbian), *ETRA*, Budva, 1996, 47-50.
- [2] Avramović, Z.Ž., Radojičić, R.Z., Savkić, D.S., "The modelling and simulation operation of a railway station in the ARS programming system" (in Serbian), *JUŽEL*, Niš, 1996, 31-34.
- [3] Avramović, Z.Ž., Radojičić, R.Z., Savkić, D.S., "Basic characteristics of object oriented programming system ARS for simulation queuing systems" (in Serbian), *YuInfo*, Brezovica, 1996, 107.
- [4] Banks, J., Carson, J. S., Sy, J.N., *Getting Started with GPSS/H*, Wolverine Software Corporation, Annadale, 1989.
- [5] Buzen, J.P., "Computational algorithms for closed queuing networks with exponential servers", *Comm. ACM*, 16 (1973) 527-531.
- [6] Gordon, G., *System Simulation*, Prentice-Hall, Englewood Cliffs, Nj, 1978.
- [7] Graham, R.L., Knuth, D.E., Patashnik, O., *Concrete mathematics: a foundation for computer science*, Addison-Wesley Publishing Company, 1988.
- [8] Kleinrock, L., *Queuing theory, Volume I: Theory*, John Wiley & Sons, Nj, 1975.
- [9] Nutaro, J. J. (2011). *Building software for simulation: theory and algorithms, with applications in C++*. John Wiley & Sons.
- [10] Pritsker, A.A.B., *Introduction to Simulation and SLAM II*, Systems Publishing Corporation, West Lafayette, Indiana, 1984.
- [11] Schriber, T.J., *Simulation using GPSS*, John Wiley, 1974.
- [12] Varga, A. (2001, June). *The OMNeT++ discrete event simulation system*. In Proceedings of the European simulation multiconference (ESM'2001) (Vol. 9, No. S 185, p. 65). sn.

Submitted: April 4, 2015.

Accepted: May 29, 2015.

THE PERSPECTIVE OF HIGH-TEMPERATURE SUPERCONDUCTIVITY ELECTRICAL EQUIPMENT APPLICATION FOR TRACTION POWER SUPPLY AND THE PROBLEMS OF ELECTROMAGNETIC COMPATIBILITY

M.P. Badjor, Yu. M. Inkov

D. Sc. Habil., professors

MSURE (MIIT)

Case study

DOI: 10.7251/JIT1501033B

UDC: 621.31.027.2

ANNOTATION

EMC analysis of superconducting and traditional electrical equipment, study of the laws of the electromagnetic interaction, the nature of the mutual influence of the parameters and operation of electrical equipment, as well as search of protection and types of arrangement of electrical equipment, in which interference will not cause disruption to the interacting elements.

The analysis of the world tendencies in the development of the electrical engineering and power engineering, including the ones for the electrified transport, shows that one of the important tendencies in the nearest future will be the employment of the high-current applied superconductivity. It is well-known, that the new opportunities are opened by the ready for the mass production high-temperature superconductors of the second generation, capable of operating at temperatures up to the temperature of the liquid nitrogen, which is a hundred times more economical than the helium temperatures. As it is estimated, after the introduction of the high-temperature superconductors of the second generation the cost of the high-temperature superconducting wires will be comparable to the cost of the resistance wires. This means that in the nearest future the development of the new superconducting electrical equipment will be started, which will excel the conventional electrical equipment at physical, technical and commercial

characteristics. Consequently, nowadays it is becoming more and more challenging the scientific research of the development, testing of models and production prototypes of various electrical equipment on the basis of the high-temperature superconducting materials, including cable power lines, transformers, electric motors, reactors and energy storage units.

The introduction and employment of the superconducting technologies and new high-temperature superconducting electrical equipment in locomotive and stationary energetic will enable to improve the traction electrical equipment safety and efficiency, to reduce the capital and maintenance costs, to provide the energy saving.

The problem of the superconducting electrical equipment employment on the transport objects is closely connected with the necessary solution of the parallel scientific, technological and design problems. One of them is the problem of the analysis of the electromagnetic interaction of the superconducting electrical equipment external fields with other types of equipment and with the conventional equipment as well. This problem is of special importance for the perspective transport vehicles, which size is more or less limited and where it is difficult to apply the easiest protection means from the external magnetic fields (EMF) – distance protection.

The advantages of the superconducting electrical equipment can be clearly seen at the increased capacity, that's why it is more reasonable to produce power (traction) equipment as superconducting and auxiliary equipment for providing transport vehicle needs (electric motors for compressors, ventilators, pumps and the electric drive control units & etc.) can be produced non- superconducting but conventional.

The problem of the electromagnetic compatibility, including the transport systems, was investigated in the terms of the conventional sources (static semiconducting converters, electrical machines, switchgear & etc.) and interference receptors (means of communication and information). The perspective of the improvement of transport means energy and technical-economic properties due to the application of the superconducting electrical equipment brings about a new aspect of the electromagnetic compatibility – the problem of the electromagnetic compatibility of superconducting and conventional electrical equipment. One of the basic questions to be investigated in the framework of the electromagnetic compatibility of superconducting and conventional electrical equipment is the study of the laws of the electromagnetic interaction, the nature of the mutual influence of the parameters and operation of electrical equipment, as well as the search of protection and types of arrangement of electrical equipment, in which interference will not cause disruption to the interacting elements.

At DC railway substations in the years to come a wide variety of superconducting electrical equipment will be applied, including non-resistance smoothing inductors, produced on the basis of high-temperature superconductivity, which will considerably increase the energy and technical properties of the substation smoothing equipment.

For the analysis and improvement of the electromagnetic and ecological conditions the methods of electromagnetic compatibility of superconducting and conventional electrical equipment in the linear focus has been worked out, which allows to analyse in general the impact of the conventional electrical equipment electromagnetic fields on the differential and integral properties of the superconducting electrical equipment.

The biggest part of the auxiliary conventional electrical equipment consists of the electrical machines and electromagnetic devices with a close air gap ferromagnetic wire, which considerably complicates the theoretical investigation of the impact of the superconducting electrical equipment external magnetic fields on the technical characteristics of the auxiliary generators and electric drive motors with an electric drive control system. The superconducting coil is supposed to be the source of the external electric fields; it is also the main element of the superconducting electrical equipment.

The investigation of the electromagnetic coupling of superconducting and conventional electrical equipment requires the development of the mathematical apparatus of analysis. At the initial stage of investigation it is worth while applying the analytical image of coupling, based on the range of assumptions allowing analysing in general the impact of each parameter of the coupling elements. The apparatus of numerical procedures of magnetic field calculations can be applied for such type of analysis.

The theoretical investigations of the dependencies of the electromagnetic coupling of the superconducting and conventional electrical equipment for the defining the conditions of their joint usage includes mathematical physics methods for the solution of the boundary problems, numerical procedures of magnetic field calculations on the basis of the secondary source concept, applied with the help of the iteration methods, numerical procedures of extremal problems solution.

The produced analysis of the transient operation mode of the superconducting electrical equipment as a part of the traction power supply and a perspective transport vehicle demonstrates that the process time is long enough independently of the type of the transport vehicle, its application, capacity, running conditions & etc. It gives the opportunity to employ the approximation for the analysis of the impact of the superconducting electrical equipment external magnetic fields on the conventional electrical equipment. The given approximation is based on the assumption of the superconducting electrical equipment external magnetic fields, as the field of constant current.

The three-dimensional non-linear numerical model of the electromagnetic coupling of the superconducting and conventional electrical equipment is worked out. It is based on the assumption of the ferromagnetic wire magnetization field as the field of the equivalent secondary sources of the surface and volume fictitious magnetic charges. The model enables to calculate the induction of the resultant magnetic field (the field of primary sources – current in the coils – and ferromagnetic wire magnetization fields) in the arbitrary point of the unlimited computational domain. This is very comfortable while analysing the coupling of several sources of the external magnetic fields and several sources under their influence. The model enables to calculate the induction in the air gap of the conventional electric equipment and its integral parameters at the non-linear characteristics of ferromagnetic wire, the longitudinal size limits and arbitrary space orientation of the conventional electric equipment.

According to [2], the standing wave of the transmitting antenna (waveguide) presents to be a complex of the continuously changing positive and negative charges with a wave length λ . These charges polarize the environment causing the appearance of volume positive and negative charges, which follow each other along the waveguide from the source to the receiver.

In the system of ETL the complex of the continuously changing positive and negative charges spaciouly remind the eddy-current toroids and move along the waveguide. The figure 1 represents this process. The toroid inner diameter is close to the wire diameter and the outer diameter is defined by the frequency, voltage magnitude and charge density inside the eddy, or, in other words, the amperage of the electric induction current.

Each of the moving volume charges possesses its own magnetic field as shown on the figure 1a and the polar extensions of these dynamic magnets in the current nodes are similar. The figure 1b illustrates the toroids 1, 2 and 3, which represent the increase of volume charges (the increase of current antinode) and corresponding magnetic fields as the blind current and the transmitted power grow.

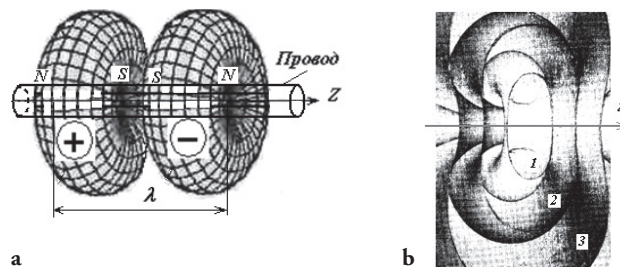


Figure 1. The models of charge and magnetic fields movement along the conductor resonance single-conductor ETL

The toroids surface 1, 2, 3 &etc. may be present-ed as the complex of “equipotential” magnetic power lines.

These magnetic fields pack each volume charge but, on the other hand, provide the movement along the wire due to mutual repulsion of the magnetic poles and the repulsion of the whole pack from the energy source.

The generating of such toroid eddies of opposite charges with inherent magnetic fields provides according to Tesla [3], *permanent energy transmission* from the source to the receiver.

Consequently, in the case of ETL we deal with dilatational waves which move not across the wire section but along it without entering it. It can be concluded, that wire resistance and its section are not important for ETL, and as its conductor it may serve thin steel wire or cable in insulation sleeve or fixed on the high-voltage insulators, as Tesla did [3].

The principle of local variable degree of unknown search field quantization is suggested for the improvement of the process of the iterative search of secondary field sources density distribution, which allows reducing the calculation time and the necessary ECM memory while preserving the accuracy of calculations. This principle is employed to construct the computer procedures for the systems with a great volume of ferromagnetic material and a close air gap.

The efficient protection measure of the conventional electric equipment from the electromagnetic coupling with superconducting electric equipment is electromagnetic screens [1].

The screening effect of the electromagnetic screen is that the electromagnetic field penetrates the screen wall and generates charges there or induces currents, which fields overlap the primary field and fully or partially compensate it.

The value of the screening effect is the screening coefficient, which is defined by the ratio of inside the screen field strength to outer field strength when the screen is absent. For magnetic field

$$\underline{Q} = \underline{H}_{IN} / \underline{H}_{OT} \tag{1}$$

In practice it is often used for calculations the term “attenuation coefficient”, which is defined as logarithm of the ratio of inner and outer field strengths

$$a_s = \ln(1/|\underline{Q}|), \text{ Hn} \quad \text{or} \quad a_s = 20 \lg(1/|\underline{Q}|), \text{ dB} \tag{2}$$

The permanent and variable fields are differentiated, the variable fields are divided into quasi-static (slowly changing) and electromagnetic (quickly changing).

Any quasi-static field change reveals simultaneously everywhere that is why the instantly perceived field picture corresponding to a definite instant value of voltage or current always coincides with the static field picture created by the direct current or voltage of the similar value. A quasi-static field may be presented as a time superposition of static fields with a similar space distribution $E_v(x, y, z)$ или $H_v(x, y, z)$, which in each case differ in strength only by a definite constant multiplier. If the receiver is located in the immediate presence from the radiation source in the so called near zone, it receives the constant (space fixed) quasi-static field. In the near zone the field changes, grows or diminishes in time simultaneously in all the points. In the far distance from the radiation source the receiver is located in the so called far zone. Independently from the radiation source design the non-constant electromagnetic wave field prevails in the far zone.

The near zone is defined not only by the distance between the source and the receiver but by the field change speed. In the time domain near or quasi-static zone is the space, which length l is so, that the field

rise time T_H exceeds the time of the electromagnetic wave crossing the length l . In the frequency domain the near zone is the space, which length is shorter the wave length ($l < \lambda$).

The difference between the near and far zones may be formalized mathematically by employing the Hertz dipole field in the spherical coordinate system (Fig. 2).

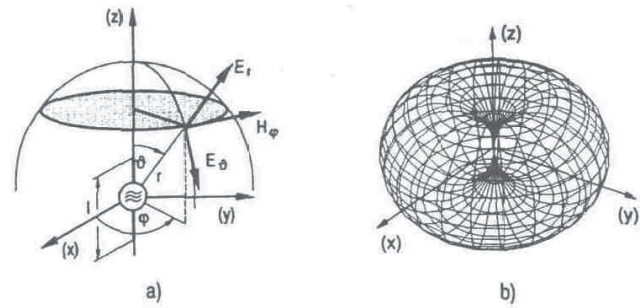


Figure 2. Hertz dipole in the spherical coordinate system (a) and the corresponding power lines of the electric and magnetic fields in the near zone (b)

The calculation of the Maxwell’s equations in the frequency domain gives the following expressions for the electric-field vectors illustrated in Fig. 2 [1]:

$$\underline{E}_g = \frac{I_m l Z_0 \lambda \sin \vartheta}{j \cdot 8\pi^2 r^3} \left[1 + j \frac{2\pi}{\lambda} r + \left(j \frac{2\pi}{\lambda} r \right)^2 \right] e^{-j \frac{2\pi}{\lambda} r} \tag{3}$$

$$\underline{E}_r = \frac{I_m l Z_0 \lambda \cos \vartheta}{j \cdot 4\pi^2 r^3} \left[1 + j \frac{2\pi}{\lambda} r \right] e^{-j \frac{2\pi}{\lambda} r} \tag{4}$$

$$\underline{E}_\varphi = \frac{I_m l \sin \vartheta}{4\pi r^2} \left[1 + j \frac{2\pi}{\lambda} r \right] e^{-j \frac{2\pi}{\lambda} r} \tag{5}$$

where I_m , - AC amplitude value; l – maximum distance between dipole charges; Z_0 – vacuum wave impedance (further $w/c = 2\pi/\lambda$, where c - light speed in vacuum). The factor $e^{-j \frac{2\pi}{\lambda} r}$ describes phase shift angle.

The equations given above are not representative, but they are easy to interpret, if we stick to two limiting cases – near and far zones.

If to assume $r \gg 2\pi/\lambda$ only the members with great exponents may be considered in (3 - 5), and the equations are simplified:

$$\underline{E}_g = \frac{I_m l Z_0 \lambda \sin \vartheta}{j \cdot 8\pi^2 r^3} \left(j \frac{2\pi}{\lambda} r \right)^2 e^{-j \frac{2\pi}{\lambda} r} \quad (6)$$

$$\underline{E}_r = \frac{I_m l Z_0 \lambda \cos \vartheta}{j \cdot 4\pi^2 r^3} \left[j \frac{2\pi}{\lambda} r \right] e^{-j \frac{2\pi}{\lambda} r} \quad (7)$$

$$\underline{H}_\varphi = \frac{I_m l \sin \vartheta}{4\pi r^2} \left[j \frac{2\pi}{\lambda} r \right] e^{-j \frac{2\pi}{\lambda} r} \quad (8)$$

Due to different exponent y , the component r of \underline{E}_r may be neglected in comparison to \underline{E}_g , so that finally only the vector \underline{E}_g and \underline{H}_φ are left. These

vectors are perpendicular to each other and the direction of the wave propagation. They oscillate in-phase and their attitude in time and space is constant:

$$\underline{E}_g / \underline{H}_\varphi = Z_0 = \sqrt{\mu_0 / \varepsilon_0} \quad (9)$$

The active impedance Z_0 is called the wave impedance of vacuum.

In the immediate proximity of the antenna ($r \gg 2\pi/\lambda$) (near zone) both the second and the third members of (3-5) are significantly less than one, and these equations are simplified:

$$\underline{E}_g = \frac{I_m l Z_0 \lambda \sin \vartheta}{j \cdot 8\pi^2 r^3} e^{-j \frac{2\pi}{\lambda} r} \quad (10)$$

$$\underline{E}_r = \frac{I_m l Z_0 \lambda \cos \vartheta}{j \cdot 4\pi^2 r^3} e^{-j \frac{2\pi}{\lambda} r} \quad (11)$$

$$\underline{H}_\varphi = \frac{I_m l \sin \vartheta}{4\pi r^2} e^{-j \frac{2\pi}{\lambda} r} \quad (12)$$

According to [1] it may be deduced the ratio $\underline{E}_g / \underline{H}_\varphi$

$$\underline{E}_g / \underline{H}_\varphi = Z_0 \lambda / (j \cdot 2\pi r) = Z_{0E} \quad (13)$$

The impedance Z_{0E} is being capacitive

$$[Z_c = 1/(j\omega C)] \text{ at } r \gg 2\pi/\lambda \text{ or } \lambda/2\pi \gg 1$$

$$|Z_{0E}| > Z_0 \quad (14)$$

The specific energy in the near zone of the high-impedance (electric) field has the prevailing electric nature, i.e.

$$w(r) = w_{\text{эл}}(r) = \frac{1}{2} \varepsilon E^2 \quad (15)$$

For the field in the proximity of a small circuit with current (FitzGerald dipole), structurally dual equations will be got in the coordinate system J and j, the calculation of which produces the active wave impedance for the far zone $Z_0 = 377 \Omega$, and for the near zone:

$$\underline{Z}_{0H} = jZ_0 \cdot 2\pi r / \lambda \quad (16)$$

The wave impedance \underline{Z}_{0H} of the loop antenna

near zone is of the inductive character ($r \gg \lambda/2\pi$ or $\lambda/2\pi \gg 1$), and

$$|\underline{Z}_{0H}| \gg Z_0 \quad (17)$$

It is the characteristics of the low resistance field, i.e. the magnetic field in the proximity to the loop antenna. The specific energy in the near zone is of the magnetic nature:

$$w(r) = w_M(r) = \frac{1}{2} \mu H^2 \quad (18)$$

In the far zone the vectors of the electric and magnetic field strength are directed at the right angle to each other and to the propagation direction. While the electric field in the near zone remains transversal, then the magnetic field contains the additional \underline{H}_r .

If the condition $l < \lambda$ is not satisfied, then it is necessary to use not the dipole equation but the equation of electric long lines.

Figure 3 illustrates the examples of quasi-static fields in the near zone.

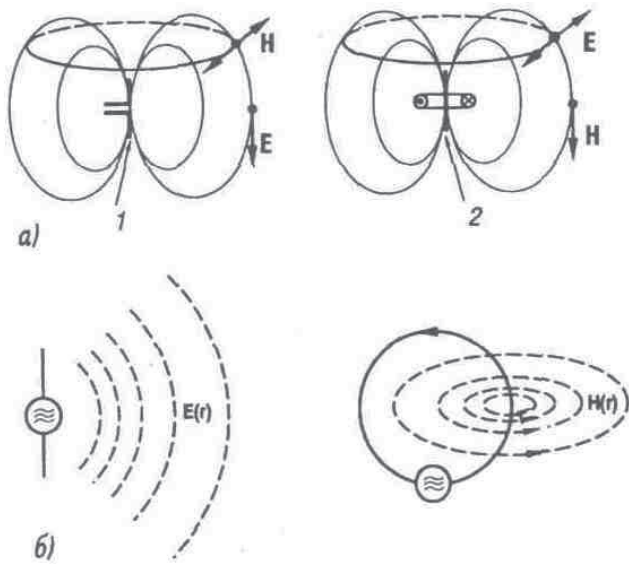


Figure 3. The ration of Hertz dipole and FitzGerald dipole (a) and schematic representation of the electric and magnetic fields in the near zone (b):
 1 – electric field ; 2 – magnetic field

With the increasing distance from the whip antenna the value of the wave impedance decreases at the rate 20 dB/decade from great to small values and asymptotically approaches the value of the wave impedance of vacuum at a great distance. On the contrary, the wave impedance of the loop antenna at first increases at the rate 20 dB per decade and then also asymptotically approaches the value of the wave impedance of vacuum at a great distance (Fig. 4).

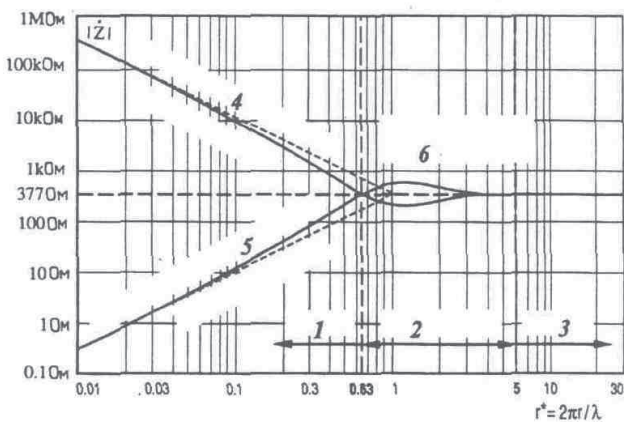


Figure 4. The device wave impedance depending on the normalized distance from the source ($r = 2r/\lambda$): 1 – near zone; 2 – transition zone; 3 – far zone; 4 – high-impedance electric field; 5 – low-impedance magnetic field; 6 – electromagnetic wave field

These distance-based wave impedances are used at the attenuation coefficient calculations by the Schelkunov’s method.

The electric field shielding by the closed conducting screen (without cracks) is infinitely large. Such screen is called Faraday cage. For the electric fields that change in time at a great rate the attenuation coefficient has a finite value. For the normal field components the following equations may be obtained by the Gauss’s law:

$$E_{H.BH} = 0 \text{ and } E_{H.BIII} = \rho_s / \delta_0 \tag{19}$$

where ρ_s – surface density of the displaced charges.

For the tangential components it is followed from the said above that $E_{K.BH} = E_{H.BIII} = 0$. Finally, it should be mentioned, that the dielectric shells exert a certain shielding effect on the electrostatic fields. In the same way as the magnetic flux passes mainly through the circuit with high magnetic conductivity (relative magnetic permeability μ_r), the electric field flux γ passes through the dielectric with high dielectric conductivity (dielectric permittivity ϵ_r).

With a large ration of the wall thickness d to the shell diameter D due to the refraction of the electric field lines on the boundary the electric flux mainly occurs in the screen wall. The attenuation coefficient is calculated by Kaden:

$$a_E = \ln(E_{BIII} / E_{BH}) = \ln(1 + 1,33\epsilon_r d / D) \tag{20}$$

The noticeable shielding occurs only at thick-walled screens with high dielectric permittivity $\epsilon_r, d \gg D$.

The following ratio of tangential E_K and normal E_H components of the electric field strength can be obtained on the basis of the Gauss’s law and induction laws:

$$E_{K1} = E_{K1} \text{ u } E_{H1} = E_{H2} = \epsilon_{r2} / \epsilon_{r1}$$

The magneto-static fields can be shielded with the help of the ferromagnetic shells with high magnetic permeability in the same way as the electrostatic fields with the help of the dielectric screens with high dielectric permittivity. Due to the refraction of the magnetic field lines on the surface boundary

of the thick-walled screens from the materials with high magnetic permeability the magnetic flux mainly passes in the screen wall.

The attenuation coefficient is calculated in the following way:

$$a_H = \ln(H_{BIII} / H_{BH}) \approx \ln(1 + 1,33\mu_r d / D)$$

In the absence of currents in the screen the following ratio of normal and tangential components of the magnetic field strength on the screen surface can be obtained due to the Gauss's law and flux continuity law

$$H_{K1} = H_{K2} \quad \text{and} \quad H_{H1} / H_{H2} = \mu_{r2} / \mu_{r1}$$

The shielding of the quasi-static electric alternating fields works in the same way as of the electrostatic fields due to the redistribution of charges. However, if in the electrostatic field the attenuation coefficient is infinitely large, then in the alternating field the frequency growth causes a phase shift, which defines the final value of the attenuation coefficient. This effect becomes noticeable at very high frequencies. Actually the attenuation coefficient is supposed to be infinitely large at the quasi-static fields. The same boundary conditions are used as for the electrostatic field. The actual screens, for example the device cases, have gaps, cracks. If the separate screen walls are not connected to each other electrically, then the difference of potential arises and the screen has almost no effect. The shielding elements should be connected together while shielding from electrostatic fields.

The electromagnetic impact is possible through the cracks between the screen elements. This impact can be reduced by using labyrinth seals. At high frequencies, the screen elements should have numerous galvanic contacts for the currents affecting the equipotential bonding could follow the shortest path. While the fully closed metal screen provides field absence inside it without screen grounding, the application of the shadow effect of three separate shielding sheets requires their grounding.

The harmful effects of gaps in the closed screens can reduce the role of the screen to the shielding ef-

fect of a single screen elements plate. The higher the screen material conductivity is, the more are the currents in the screen at the similar induction electric field strength, and the higher is the attenuation coefficient. As the static magnetic field cannot induct currents, the non-ferromagnetic shells for constant magnetic fields ($f = 0$) have no shielding effect. On the other hand, the attenuation coefficient of quasi-static magnetic field tends to infinity with the frequency increase. This tendency has a limit on the frequencies where, along with the quasi-static magnetic field the magnetic field of displaced currents (electromagnetic waves) must also be taken into account. With increasing frequency we can no longer ignore the effect of displacement currents. The impact of the displaced currents can't be ignored any longer due to the frequency increase.

To manufacture the screens it is used the materials, which have high conductivity for the existing fields fluxes and which are able to create an opposing magnetic field due to the induction. The screen from good conductive metals and ferromagnetic materials are used most frequently. The comparison of the characteristics of the two screens with the same thickness and made of iron and copper explains the features of their shielding action (Fig. 5).

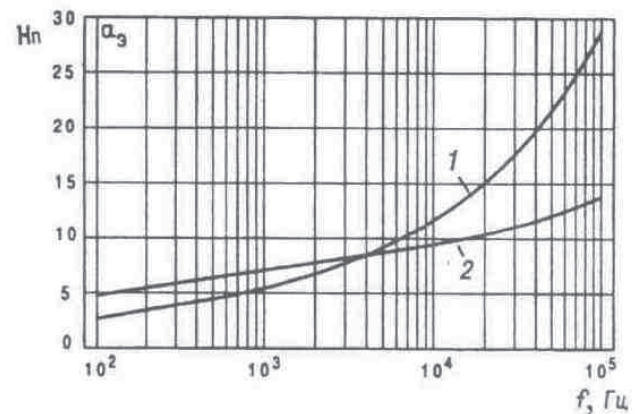


Figure 5. The ration of attenuation coefficient a_g of the magnetic field of the cylindrical screen from frequency f : 1 – for iron screen ($r_0 = 5$ m, $d_0 = 0,1$ mm, $\sigma = 7 \cdot 10^6$ Cm/m, $\mu_r = 200$); 2 – for copper screen ($r_0 = 5$ m, $d_0 = 0,1$ mm, $\sigma = 58 \cdot 10^6$ Cm/m, $\mu_r = 1$)

In the range up to 100 kHz, the penetration depth of the electromagnetic field is greater than the thickness of the screen wall, and a material with high conductivity has a higher attenuation coefficient. The shielding effect here is based only on the screen attenuation, which acts as a shorted turn.

The analytical calculation of the shielding effect of electromagnetic screens requires the solution of Maxwell's equations for the areas inside and outside of the screen, and also in its wall. The result of the solution is the values of the shielding coefficient or attenuation coefficient. This method provides a deeper, beyond the known approximation formulae, understanding of the principle of electromagnetic screens and the screen operation becomes available for accurate quantitative assessment. However, this method is mathematically intensive, with approximate formulae the screens calculation is possible with the help of a grid method. The attenuation graphs for the cabin with an edge length 2 m calculated by this method are presented in Fig.6.

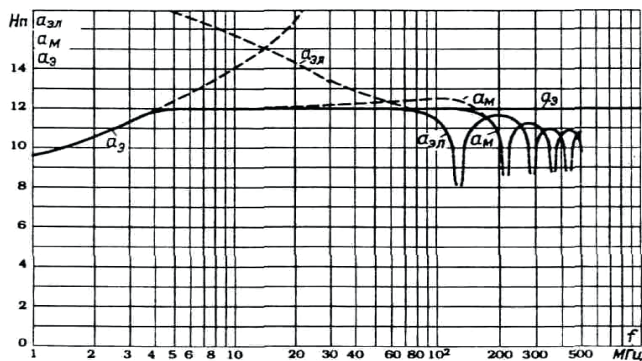


Figure 6. The attenuation coefficients of the measuring cabin with an edge length of 2m and copper foil screen thickness of 0.1 mm.

It should be noted that the spherical screens in practice are very rare; more often the question arises whether it is possible to calculate the shielding effect of the rectangular screening cabin. Taking into account the significant difficulties, it should not be tried to calculate the attenuation coefficient of the fields in the rectangular cabin accurately and analytically but it should be replaced with the sphere the radius r_0 of which equals to half of the length of the cabin edges. Due to the edge effect the shielding effect near the cabin corners is weaker as the current in the screen wall should pass the longer way, which results in a high active and inductive voltage drop

along the wall. The edge effect can be smoothed by the rounding of corners and increasing the wall thickness near the corners.

The attenuation coefficient for the quasi-static magnetic fields theoretically reaches high values, however, in practice due to the door gaps, lattice ventilation widows, power supply input & etc. it is limited.

The method of calculation of the shielding effect of multilayer cylindrical and flat ferromagnetic (magneto static) screens in the linear approximation is based on the recurrence relations, which allows calculating the magnetic field induction in the field behind the screen for an arbitrary number of layers of the screen. Multilayer cylindrical screens provide a higher ratio of the shielding effect than single-layer screens of similar thickness with practically a very slight increase in the weight and dimensions. The cylindrical screens are more effective than the flat ones. Flat multilayer and single-layer screens of equal thickness provide almost the same shielding effect.

The principles of the numerical calculation of the ferromagnetic screen with a complex shape are based on the fact that the screen can be represented as a set of discrete elements. The size and position of each element are defined on the basis of the condition of minimization of the magnetic field energy in the given volume (shielded area), due to this there arises a possibility to synthesize a complex shape screen. The active screens synthesizing method is based on the gradient methods for solving extremal problems and allows to calculate the geometrical dimensions and the space position of axisymmetric shielding coils with rectangular cross section for superconducting coils of the similar geometry, while maintaining the predetermined intensity of the entire system.

The areas of numerical modelling are identified and the nonlinear numerical models are worked out, what allows analyzing the interaction of the conventional and superconducting electrical equipment electric field sources with the unlimited area of the magnetic field distribution and the lack of symmetry of the field distribution in space. The algorithm and software package are developed to determine the ef-

fect of electromagnetic fields on the integral parameters of conventional and superconducting electrical equipment. There have been conducted the research and the definition of the parameters and sizes of the superconducting inductive reactors of the smoothing filters for traction substations, which minimize the space occupied and ensure the best application of superconducting material at a given power intensity.

The obtained results can be considered as the basis of the research area related to electromagnetic compatibility of power superconducting and conventional electrical equipment for traction power supply and perspective vehicles.

REFERENCES:

- [1] Badjor, M.P. (2002). Electromagnetic compatibility. Manual for Higher educational institutions. - M.: Transpot, 640 p.
- [2] Strebkov, D.S. (2005). High-temperature quasi-superconductivity of the conductors for capacitive currents. Scientific papers of RAAS №4, P.56-58.
- [3] Tesla, N. (1999). World System of wireless Transmission of Energy. Telegraph and Telephone Age, October 16.1927. Published in a book: Nikola Tesla. Selected works. Articles. Beograd, p. 280.

Submitted: April 30, 2015.

Accepted: May 8, 2015.

SAFETY AND RISK MANAGEMENT

V.M. Lisenkov, P.F. Bestemyanov

D. Sc. Habil., professors

MSURE (MIIT)

Case study

DOI: 10.7251/JIT1501042L

UDC: 331.45/46:656.2

Abstract: The article is devoted to the problem of creating a system of security and risk management. Formulated in relation to the process of movement of trains:

- factor of safety of the train
- the probability of traversing the trains on a particular route without transfer of its movement in a dangerous condition;
- a measure of risk of the transfer movement of the train in a dangerous state
- transition probability of motion in a dangerous state when the movement of trains on a given route.

The objectives of security and risk management are: to provide values of their indicators are not worse than normative, namely, the values of the performance security shall be not less than the normative, and the values of indicators of risk - not more than normative. Proposed functional framework and organizational structure for the management of safety and risks.

Keywords: safety index, a measure of risk, a dangerous condition, standard indicators of safety and risk.

SAFETY AND RISK INDEX

Safety and risk management gain particular significance when managing responsible technological processes (RTP), which lack of security leads to great financial losses and loss of life.

RTP is distinguished by two groups of states – dangerous (DS) and non-hazardous (NS). Transitions of RTP states from NS to DS are accompanied by the emergence of damaging factors whose impact on the external environment objects and RTP objects causes loss and damage.

With this consideration in mind we can formulate the following definition of security RTP - this characteristic of RTP not to move from NS to DS during some estimated time. Transitions of RTP into DS are random events, so the measure of safety, that would numerically estimate the security, must be a probabilistic observation. Thus, safety indicator – is the probability that the RTP won't turn from of NS to DS for the estimated time. Obviously, the larger the indicator, the higher is safety.

Practically, it is important to know what the minimum level of safety should be, for losses and damages not to exceed to an estimated level. This minimum level of safety normalizes and the actual levels of safety should not be smaller.

The word risk, according to the norms of the Russian language [1, 2], means the possibility of occurrence of an unwanted event. In this case, when considering RTP, the undesirable event is the transition of RTP into a dangerous state. With this consideration in mind, linguistically correct is the following definition of risk transition of RTP from DS: risk transition of RTP into DS - is the ability to turn into RTP from NS into DS.

Taking into account that the transition of RTP into DS is random, risk index as well as safety index, should be of probabilistic nature, that is: risk rate transition of RTP from NS into DS – is the probability of transition of RTP from NS into DS.

Obviously, the larger the risk transitions of RTP into DS, the lower is safety. Therefore, in this case the maximum value of risk index is limited. Such index value is called normative.

Transitions of RTP into DS occur under the influence of dangerous destabilizing factors (DDF) in the form of dangerous hardware failures, dangerous errors in software and dangerous mistakes of the personnel. DDF events are random and undesirable. Therefore, on the analogy of the above indexes for RTP, it is possible to formulate a number of additional indexes to assess the safety and risks of the individual components of RTP – technical equipment of specific functionality, software and personnel:

- safety index of technical equipment is the probability that the technical equipment won't have any dangerous failures during estimated time;
- risk index of dangerous failure is the probability of occurrence of a dangerous failure during the estimated time.

In the study [3] there are other types of indexes, including other types of RTP, for example, train movement.

With regard to the train movement:

- safety index of the train movement is the probability of a train going on a certain route without transition of its movement into a dangerous state;
- risk index of the train transition into a dangerous state is the probability of transition of train movement into DS when going on a scheduled route.

Since the transition of trains in the DS ends with loss and damage, it is possible to use the following indexes:

- risk index of losing M_i during train movement is the probability of losing M_i due to the transition of movement into the DS on a scheduled route;
- risk index of damaging N_i during train movement is the probability of damaging N_i due to the transition of train movement into the DS

on a scheduled route.

The study shows all possible safety indexes and calculations in respect to the transportation process and trains movement.

In the future, in order to reduce the text instead of “probability of transition RTP and NS into DS” there will be used - the transition probability of RTP into DS.

OBJECTIVES AND MANAGEMENT PROCESSES.

The objectives of the safety and risk management of RTP are: to provide the index values just as well as the standard, that is the index values of safety should not be less than the standard, and the values of risk indexes should not be more than the standard. At that there should be observed resource limits.

With regard to this RTP as the train movement on a scheduled route, the purpose of safety management is to ensure the safety index movement is not lower than the standard value. As for the risk management purposes, they provide safety index movement does not exceeding the standard values.

Process safety and risk management consists of changing their indexes until you reach the purpose of management. Thus special techniques are used: endurance, structural, parry CRF.

To implement the safety and risk management process of RTP there must be the complex of functionally related hardware, software and personnel, which are capable of implementing the above methods.

Safety and risk management is possible only for certain standard values of safety and risk of RTP as a whole and its individual functional components. At the stage of design and production of technical equipment, these standard values should be provided and confirmed by a safety certificate. In the process of operation of RTP there should be monitored the actual values and risks. If the actual values are worse than the standard, there should be developed and implemented measures for the elimination of this situation.

In order to do this efficiently, it must be based on well-developed:

- regulatory framework;
- functional baseline;
- organizational structure;
- legal and regulatory framework;
- technological base;
- scientific methodological basis;
- personnel framework;
- conceptual framework.

The more perfect the listed frameworks are, the smaller amount of resources will be required to achieve safety and risk management.

Features of construction of these frameworks are discussed below.

THE LEGAL FRAMEWORK OF SAFETY AND RISK MANAGEMENT.

Legislative framework consists of three Federal Laws of the Russian Federation

- «Consumer rights protection»
- «Technical Regulation»
- «Railway transport in the Russian Federation».

The first two laws form the legal framework of safety management systems and risk of RTP for any functional purpose, the third forms the legal framework of safety and risk management only on the railways.

In the «Consumer rights protection» it is claimed: «This law regulates relations between consumers and employers, sets out the rights of consumers to purchase goods (work, services) of good quality, the safety of their life and health ... ».

Thus, according to this law, the services for passengers and cargo must be safe especially to the consumers of these services, i.e. concerning passengers and not those who provide these services, i.e. railways.

According to the Federal Law about «Technical Regulation»: «regulates relations arising in: development, accepting, application and enforcement of

mandatory requirements for products or related processes of design (including research), manufacturing, construction, installation, commissioning “. According to Article 7 of the Law, mandatory requirements include requirements of mechanical, thermal, radiation security, etc.

According to this law, “the harm risk degree” should be taken into account in determining the characteristics and parameters of technical means.

In addition, and in accordance with the Federal Law about “Consumer Rights Protection”, the mandatory requirement is the requirement of products and services safety.”

According to the Federal Law about “Railway Transport in the Russian Federation” the mandatory requirement is the requirement to ensure the absence of “unacceptable risk” accidents occurrence and health injury of citizens, environmental damage, and property of individuals or legal entities.

Thus, according to the Federal Law about “Consumer Rights Protection”, “Railway Transport in the Russian Federation”, “Technical Regulation”, which form the legal framework of safety and risk management, the mandatory are:

- security requirement of products and services in regard to passengers, the environment, the goods transported, the transport system;
- quantitative (probabilistic) requirement of “risk level” of harm to consumers of transport services and the environment and to ensure that this “level” is not more than the “acceptable” value, i.e. not more than the standard value.

FUNCTIONAL BASELINE MANAGEMENT

The functional baseline below refers to a set of functions that must be performed in the management process to achieve the most effective security and risk management. These features include:

- specification and justification of a complete range of safety and risk performance; in solving certain problems there can only be used a part of the indexes;

- task of harmonized between each other normative values of the indexes of transport safety in general, traffic safety, safety of hardware operation and software, operators, as well as the standard values of all types of risks. Depending on the solvable problem operation it may be required knowledge of the standard values of the indexes;
- specification of the parameters and characteristics of hardware and software, as well as the professional characteristics of operators, which provide normative values of their safety and risk performance;
- development of classifiers of dangerous destabilizing factors on the basis of analyzing the causes of the transition into dangerous states and on the basis of special methods of identification of dangerous hardware failures;
- frequency response analysis of CRF;
- specification of safety indexes and risks of complex devices via the CRF probability, for example, by the method of event tree analysis;
- efficiency analysis of ensuring methods of standard values of safety and risks;
- provision of given safety parameters and characteristics indexes at all stages of their life cycles;
- certification of technical means in terms of the safety of operation;
- licensing of the company performance in view of its ability to produce hardware with planned safety indexes of functioning (presence of the required technological base, personnel, methodological support, etc.);
- control of the use of certified equipment;
- a statistical analysis of operational safety indexes of trains movement, operation of technical equipment and operators, the identification of the CRF and their occurrence;
- forecasting possible changes in safety and risks indexes due to changes in operating conditions of technical equipment, production technology, etc. ;
- programs development of preventive operational measures aimed at preventing the CRF and the transition into dangerous states;
- development of long-term programs of providing normative safety and risks values.

If at least one of these functions won't be accomplished during the performance, the process of safety and risk management won't be as effective as possible. But there may be cases where the accomplishment of all these functions is not necessary.

ORGANIZATIONAL STRUCTURE OF CONTROL FACILITIES.

For performance of all listed above functions it is necessary to have a set of the organizations, enterprises of the technical means and the personnel, which are in a functional interrelation, which it is possible to call a control system of safety and risks. The system has to possess a certain organizational structure. The modern System has the three-level hierarchical structure including:

- federal,
- branch and
- corporate (separate corporations, organizations, enterprises, companies, etc.) levels.

The Federal Assembly, the President and the Government of the Russian Federation refer to the Federal hierarchical level. According to the Federal law "On technical regulation" they have to:

- adopt the laws of the Russian Federation relating to area of safety of production and services, including safety of rail transportation;
- accept the technical regulations in the form of Federal laws of the Russian Federation, decrees of the Russian President and resolutions of the Government of the Russian Federation defining the relations between all participants of transportation process arising at safety of transportations and freights.

To the branch hierarchical level of System refer the following:

- the ministries, the state committees, agencies the main function of which is assistance to execution of the main functions of bodies of federal level at management of safety;
- the state control (supervision) authorities for observance of requirements of technical regulations;
- national authority of the Russian Federation on standardization, technical committees on standardization;

- body for certification, test laboratories (centers);
- body for accreditation of participants of transportation process.

Governing bodies of branch level have no right to publish normative documents of Federal level in the field of management of safety, obligatory for execution.

The main function of structural components of System of corporate level (corporations, the companies, the enterprises, etc.) is ensuring standard values of indicators of safety and risks at various stages of life cycles of technical means and the personnel by selection of the corresponding characteristics and parameters of technical means and the personnel.

The functional and organizational structure of System of each organization is defined by its concrete functions at safety of transportations.

Thus, the control system of safety and risks is the centralized state control system for traffic safety of trains as the state establishes standard indicators of safety and risks and exercises the supervision of application only of the technical means certified on indicators of safety.

REGULATORY LEGAL BASE OF SYSTEM

Part of process of management of safety and risks is technical regulation, i.e. legal regulation of the relations in the field of establishment, applications and executions of obligatory requirements to production or to related design processes (including researches, productions, constructions, installation, adjustment, operation of storage, transportation, realization and utilization, and also in the field of establishment and application on a voluntary basis of requirements to production, design processes, including researches, productions, constructions, installation, adjustment, operation, storage, transportation, to realization and utilization, performance of work or rendering services and legal regulation of the relations in the field of an assessment of compliance of production to obligatory requirements).

The regulatory legal base of technical regulation is formed by:

- technical regulations;
- national standards;
- sets of rules.

The technical regulations – the document which is accepted by the international treaty of the Russian Federation ratified in the order established by the legislation of the Russian Federation, or the intergovernmental agreement concluded in the order established by the legislation of the Russian Federation, either the Federal law, or the decree of the President of the Russian Federation, or the resolution of the government of the Russian Federation. It establishes requirements to objects of technical regulation (to production, including buildings, structures and constructions or to the design processes connected with requirements to production (including researches), productions, constructions, installation, adjustment, operation, storage, transportation, realization and utilization obligatory for application and execution.

Technical regulations are accepted for:

- protection of life and health of citizens, property of natural or legal entities, state or municipal property;
- environmental protections, life and health of animals and plants;
- preventions of the actions misleading consumers.

Adoption of technical regulations in other purposes isn't allowed.

Technical regulations taking into account the degree of risk of harm establish minimum necessary requirements ensuring mechanical safety electric, thermal, biological, safety of radiations and other types of safety.

The technical regulations have to contain requirements to characteristics of production, production processes, etc., but shouldn't contain the requirements to designs and execution, except for the cases if due to the lack of requirements to a design and execution taking into account degree of risk of harm the achievement of the purpose of adoption of technical regulations formulated above isn't provided.

The words “taking into account degree of risk of harm” assume knowledge of value of an indicator of risk at which admissible losses and damages at transportation process aren't provided.

Technical regulations are subdivided on:

- all-technical technical regulations and
- special technical regulations

They differ in that the requirements of the general technical regulations are obligatory for application and observance concerning any kinds of production, production processes, etc., and the requirements of special technical regulations consider technological and other features of separate types of production, production processes, etc.

The general technical regulations, for example concerning safe operation and utilization of cars and the equipment, fire safety, electromagnetic compatibility, etc.

Technical the regulations have to contain a list and (or) the description of objects of technical regulation, the requirement to these objects and rules of their identification for application of technical regulations.

The documentary certificate of compliance of production and (or) other objects of technical regulation to the requirements of technical regulations, provisions of standards and sets of rules is called as compliance confirmation.

Forms of confirmation of compliance are subdivided into voluntary and obligatory confirmation of compliance.

Voluntary confirmation of compliance is carried out in the form of voluntary certification.

Obligatory confirmation of compliance is carried out in the forms of: adoption of the declaration on compliance (compliance declaring); obligatory certification.

Voluntary confirmation of compliance is carried out at the initiative of the applicant on terms of the

contract between the applicant and certification body. It can be carried out for establishment of compliance to the national standards, standards of the organizations, to the sets of rules, systems of voluntary certification, to the conditions of contracts.

The certificate of conformity on the objects, which passed voluntary certification, gives out body for certification.

Obligatory confirmation of compliance is carried out only in the cases established by the corresponding technical regulations and is exclusive on compliance to requirements of technical regulations.

Production released in the territory of the Russian Federation can only be object of obligatory confirmation of compliance.

Forms and schemes of obligatory confirmation of compliance can be established only by technical regulations taking into account degree of risk of impossibility of achievement of the objectives of technical regulations.

Declaring of compliance is carried out on one of the following schemes:

- adoption of the declaration on compliance on the basis of own proofs;
- adoption of the declaration on compliance on the basis of own proofs, the evidence obtained with participation of body for certification and (or) the accredited test laboratory (center).

Obligatory certification is carried out by the body for certification accredited in the order established by the Government of the Russian Federation.

The body for certification attracts the test laboratories accredited in the order established by the Government of the Russian Federation on a contractual basis for carrying out researches (tests) and measurements; exercises control of objects of certification if such control is provided by the corresponding scheme of obligatory certification and the contract.

The state control (supervision) for observance of requirements of technical regulations is exercised

concerning production and other objects of technical regulation.

Concerning production the state control (supervision) of observance of requirements of technical regulations is exercised only at a stage of the address of production.

The national standard – the document in which for voluntary repeated use the characteristics of production, rules of their implementation and the characteristic of processes of design are established (including researches, productions, constructions, installation, adjustment, operation, storage, realization and utilization, performance of work and services).

The purposes of standardization are:

- the increase of level of life safety and health of citizens, property of natural and legal entities, the state or municipal property, objects taking into account the risk of emergency situations of natural and technogenic character, increase of the level of ecological safety, safety of life and health of animals and plants;
- ensuring competitiveness and quality of production (works, services), unities of measurements, rational use of resources, interchangeability of technical means (cars and equipment, their components, components and materials), technical and information compatibility, comparability of results of researches (tests) and measurements, technical and economic data, carrying out analysis of characteristics of production (works, services), executions of the state orders, voluntary confirmation of compliance of production (works, services);
- assistance to observance of requirements of technical regulations;
- creation of systems of classification and coding of technical and economic and social information, systems of cataloguing of production (works, services) systems of ensuring quality of production (works, services), systems of search and data transmission, assistance to work on unification.

Develops and approves national standards national authority on standardization.

Provisions of the national standard have advisory nature, except for those a case when on it links in technical regulations take place.

The set of rules documents of standardization which contains technical rules and (or) the description of processes of design (including researches, productions, constructions, installation, adjustment, operation, storage, transportation, realization, utilization of production and which is applied on a voluntary basis).

Development and the approval of sets of rules are carried out by federal executive authorities within their powers.

TECHNICAL BASE OF SYSTEM

The technical base of a control system of safety is formed by the technical means of two main groups differing in a functional purpose:

- technical means of safety of train service and
- the technical means intended for the analysis of the actual and predicted traffic safety and functioning of the technical means influencing traffic safety.

Special systems of safety of train service, for example, of system of automatic lock-out, the automatic locomotive alarm system, etc. treat the first group.

The automated systems treat the second group:

- collection of information about dangerous failures of hardware and the reasons of their emergence; about dangerous errors of software and the personnel, about the reasons of their emergence; about transitions of the movement to dangerous states, about losses and damages;
- transfers of this information in the device of calculation of the actual values of indicators;
- calculation of the actual (operational) values of indicators of safety of functioning of technical means and personnel, and also traffic safety indicators in general;
- estimates of residual safe resources of technical means;
- calculation of expected values of indicators of traffic safety of trains and functioning of technical means;

- formations of operational recommendations about prevention of decrease in the actual indicators of safety are lower than standard level.

Without the developed technical base of System its effective functioning, i.e. effective management of safety and risks isn't possible.

NORMALIZING PRINCIPLES OF SAFETY INDEXES

Normalizing of safety indexes is the process of setting their normalized values (standards). Normalized value of safety indicator – limited value, for instance, min allowed value of traffic safety indicator $P(S_\rho)$, max allowed value of loss risk indicator $Q(M_\rho)$ and damage risk indicator $Q(N_\rho)$.

It is possible to use two principles in setting normalized values of safety indexes. First principle is based on economic and second one – on social approach to normalizing task solution. According to the first principle normalized values of safety indexes are set on the basis of economic expediency evaluation while the second principle is based on estimation of public opinion about necessary level of safe transportation.

According to the 1st principle the resource level for normalizing of indexes can be limited or not.

As a rule, traffic safety improving is concerned with investment and that is why economic expediency of traffic safety improving projects is determined according various evaluation methods of investment projects [4].

Investment project's efficiency is characterized by a rating system:

- commercial efficiency, which considers financial implications of project implementation for its direct participants;
- budget efficiency, which considers financial implications of project implementation for federal, regional or sectorial budgets;
- economical efficiency, considering costs and effects which are concerned with project implementation and which come out of project participants' direct financial interests and all-low cost measurement.

Future costs and effects' estimation for efficiency determination of investment project is carried out within calculated period which duration is called "time horizon". Time horizon is measured by a number of calculated intervals each of which can be equal to a month, a quarter or a year.

It is recommended to compare different variations of traffic safety improving by using such indexes as net present value (integral effect), profitability index, internal rate of return, pay-off period, etc.

During transportation process implementation it is convenient to use a formula of net present value for safety indexes' optimization task solution in economic context:

$$\mathcal{E}_{umm} = \sum_{t=0}^T (R_t - Z_t) \cdot \frac{1}{(1+E)^t}, \quad (1)$$

where T - time horizon equal to calculated period number on which writing-off of technical resource occurred;

t - calculated interval;

R_t - results, taken out on t -calculated interval;

Z_t - costs, born on the same interval;

E - discount rate, equal to acceptable for investor rate of return on equity.

Discounting is understood as reduction of timely asynchronous costs, results, effects to their values for any one time moment, for instance primary moment ($t=0$).

Following from formula (1), for increasing value of \mathcal{E}_{umm} it is necessary, in particular, to decrease costs Z_t . In general costs are determined as investment costs K and current costs C , that is

$$Z = K + C; \quad (2)$$

discounted investment costs' amount

$$K = \sum_{t=0}^T K_t \cdot \frac{1}{(1+E)^t} \quad (3)$$

for K_t - investment costs for t - interval;

discounted current costs' amount

$$C = \sum_{t=0}^T C_t \cdot \frac{1}{(1+E)^t} \quad (4)$$

where C_t - current costs for t - interval.

For normalizing safety indexes' task it is useful to consider only costs Z_B , necessity of those is determined by target safety level:

$$Z_B = K_B + C_B, \tag{5}$$

where

$$K_B = \sum_{t=0}^T K_{Bt} \cdot \frac{1}{(1+E)^t}, \tag{6}$$

$$\tag{7}$$

$$C_B = \sum_{t=0}^T C_{Bt} \cdot \frac{1}{(1+E)^t}.$$

Current costs C_B are divided into two parts – 1st one C_{B1} is determined by costs, which are necessary for controlling of target safety level, and the 2nd one C_{B2} - is determined by damage suffered from traffic movement to dangerous condition:

$$C_B = C_{B1} + C_{B2}. \tag{19.8}$$

This is the key difference between normalizing reliability and normalizing safety.

As a rule, increasing of traffic safety level is only possible as a result of increasing indexes K_B and C_{B1} . However, economic damage index C_{B2} decreases as a result of traffic safety level increase. Picture no.1 contains a diagram of idealized relationship between cost $K_B + C_{B1}$, damage C_{B2} and traffic safety level. Follow from total costs' diagram there is some optimal value of traffic safety index $P_{opt}(S_0)$, wherein total costs have minimum value and net present value \mathcal{D}_{umm} from transportation, as safety function, reaches its maximum value.

Therein lies a determination principle of economically proved traffic safety index.

In case of volume limitation in consequence of decreasing K_B and C_{B1} line $(K_B + C_{B1})$ may not cross line C_{B2} so $P_{opt}(S_0)$ cannot be achieved.

As for socially proved traffic safety standards they represent standards which are only sufficient against morality norms and ethics of certain society. Such approach takes into account the fact that absolute traffic safety cannot be principally reached. More-

over, traffic safety level depends not only on resources volume supplied but on extent of development of science, technique and technological base of the society. It follows here from that social requirements to traffic safety can be really met only in the framework of scientific knowledge, mature technology as well as state and industry sector's economic health.

Normalizing traffic safety indexes' results according to these two approaches scarcely ever match each other. In such case two situations are possible: economically proved traffic safety index value $P_{opt}(S_0)$ is higher than the social one, then it is excepted as a standard; socially proved safety index value is higher than economically proved one – then the first one becomes a standard.

When social requirements to traffic safety is much more strict than economically proved one the government is to make the following decisions:

- to oblige railroaders to increase traffic safety level by decreasing economical efficiency for transportation;
- to devote additional funds from the state budget to railroads for the development of traffic safety to a socially proved level;
- not to take public opinion into account.

Thus, socially proved determination principle consists of matching safety standards and morality norms and ethics of certain society.

DETERMINATION METHODS OF ECONOMICALLY OPTIMAL SAFETY STANDARDS

For practical task solutions of economical safety standards' optimization continuous dependence of volumes $(K_B + C_{B1})$ and C_{B2} from safety index value $P(S_0)$, cannot be determined, as set on the picture no. 1. In fact these diagrams are plotted point by point which belong to different system variations which supply different values of safety indexes and are characterized by certain volume of investment and current costs needed to insure such indexes. Different system variations are characterized by different methods of traffic safety improving. These methods can be alternative, when it is only possible to use on of them, and nonalternative, when it is possible to use them together.

Determination of standards for federal level considers nonrecurrent and current costs of all traffic safety improving project's participants as well as transport services consumers' costs. However, multiple counting of same costs is to be excluded as well as costs of one participants in results of other participants.

Hereinbefore, in general costs are divided into various types – freight loss, loss of railroad technical facilities, loss of ecological character, loss of business entity, social character loss, loss of health and passenger lives, loss of technical staff, and loss of population. Loss value term of M_i type is regarded as economic damage N_i suffered from this type of loss.

Each method of supplying of one and the same safety index value is characterized by its own volume of economic damage

$$C_{B2} = \sum_i N_i Q(N_i), \quad (9)$$

It is possible to change parameters which influence economical efficiency of transportation process in case of changing of safety indexes for technical facilities. For example, increasing of underlying strength of technical facilities' elements leads to both safety and reliability increase. In addition there are safety improving methods according which reliability of technical facility decreases and economical damage suffered from non-dangerous failure increases as a result.

Safety standards' optimization task solution is possible under certain limits for types of losses. For instance, in case of safety normalizing of passenger-train traffic only passenger health and lives are regarded as possible losses. In such case it is said about safety indexes optimization in one or another narrow sense.

For building dependences shown on picture no. 1 there is a method which is based on Pareto diagrams' initial building shown on pictures no. 2 and 3. Alternative variations of traffic safety indexes' increase $P(S_0)$ are situated on horizontal axis of such diagrams. It is essential that there should be an optimal value variation $P_{opt}(S_0)$ among these N_B variations. The points corresponding to the same options of improving safety

are shown in a system of coordinates $((K_B + C_{B1}); P(S_0))$ in picture 4. With the help of these points we plot a graph of dependency $((K_B + C_{B1}); P(S_0))$, which must be plotted in such a way, that the minimal value of $(K_B + C_{B1})$ should be the case, no matter what the value of $P(S_0)$ is. The options that don't match the requirements should be considered economically unfavorable and shouldn't be used while plotting a graph.

Graphic coordinates of the unknown dependency are found using the following way. With the help of additional axes we limit the space of the right lower quadrant for each of the points. The point is considered to be pertaining to the required graph if there are no points pertaining to other options within this quadrant. The dependency graph should go through a sequence of such points $((K_B + C_{B1}); P(S_0))$.

In cases where the option to improve traffic safety are not an alternative, the plotting of dominant sequence comes to the choice of such sequence of options in which the lowest value $P(S_0)$ corresponds to the lowest extent of expenses. Firstly a Pareto graph should be built $(K_B + C_{B1})$ (pic.5), it stands for cost-efficiency in case of different options of improving safety. As the indicator of the use of safety improving cost we use the relation of safety improving index $\Delta P(S_0)$ to the safety expenses index $\Delta(K_B + C_{B1})$.

$$\mathfrak{E}_s = \frac{\Delta P(S_0)}{\Delta(K_B + C_{B1})}. \quad (10)$$

Here $\Delta P(S_0)$ means the index of traffic safety and related costs, and $\Delta(K_B + C_{B1})$ means the basic option. It can be an option with a minimum safety level or an option used in the running of a subsystem responsible for train (shunting) operation. This graph gives us a visual representation of the relative efficiency of the options. So it is possible to determine the sequence of their application in order to increase traffic safety index. It is obvious that the first option to be used is the option 6, then the options 8 and 7, etc.

$$\begin{aligned} \text{№1} &- 6, \\ \text{№2} &- 6+8, \\ \text{№3} &- 6+8+7, \\ \text{№4} &- 6+8+7+3, \\ \text{№5} &- 6+8+7+3+9, \\ \text{№6} &- 6+8+7+3+9+4, \end{aligned} \quad (11)$$

- №7 - 6+8+7+3+9+4+5,
- №8 - 6+8+7+3+9+4+5+1,
- №9 - 6+8+7+3+9+4+5+1+2,
- №10 - 6+8+7+3+9+4+5+1+2+10.

Using this sequence of options 6, 8, 7, 3, 9, 4, 1,2,10 we plot a graph of dependency $((K_B + C_{B1}); P(S_0))$ (pic. 6). The results of safety index improvement, in case of a simultaneous use of several options, are added (integrated), i.e. they possess the property of additivity.

In other cases we can have alternative as well as non alternative options. As a result, to plot the graph $((K_B + C_{B1}); P(S_0))$ they are all divided into alternate groups, each of which combines non alternative groups. For example let's suppose that the following groups are alternative.

- №1 - 2,4,9;
- №2 - 1,3,7;
- №3 - 5,6,8,10.

For each group we determine the sequence of options according to the rule, used to plot the graph of non alternative options $((K_B + C_{B1}); P(S_0))$.

- №1 - 9, (9+4), (9+4+2);
- №2 - 7, (7+3), (7+3+1);
- №3 - 6, (6+8), (6+8+5), (6+8+5+10).

Then each option subsequently is depicted with a point in the system of coordinates $((K_B + C_{B1}); P(S_0))$ according to its efficiency.

For the dominant sequence we choose only those points that comply with the rule, which was laid down while we were considering alternative options.

To determine the economically optimal value of the traffic safety standards we need to plot and additional dependency graph $((K_B + C_{B1}); P(S_0))$. That is why we need to determine the extent of economic damage C_{B2} for each of the options of traffic safety improvement, which were examined above in the graph $((K_B + C_{B1}); P(S_0))$.

The damage is the result of the impact on the train and the environment in which it moves made by damaging factors H_j , which emerge when a train transits into a dangerous condition S_{ok} . Therefore,

to reduce the losses and the damage it is necessary to reduce the likelihood of dangerous conditions of motion $Q(S_{ok})$. Also we have to reduce conditional probabilities of damaging factors H_j in these conditions $Q(H_j / S_{ok})$.

It is important to note that when the value of $Q(S_{ok})$ is the same, the probability rate $Q(H_j / S_{ok})$ may be different. For example, to reduce the likelihood of corrosive liquids spills the tanks must be equipped with special protective devices. It reduces the likelihood of a damaging factor in the form of corrosive liquids such as sulfuric acid. Another example is the high-speed train with special zone which can absorb impact energy. It reduces the likelihood of forming such an inertial force that the impact of this force would have led to the passenger's death.

Therefore, the level of economic damage depends not only on traffic safety, but on rolling stock properties to reduce the levels of losses in the accidents by eliminating the damaging factors.

In addition the extent of damage depends on the protective measures efficiency; these measures are devised in case of emergency.

Thus in determining an economically viable factor of traffic safety it is necessary to take the constraints imposed on all other factors into account, because the affect the damage from the crash.

In general while we determine the dependency $(3_B; P(S_0))$ it is necessary to evaluate the economic feasibility of measures aimed to reduce the amount of losses carried out by all the stakeholders. To do this we apply a combined Pareto chart (picture 7). The horizontal axis is responsible for the options N_B of reducing the damage, the positive vertical axis is responsible for additional costs $\Delta(K_B + C_{B1})$ and the negative vertical axis is responsible for reducing the damage. C_{B2}

Economically viable are those activities for which the following condition is true $\Delta C_{B2} > \Delta(K_B + C_{B1})$.

The graph shows that economically viable are options 1,2,4,6,7,8,9. If these options are not an alter-

native, their application is determined by the order of their succession 7,2,8,4,6,1,9. The efficiency of options 1, 9 and 4, 6 is the same, so the order of their use does not matter.

Let's have a look at picture 1. Solid lines show the most rational option of improving $P(S_0)$ and all economically viable options of reducing the damage. Then, if one or more of cost-effective measures are not used, the graph of dependency $((K_B + C_{BI}); P(S_0))$ will lie a little bit lower than the corresponding chart. But the graph of dependency $((C_B; P(S_0))$ will lie higher. It will increase $P_{opt}(S_0)$ and the minimal value of Z_B .

Optimal economic value of safety indicator was determined with the help of the dependency graph $((C_B; P(S_0))$. The saddle point of this graph corresponds to the minimum Z_B and is determined by the condition:

$$K_B + C_{BI} = C_{B2}. \quad (12)$$

Then the minimal value of the costs Z_B can be found from the condition (12) and without the use of graphs, which have been used only for purposes of clarity of the optimization method of traffic safety.

It is possible that none of the real options corresponds to the saddle point $((C_B; P(S_0))$, and then we accept the one, that closely complies with our condition, as optimal (19.12).

After determining the optimal value of the safety indicator $P_{opt}(S_0)$ and outlining the system of measures for its maintenance, we can determine the safety performance standards for all the structural components of the subsystem of the train (shunting) operation. Safety performance standards are accepted values of the structural components of security subsystem, which provides economically optimal value of the traffic safety indicator.

SOCIAL SAFETY STANDARD.

Social safety standard is established only with respect to one type of loss, namely, loss of life and relative health of the passenger. Immediately we have to standardize the value of the indicator of risk of death

when the train transits into a dangerous state. It is not possible to use rigorous scientific methods or at least the methods used in determining cost-optimal safety standards.

The establishment of social norms of a passenger's death, which was a result of train derailment largely depends on the social, political and economic systems of the country. The more progressive the society is, the more developed and focused on solving of social problems is the economy of the state. And the higher the country values an individual and their safety.

However, the severity of the public requirements for traffic safety, as well as for other important technological processes, depends on the psyche of an individual.

Thus, the results of the studies suggest that if the probability of death is 10^{-6} a year and it is the result of technogenic emergencies, the public usually does not express undue concern. Based on this, many experts take the value of 10^{-6} as a normative value of the technogenic risk indicator.

We can assume that it is a psychologically reasonable standard which measures the risk of death.

In addition, people's attitude towards the value of this type of risk depends on how free they are to decide — to expose themselves to the risk or not. For example, the athlete himself takes the decision to participate in a car race on mountain roads with the aim of establishing a sports record. Another thing is when a person from force of circumstances is forced to use the services of railway transportation. In these cases, the difference in the assessment of acceptable loss of life reaches 3 orders of magnitude, namely, in the latter case the safety requirements are stricter.

Another feature of the human psyche is that people consider single emergencies with severe consequences less acceptable than a large number of accidents with less severe consequences. For example, the public reacts more sharply to relatively rare derailments with severe consequences than to the daily deaths in car accidents. This being said, train wreck

is considered to be a truly extraordinary event, and car accidents are considered to be everyday phenomena, an inevitable attribute of modern city life. At the same time we know that the automobile safety is substantially lower than the train safety.

Thus, the establishment of social norms of risk of death indicator as the passenger travel by train, we should take into account the real state of the society as well as the state of overall security of the individual in society. We should also take into account the current state of train safety.

If the social norm of the risk of death of the passenger is more strict than economically feasible, then it should underlie the safety standards of structural components, which are parts of train and shunting operation. To do this we use the methods discussed above to determine the most economically rational option of implementing of a subsystem, which can provide the risk of death standard. The safety values of structural components of such a system are accepted as normative.

Submitted: April 30, 2015.

Accepted: May 8, 2015.

WATER TREEING IN EXTRUDED CABLE INSULATION AS REHBINDER ELECTRICAL EFFECT

Iz. B. Peshkov¹, M. Yu. Shuvalov², V.L. Ovsienko³

¹*D. Sc. Habil., professor*, ²*D. Sc. Habil.*, ³*Ph. D.*,
JSC VNIKP

Case study

DOI: 10.7251/JIT1501055P

UDC: 621.315:66.017

Abstract: The paper contains systematic comparison of signs and properties of the water treeing phenomenon (the basic mechanism of degradation of medium voltage electric cable extruded insulation which develops under combined action of electric stress and water) and Reh binder Effect – the reduction of mechanical strength of solids due to physical and chemical action of liquid medium.

The analysis of the published data permits to distinguish 13 indications of the Reh binder Effect. The authors show successively the direct analogy of the water treeing and the Reh binder Effect using the above mentioned indications, including decrease of work of the development of new surfaces in the course of destruction, chemical specificity, role of material defects, two-stage destruction nature, etc. The analogy obtained is accepted as a working hypothesis which permits to bring certain order into theoretical and experimental studies of the water treeing.

Key words: water treeing, Reh binder Effect, destruction, medium, defects.

Today XLPE cables are the basic types of 10-500 kV AC power cables. These cables are used for feeding cities and energy-intensive manufacturing facilities, as well as for carrying energy from electric power stations. Polymer cable insulation operates under the exposure to high electric stresses; therefore polyethylene insulation of medium and high-voltage cable has to meet strict electric strength and reliability requirements over the operation period of several decades.

However if there are cavities and microimpurities in the polymer insulation, then in the course of operation degradation known as treeing begin to develop within the insulation material. Treeing may be caused both by contaminants in the original polyethylene and imperfection of cable manufacturing process.

In the long run treeing leads to cable failure in operation. Therefore the investigation of tree initia-

tion and development is of paramount importance. The main form of electrical insulation breakdown is associated with dendric tree-like growth known as electrical trees (ET). The main factors of ET growth are electric stress and temperature. Ageing known as water treeing [3, 8, 7] occur in the insulation under the simultaneous exposure to electric field and water diffusion into the insulation from the environment.

Electrical and water trees (WTs) tend to grow from the defects of the cable insulating system. ETs initiate slowly but grow quickly. On the contrary, WTs initiate quickly but grow relatively slowly. In medium voltage cables WTs form the basic mechanism of degradation of extruded insulation.

Despite the dramatic progress achieved over the recent 20-30 years in the field of development of more reliable dielectric materials and their processing into high-performance products, WTs still remain

the main concern of major companies producing both insulating and semiconducting materials and cables, as well as of cable operating companies.

This concern is dictated by the desire to create more durable materials and cable constructions, as well as to develop more reliable and valid methods for the assessment of WT resistance of the electrical insulation system and its service life forecast.

The WT problem continues to be of critical importance due to both the complexity of physical and chemical nature of ageing and complexity of the above mentioned goals. For deeper understanding and more effective study of the WT development mechanisms a “system working hypothesis” is offered in order to bring a certain order into the experimental investigation and mathematical modeling of the process (both are necessary for the successive solution of the above mentioned problems).

A statement about the analogy between the WT development in the insulation and the Rehbinder effect is accepted as this “system hypothesis”.

As is well known [13], the Rehbinder effect (RE) is the drop in mechanical strength of solids through the reversible physicochemical action of a particular medium associated with the increase of specific free energy and as a result – with the decrease of work of the development of new surfaces in the course of destruction.

The analysis of typical indications of the RE which are known from scientific publications shows that XLPE cable insulation ageing due to combined action of electrical field and water resulting in the decrease of dielectric strength and WT development has similar features, i.e. it can be considered as a certain electrochemical demonstration of the RE. This can be seen from the Table below where both processes are compared.

No.	Indications of RE	Corresponding features of electrochemical ageing of polymer cable insulation in the presence of moisture
1	Exposure to external destructive force – mechanical stresses.	Exposure to external destructive force – electric field.
2	Facilitation of destruction under combined impact of external forces and liquid medium [12].	Significant decrease in dielectric strength under combined action of electric field and water.

3	RE is related to decrease of work of the development of new surfaces in the course of destruction [13].	In this case new surfaces are surfaces of microcavities comprising WTs. In the absence of the medium the work of development of new surfaces raises dramatically, which is manifested in a considerable increase of “destructive” electric stresses when wet ageing transforms into dry ageing.
4	Reversibility: the strength recovers after the removal of the medium [13, 9] and the load [9]. As regards the thermodynamics, RE represents weakly non-equilibrium processes [12].	When water is removed from the insulation the electric strength recovers and WTs dry up. ¹⁾ After the electric field is switched off and the cable is conditioned in water the electric strength recovers [6], at least partially.
5	RE may subside with the rise in the temperature due to dissipation of deformative microinhomogeneities and healing of microcracks, diffusion dispersal of the medium, reduction of active component adsorption [9].	Ageing under operation conditions or in tests at elevated temperature (for example, 90°C) is expressed much less than at low temperatures (20÷40°C). WTs develop in a less intensive way, the dielectric strength decreases to a smaller extent.
6	Contact with the medium has to be relatively long [13].	WTs grow over a prolonged period – from several weeks/months (accelerated laboratory tests) to years and decades (commercial operation).
7	Chemical specificity with regard to the nature of the material, medium and additives [9].	WT growth dynamics and their subtle properties (for example, spectral properties) depend strongly on the composition of the insulation system under destruction, the electrolyte composition and the chemical nature of the defects at which WTs initiate.
8	Essential role of the structure defects [13, 9].	WTs always initiate at the defects, and not only technological defects, like foreign inclusions or cavities, but also “molecular” polymer defects are essential for their development.
9	Specific role of the solid grain boundaries: destruction develops at the grain boundaries [9].	WTs develop in the amorphous phase of cross-linked polyethylene, i.e. at the crystallite boundaries.
10	The medium should be related to the material under destruction [9].	Hear the medium is water. As shown in [10], WTs in cross-linked polyethylene are hydrophilic.
11	Destruction proceeds in two stages ²⁾ : 1) gradual initiation and development of equilibrium microcracks; 2) fast propagation of non-equilibrium crack over the entire body cross-section [9].	Destruction also has two stages: 1) gradual initiation and development of WTs; 2) fast propagation of ET (initiated at WT as at “secondary” defect) over the entire insulation thickness.
12	Surface diffusion along the crack walls.	Surface diffusion along the cavity walls (and, perhaps, submicroscopic channels, presumably connecting these cavities).
13	Time (t) dependence of the crack length (l_c) is approximated by the power function [11]: $l_c \sim t^{0.31}$	Experimentally obtained time dependence of WT length (l_w) is approximated by the power function [4]: $l_w \sim t^\beta$, $\beta \approx 0.2 \div 0.4$

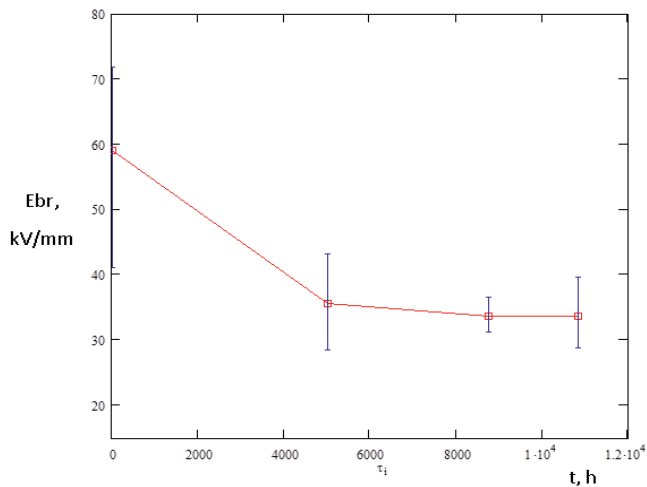
¹⁾ The idea of reversibility as applied to WT should be treated with some care. It seems reasonable to speak about partial physical-chemical reversibility.

²⁾ This is characteristic of other types of destruction.

Below we deal with a variety of experimental data which illustrate the typical features of the RE in respect to the electrochemical ageing of extruded cross-linked polyethylene cable insulation with reference to the processes described in the Table.

Dielectric strength reduction due to ageing (item 2).

Accelerated ageing tests of full-scale specimens of medium-voltage cable are being conducted in VNIIEP at present; the tests comply with the norms of CENELEC (HD 605, HD 620). The electric strength data obtained by now and averaged over some manufacturing plants are given in Fig. 1 versus



test duration.

Figure 1. Dependence of dielectric strength (E_{br}) of full-scale 10 kV cable specimens on time (t) of accelerated electrochemical ageing tests carried out in accordance with CENELEC norms

Significant increase in the work of development of new surfaces in the absence of active medium which is represented by a sharp increase of destructive electric stresses (item 3).

WTs initiate even at electric stresses (E) equal to 2-3 kV/mm and probably at lower stresses. At the same time the electrical ageing at moderate temperatures in the absence of moisture in the insulation is registered only at E values within tens of kV/mm. This is confirmed by the experimental data given in [14].

Specimens of 1 mm thickness cut out of 110 kV cable insulation were aged at a temperature of 40°C and E=23 kV/mm. Examination of the specimens after 5000 hours of ageing revealed no signs of ageing.

In addition test of a full-scale specimen of a 110 kV cable as carried out at continuously applied voltage, with E=13 kV/mm at the inner screen and constant heating, the conductor temperature was 130°C. The breakdown occurred after 23800 hours of testing, whereupon the insulation was examined using the FTIR spectrophotometry, thermal analysis, video microscopy and other techniques which revealed some signs of thermal ageing and no signs of electrical ageing.

If exposure to water had been “included” into the performed tests one could have with certainty expected mass initiation of WTs and most likely early failures of the test specimens.

Reversibility (item 4) – this property requires additional analysis.

Weakening of the RE with the rise of temperature (item 5) is illustrated by two length histograms of WTs revealed in two different parts of the same cable after 12 years of operation (Fig. 2 a, b). The difference between the parts lies in the following: due to the outer source of heat one part of the cable was heated to a higher temperature which prevented WT growth. As a result the mean sizes of the trees exhibit two-fold difference.

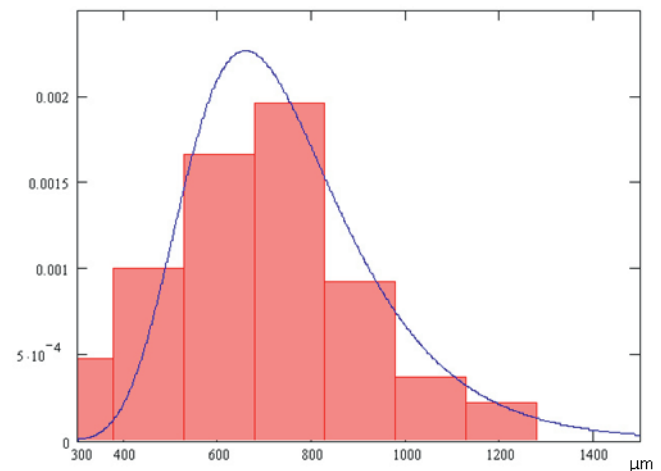


Figure 2a. Histogram of “bow-tie” water tree lengths and approximating density of type 1 maximum value distribution (detailed description of this distribution is given, e.g., in [5]). The trees were revealed in the cable specimen after 12 years of operation at moderate temperature

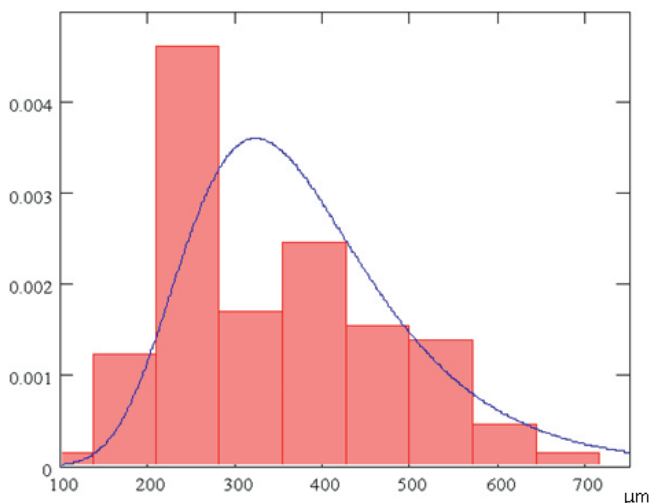


Figure 2b. Histogram of bow-tie water tree lengths and approximating probability density. The trees were found in another specimen of the same cable: the specimen was taken from a cable line section that was in operation at elevated temperature

This phenomenon also requires additional consideration.

Chemical specificity (item 7). There are many scientific papers which show the dependence of the WT growth rate on the chemical composition of insulating and semiconducting compounds, for example, [3, 8], and electrolyte composition [2]. Consideration must be given to the differences in the chemical nature of WT which are resulting from the differences in the composition of the defects that give rise to treeing.

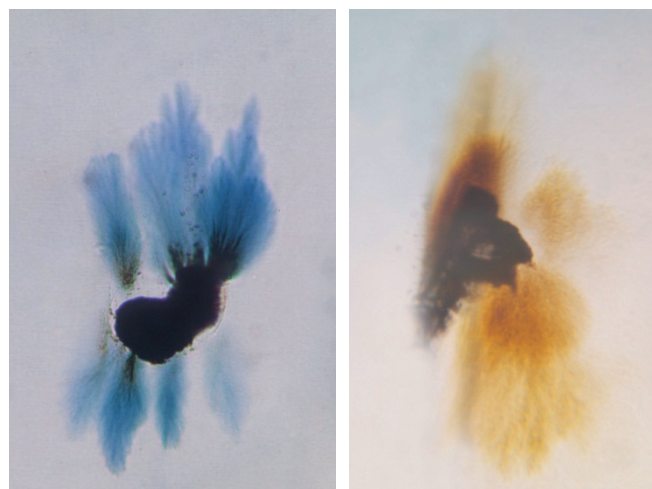


Figure 3. Bow-tie water trees possessing intrinsic optical absorption in different spectral regions. The distinctions are caused by the difference in the chemical nature of the defects at which the trees grew.

Such chemical “individuality” of some WTs is demonstrated in Fig. 3. Optical contrast of the trees against the surrounding dielectric is resulting from the primary absorption.

Role of defects (item 8). On the whole it is safe to say that there is a positive correlation between the sizes of defects and trees; large WTs growing at large defects are shown in Fig. 4 a, b, c. However this correlation is not strict: while examining cables that failed in operation one could sometimes come across large trees growing from small inclusions. The WT growth rate seems to be dependent on a variety of defect characteristics: its form and dielectric constant (and hence local increase of electric stress), hydrophilic property and water solubility of substances comprising the defect, their chemical activity, compatibility of the defect and the surrounding polymer. A large WT growing from a small-size defect is shown in Fig. 4 d.

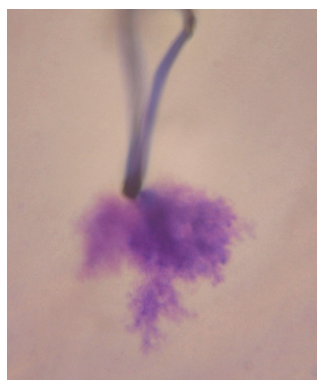


Figure 4a. Water tree growing from the hydrophilic cellulose material fiber. Stained with methylene blue.



Figure 4b. Vented water tree growing from the semicon screen protrusion. Stained with methylene blue.

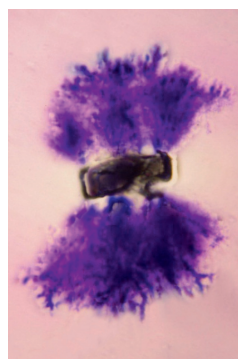


Figure 4c. Bow-tie water tree growing from a foreign inclusion in the insulation bulk. Stained with methylene blue.



Figure 4d. Bow-tie water tree of 1.5 mm length growing from a small inclusion. In this case the image contrast is provided with the help of the so-called Reihberg illumination (color variant of the dark field microscopic method) – “optical staining” based on the use of light filters instead of staining the insulation slices containing water trees (see photo in Fig. 4a-c and Fig. 6) with a special staining agent.

WT development in the amorphous phase of the material (item 9). Comparative investigation with the aid of a polarizing and a phase-contrast microscope shows that WTs, as well as other types of degradation of amorphous-crystalline polymers, develop practically in the amorphous phase of the material.

Indeed, as may be seen in Fig. 5 a, b, birefringence, determined by the dielectric crystalline phase organization, undergoes no changes inside the WT as compared with the intact insulation, and as a result the WT is practically invisible in the polarization contrast and at the same time it is perfectly visible in the phase contrast. It means that the crystalline phase of the polyethylene inside the WT remains intact. It is fair to say that this simple proof of the crystalline phase intactness is effective only for “young” and relatively small WTs. Large WTs often scatter light in such a way that they introduce an amplitude contrast into the optical image which does not disappear when the polarizer and the analyzer are in a crossed position. Nevertheless this difficulty may be overcome by using the special technique of video-enhanced polarization microscopy [1].

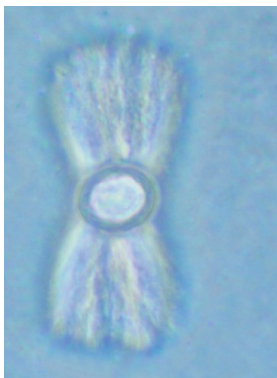


Figure 5a. Bow-tie water tree. The photomicrograph was obtained with the use of the phase contrast method.



Fig. 5b. The same as in Fig. 5a but polarization contrast is used instead of phase contrast. The water tree is practically invisible.

Two-stage cable destruction (item 11). In case of the electrochemical ageing of the extruded power cable insulation the failure condition is achieved in the following way. At first WTs are developing over a long period of time; then as their dimensions and the extent of polymer degradation within the WT reach some critical level (enter a certain critical region),

electrical trees originate at the water trees as secondary defects and rather quickly they grow through the entire insulating layer causing a breakdown. Photos of WTs at which electrical trees began to grow are shown in Fig. 6.

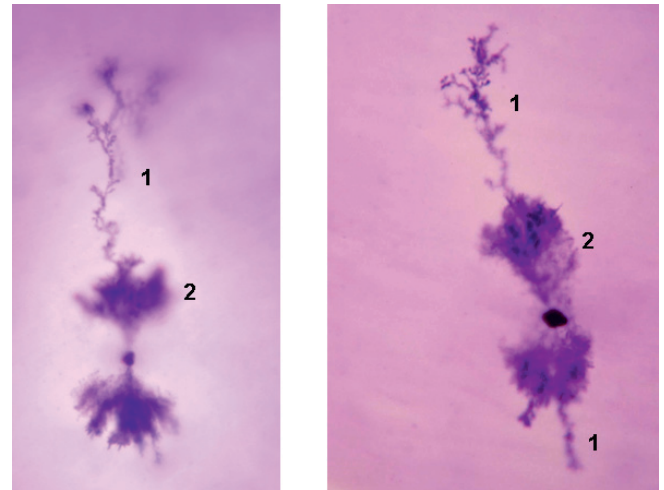


Fig. 6. Electrical trees (1) growing from water trees (2), stained with methylene blue

Therefore on the basis of both our own and foreign test data we may say that there is a rather close analogy between the Reh binder effect and the WT development. However this analogy cannot be absolutely full for variety of reasons, including the following:

- RE in its traditional meaning refers to mechanical destruction phenomena while WT growth is an electrochemical process;
- RE covers a wide spectrum of phenomena [12] and thus it cannot be determined comprehensively;
- RE suggests that no chemical reactions [11] occur in the degraded material or a “moderate” chemical interaction takes place [12]. At the same time it is known [10] that the WT development is accompanied by local oxidation of the dielectric. Therefore the electrochemical ageing of the extruded power cable insulation should be viewed as only partly reversible process (in the sense that was mentioned earlier – after the moisture is removed the WTs dry up and the cable dielectric strength recovers). With respect to thermodynamics it is proper to regard the WT growth as a relatively weakly non-equilibrium process [14].

REFERENCES

- [1] Allen, R.D., Allen N.S. (1983) *Video-enhanced Microscopy with a Computer Frame Memory*. Journal of Microscopy, Vol. 129, pt 1, January 1983. p.p. 3-17.
- [2] Bamji S., Bulinski A., Densley J. et al. (1984) *Water Treeng in Polymeric Insulation*. CIGRE, 1984, Paper 15-07, 7 p.p.
- [3] Bostrom, J.O., Campus, A., Hampton, R.N., Heikalla, P., Jager, K.M. et al. (2005) *Copolymer compounds of cross-linked polyethylene (SuperCOPO) for medium voltage power cables*. Cables and Wires, № 5 (294), 2005, p.p. 7-22 (in Russian).
- [4] Gototh H., Okamoto T., Suzuki S., Tanaka T. (1984) *Method for Estimation of the Remaining Life-time of 6.6 kV XLPE Cables after their First Failure in Service*. IEEE Transactions. Vol. PAS-103, №9, 1984, p.p. 2428-2434.
- [5] Gumbel, E. (1965) *Statistics of extremes*. : “Mir”, 1965 – 450 p.p. (in Russian).
- [6] Katz C., Fryszczyn B. (1985) *Recovery of Dielectric Strength in Cables Containing Water Trees*. International Conference on Properties and Applications of Dielectric Materials, Xian, China, June 24-29, 1985. Vol. 2, p.p. 526-530.
- [7] Leppanen, J., Chamov, A.V. (2005) *Insulating technology for medium-voltage cables of improved reliability*. Cables and Wires, № 5 (294), 2005, p.p. 32-34 (in Russian).
- [8] Mendelsohn, A., Aarts, M. (2005) *Global experience of using water-tree retardant cross-linked polyethylene insulation for long-life medium-voltage cables*. Cables and Wires, № 5 (294), 2005, p.p. 23-29 (in Russian).
- [9] Rehbinder, P.A. (1979). *Surface phenomena in disperse systems*. Selecta M.: “Nauka”, 1979 (in Russian).
- [10] Ross, R., Geurts, V.S.M., Smit, J.J. et al. (1990) *The Hydrophilic Nature of Water Trees*. IEEE International Symposium on Electrical Insulation. Toronto, Canada, June 3-6, 1990. p.p. 169-172.
- [11] Shchukin, D.E., Summ, B.D. (1969) *Role of processes of adsorption-active medium distribution over the surface of solids in the effect of strength reduction through adsorption*. Collected works. Surface diffusion and diffluence. Ed. by Prof. Ya.E. Geguzin. M.: “Nauka”, 1969, p.p. 161-187 (in Russian).
- [12] Shchukin. E.D. (1976) *Reduction of surface energy and change in mechanical properties of solids under environmental exposure*. “Physical-chemical mechanics of materials”, 1976, v. 12, №1, p.p. 3-21 (in Russian).
- [13] Shchukin, E.D., Pertsev, A.V., Amelina, E.A. (1992) *Colloid chemistry*. M.: “Vyshaya shkola”, 1992 (in Russian).
- [14] Shuvalov, M.Yu. (2000) *Investigation of high voltage cables, development of improved methods of electrical design and microdiagnostics*. Doct. of Sc. M.: JSC VNIIEP, 2000, 342 p (in Russian).

Submitted: April 30, 2015.

Accepted: May 8, 2015.

CONTROL SYSTEMS FOR AUTOMATED VESSEL PILOTING THROUGH LOCAL STATIONARY OBSTACLES

Dovgobrod Georgy Moiseevich¹, Klyachko Lev Mikhaylovich²

¹Ph.D. (Engineering), ²D.Sc.(Shipbuilding)

OJSC “Central Scientific Research Institute “Kurs”, Moscow, Russian Federation,

e-mail: grsud@kyrs.ru

Case study

DOI: 10.7251/JIT1501061M

UDC: 656.61.052

Abstract: To reduce the “human factor” component in the causes of accidents during pilot age of vessels along areas of fairways with local stationary obstacles we propose a device which provides: a) real-time presentation on a graphical display of information on current and predicted positions of a vessel with regard to a stationary obstacle; b) automated or semi-automated piloting of a vessel in to a straight path for safe passage of an obstacle. Specified device will allow reducing the risk of accidents while piloting a vessel along difficult parts of fairways.

Key words: control systems, navigation, microcontroller.

Each year, in Saint-Petersburg a number of vessel collision events with bridge piers takes place during the passage of cargo ship caravans along the Neva [1]. In order to reduce the “human factor” component in the causes of accidents during pilot age of vessels along areas of the fairways with local stationary obstacles a device for vessel piloting (DVP) has been developed in OJSC “CSRI “Kurs”. DVP is designed for:

- Delivery of information to navigator on current and predicted positions of a vessel with regard to a local stationary obstacle (for example, piers of a bridge);
- Automated or semi-automated piloting of a vessel into a straight path for safe passage of an obstacle.

STRUCTURAL DIAGRAM OF A DEVICE FOR VESSEL PILOTING (DVP)

The following designations are used below:

D_v – a tuple of a vessel geometrical parameters $D_v - \{d, l_b, l_{st}\}$ where d is a vessel hull beam, l_b, l_{st} are dis-

tances from bow and stern to a vessel center of mass respectively.

T_{pr} - one-dimensional (linear) array of tuples of parameters of preset straight-line motion paths in the vicinity of a j -th obstacle $T_{prj} = \{\phi_{pr}, \lambda_{pr}, \phi_{pr}, l_{pr}, L\}_j$, where ϕ_{pr}, λ_{pr} are the latitude and the longitude of an initial point, l_{pr} is the length of a preset path, L is the length of a maneuvering area in front of an obstacle.

Structural diagram of a DVP is presented in Figure 1. Connections shown dashed may be absent in a simplified version of a device. Units of a DVP gear are designed to fulfill the following functions. *Graphical screen* 1 displays on a screen in visual form symbolic representations of current and projected positions of a vessel with regard to an obstacle. *Control unit* 2 is used to control DVP operation. *Angular speed sensor* (ASS) 3 measures angular speed of a vessel hull turning rate in horizontal plane w . *Heading sensor* 4 measures the current heading of a vessel ϕ_h . *Global positioning system* (GPS) *receiver* 5 measures current velocity vector of longitudinal vessel movement V_v

and the vessel current coordinates f_v, l_v . *Microcontroller 6* performs calculations of the following values with period τ (See Figure 2): x_{vl}, x_{vr} coordinates of the current projection of a vessel hull and of its center of mass x_{cm} on oX axis in the local coordinates system XOY, x_{vl}^p, x_{vr}^p coordinates of predicted over time Dt position of a vessel hull projection and of its center of mass onto OX axis, the current distance to an obstacle L , obstacle approach speed V_{ap} . It displays on a graphical screen in a visual form current and predicted geometric parameters of the mutual position of the vessel and the obstacle X_v, X_v^p, L, V_{ap} . It stores the vessel motion actual parameters T_{ac} in permanent memory. It estimates V_v, f_v, l_v in case of short-term signals from SNS receiver drop out. *Rudder feedback 7* measures the current rudder position δ . *Digital interface 8* is used to enter the coordinates of the obstacles S_{ob} , of preset motion paths in the vicinity of obstacles T_{pr} , of vessel geometric parameters D_v , of prediction time Dt , and to feed the actual path and other vessel motion parameters T_{ac} into a PC for further analysis. *Interface with the steering gear actuator 9* is used to transfer rudder deflection calculated value d_{pr} into the actuator. *Permanent memory 10* is used for storage of: coordinates of obstacles S_{ob} , preset motion paths in the vicinity of obstacles T_{pr} , vessel geometric parameters D_v , prediction time Dt , actual path and other vessel motion parameters T_{ac} .

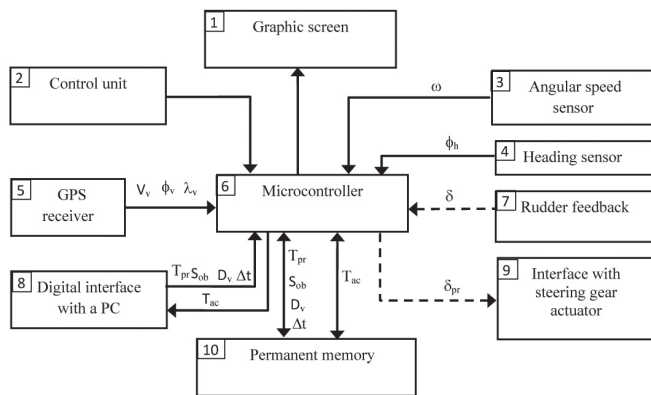


Figure 1. Structural diagram of a vessel piloting device

DVP OPERATION DESCRIPTION

Let us consider geometric layout of a vessel entering a preset path for passing an obstacle presented in Figure 2. XOY is a local system of coordinates connected with definite stationary obstacle. OY axis has a direction of a preset motion path in the vicinity of

an obstacle. OX axis is perpendicular to OY axis. The origin of coordinates “O” lies at the initial point of a preset path for passing through an obstacle $\{f_{pr}, l_{pr}\}$.

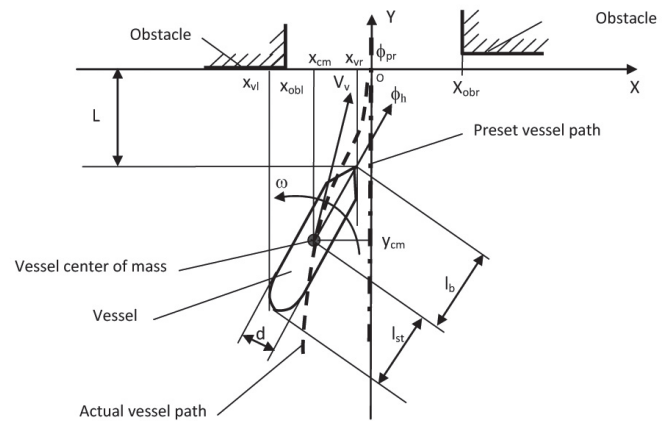


Figure 2. Geometric layout of a vessel entering a preset path of passing through an obstacle

Along the entire length of a ship fairway serviced by DVP when a vessel is in motion DVP operates in one of the two modes: a) next obstacle approach state and b) piloting state. In the state of next obstacle approach DVP monitors the current distance from a vessel to the next obstacle and when a vessel enters the vicinity of an obstacle passes into “piloting state” mode. By “the vicinity of an obstacle” we mean a part of water area near an obstacle sufficient for entering a preset path for passing an obstacle. After the state of piloting has set in a navigator may choose one of the three modes to pilot a vessel into a preset path to pass obstacles and to move along this path:

3. Manual control without an advisor.
4. Manual control with an advisor.
5. Automatic control.

In manual control modes a navigator uses displayed on a screen information on a preset path, on current and predicted vessel position, on an obstacle position and pilots a vessel into a preset path to pass an obstacle. In manual control mode with an advisor the screen displays a recommended value of rudder deflection. In this case to control a vessel motion it is enough for a navigator to match the images of the current rudder position with a recommended one with the help of rudder control gear. When passing an obstacle a navigator uses information presented on the screen in order to counteract vessel deviation

from a preset path in manual control modes and to control the process of motion in automatic mode. After piloting a vessel through an obstacle DVP passes into the state of “next obstacle approach”.

Model view of a screen with information on the state of vessel piloting is shown in Figure 3 [2]. Symbolic presentations of a vessel hull edge lines are accomplished in a form of a vessel hull schematic drawings halves in plan view. When the angle of drift is equal to zero vessel hull halves are joined into a complete view of a vessel hull. When the angle of drift is not equal to zero vessel hull halves are pushed apart at a distance proportionate to the angle of drift. The position of the vessel hull projection edge lines x_{vr} , x_{vl} onto OX axis and the projections of the left and the right obstacles onto OX axis are displayed on a screen in the scale of OX axis.

In case of ideal current state of the vessel piloting process the vessel center of mass should lie on a preset motion path, a current speed vector of the vessel longitudinal motion should coincide with a preset vessel motion path and the vessel boards should be ultimately removed from the obstacles. Model screen view with information on ideal vessel piloting state is shown in Figure 4. Points O, x_{cm} , X_{cm}^p coincide; halves of a vessel hull joins into a complete image of a vessel hull projection onto a horizontal plane.

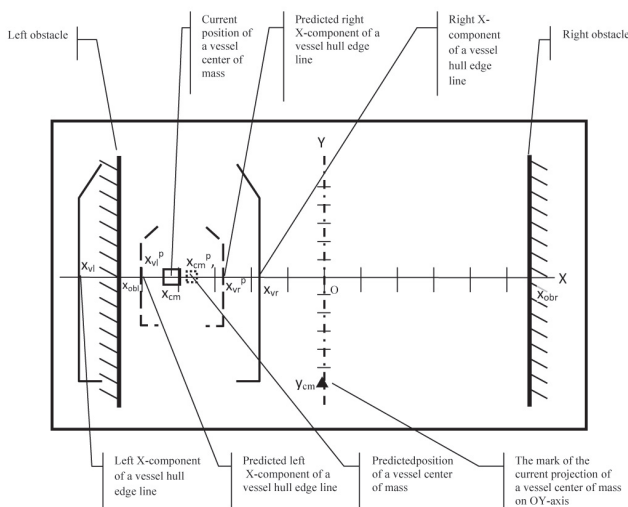


Figure 3. Model screen view with information on the state of vessel piloting process

To calculate a predicted position of the vessel hull projections edge lines (x_{vl}^p, x_{vr}^p) onto OX axis for time value $t+Dt$ one can accept that V_v and ω are constant for time interval Dt . To calculate a predicted position of a vessel center of mass one can use vector expression (1) where symbol “T” stands for transposition operation.

$$(x_{cm}^p, y_{cm}^p)^T = (x_{cm}, y_{cm})^T + V_v^T \Delta t \tag{1}$$

For proximate calculation of predicted position of the most jutting out vessel hull points expressions (2) are used. In the expressions (2) it is accepted that a vessel hull projection onto a horizontal plane is approximated by a rectangle with adjacent to it semi-circles corresponding to bow and stern. For proximate calculation of the current position of the most jutting out vessel hull points expressions similar to expression (2) are used.

$$(x_{std}^p, y_{std}^p)^T = (x_{cm}^p, y_{cm}^p)^T - (l_{st} - d/2) * (\sin(\phi_h - \phi_{pr} + \omega * \Delta t), \cos(\phi_h - \phi_{pr} + \omega * \Delta t))^T$$

$$(x_{bd}^p, y_{bd}^p)^T = (x_{cm}^p, y_{cm}^p)^T + (l_b - d/2) * (\sin(\phi_h - \phi_{pr} + \omega * \Delta t), \cos(\phi_h - \phi_{pr} + \omega * \Delta t))^T \tag{2}$$

$$x_{vl}^p = \min(x_{std}^p - d/2, x_{bd}^p - d/2)$$

$$x_{vr}^p = \max(x_{std}^p + d/2, x_{bd}^p + d/2)$$

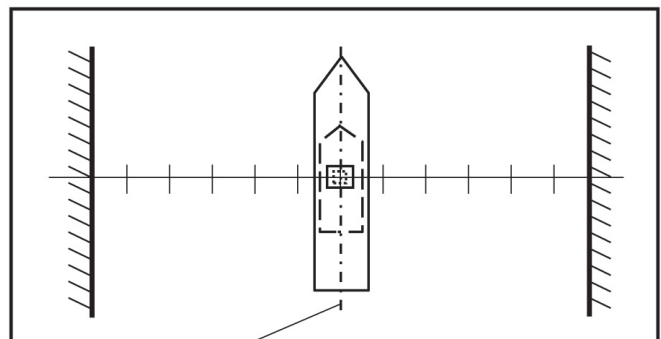


Figure 4. Model screen view with information on ideal state of a vessel piloting process

The process of vessel piloting along a part of the fairway with a local stationary obstacle consists from two stages:

- Piloting a vessel into a safe path to pass an obstacle.
- Keeping a vessel on a safe path for passing an obstacle.

A navigator's task for the case of manual control consists in keeping minimal distance between points O , x_{cm}^v , x_{cm}^p with the aid of vessel steering and propulsive thrust control gear, and in controlling that symbolic presentations of the vessel hull projection edge lines onto OX axis preset by points x_{vl}^v , x_{vr}^v , x_{vl}^p , x_{vr}^p do not overlap on a screen the images of obstacles preset by points x_{obl} , x_{odr} .

In the capacity of an operating path for piloting a vessel into the path to pass an obstacle Bernstein basis fifth-degree polynomial curves are applied [3]. Specified operating paths are physically realizable.

In manual control modes with an advisor and in automatic control mode the calculation of control signal is accomplished with the use of nonlinear control law described in article [4].

SUMMARY

DVP will permit a navigator to pilot a vessel in advance into a preset path for safe passing of a sta-

tionary obstacle. When piloting a vessel through an area with stationary obstacles with the appliance of DVP a navigator may use not only eye estimations of a vessel position in relation to an obstacle but also objective estimations of current and predicted mutual position of a vessel and an obstacle. Additional objective data will provide a rise of accuracy of vessel motion control in the vicinity of an obstacle and thereafter lead to reduction in the number of accidents. Navigator's control of the vessel motion using data displayed on a screen will allow to accurately pilot a vessel in the vicinity of obstacles at night-time and at adverse weather conditions.

Actual path and other vessel motion parameters (T_{ac}) storage in permanent memory will permit to fulfill objective accident-incident analysis.

The device may be manufactured as a separate element for installation in a pilot room or as a self-contained portable device with no connection to rudder translator and steering gear actuator and there after without automatic control mode. DVP operation algorithm may be realized as a separate task within bridge vessel motion control system.

REFERENCES:

- [1] Dovgobrod, G.M. (2011 and 2012). *Development of Adaptive Algorithm for Vessel Motion Control on a Nonlinear Path Using a Method of Backstepping Control Synthesis* Giroscopiya I Navigatsiya, 2011, №4, p.22-31 (English version: G. M. Dovgobrod, *Development of an Adaptive Algorithm for a Ship Motion Control on a Nonlinear Path*, *Gyroscopy and Navigation*, No. 1, 2012, p. 41-46)
- [2] Dovgobrod, G.M., Klyachko, L.M. (2006). Patent for an invention *Device for Generation and Display of Information for Vessel Piloting through Narrow Parts of the Fairways* №2318187, priority date 15.06.2006
- [3] Dovgobrod, G.M., Klyachko, L.M., Rogozhnikov A.V. (2009). *The Use of Parametric Approximation in the Process of Vehicles Motion Paths Planning* Izvestiya vysshikh uchebnykh zavedenii. Instrument engineering. 2009. V.52, №9, p.11-17
- [4] Rossiyskaya Gazeta, 02.08.2005, №167 (3836)

Submitted: April 30, 2015.

Accepted: May 8, 2015.

PROSPECTS OF HIGH TECHNOLOGIES IN THE REMOTE DIAGNOSIS OF THE TRACK

Lievin, Boris A.¹, Nedorchuk, Boris L.

¹professor, rector

Moscow State University of Railway Engineering (MIIT), Moscow, Russia

Case study

UDC: 656.2:62

DOI: 10.7251/JIT1501065L

Abstract: The article assesses trends of development of devices for control and diagnostics of railway tracks, highlights the growing importance of advanced technologies that make use of more sophisticated methods of remote monitoring of the technical condition and ensure safe operation of railroad bed. In particular, the authors analyze in detail the results of their own developments, with an emphasis on options for optical control with the use of aircraft and video recording, significantly expanding the possibilities of monitoring and quality of observations, and at the same time forecast (considering experimental data and economic factors) promising areas of engineering research.

Keywords: railway, track monitoring, remote diagnostics, aerial photography, optical sensors, polarization of reflected light, infrared technology, satellite communications.

INTRODUCTION

As we know, a number of immutable factors (primarily, the need to increase operating speeds on the railways, to achieve additional traffic safety guarantees with account for not only “uncreated” man-made threats) forces constantly to look for more efficient and reliable control devices in all respects of tracking of technical condition of the track, conditions of the right-of-way.

There is a fairly definite picture of vectors of engineering research where high-tech solutions and projects claim to dominate. Some of them are implemented; others are likely to have different degrees of readiness and experimental verification.

VECTOR DISPOSITION

The general trend in the situation, from the very origins guided by enforcement promises, have remained the same for nearly two centuries: live visual inspection with direct participation of a person

(track patrolman), as soon as the slightest opportunity appeared, was immediately supplemented by independent technical expertise, objective data of instruments and measurement, engineering analysis. Moreover, with the increasing complexity of track measuring equipment which was put on the track carts, placed in special cars, troubleshooting gradually transformed from a contact to a non-contact one, using as instruments the most promising means of detection of defects, technological risks, direct threats to traffic safety.

If we take into account methods of troubleshooting of the state of the track (railway complex elements), which have become known in recent years, then used and proposed methods can be grouped as follows.

1. **Mechanical methods.** These include, for example, a system of rail structures diagnostics, created on the basis of micromechanical sensor elements [11]; a technique to assess dynamic effects of the vehicle on the track, built on the spectral analysis of the responses received to the shock pulse and in-

volving monitoring with the use of vibration sensors that convert mechanical vibrations recorded by them into electric signal [18, 14]; a method of continuous change of the vertical forces in the contact area of wheel and rail with dynamometric wheel sets, allowing to fix deformation of a spoke or a disc, and thus the state of individual sections of the track [16].

2. **Ultrasonic methods.** An example where by multiple reflection of the ultrasonic pulse from the boundaries of the control object by SAFT method imaging of defects in rail base blades is provided is shown in [2]; similar opportunities for ultrasonic inspection are provided by examination of the surface of the rail in order to detect appearance of cracks and fractures during tracking the dynamics of the defect in order to prevent accidents on the road [e.g. 9].

3. **Signal- reproducing means.** Highlighting of that category by us is based on the fact that in the process of troubleshooting new narrowly functional, but very useful clips and repeaters of controlled data are offered, including acceleration sensors used for inertial measurement of track irregularities [3], as well as angular movement sensors used for monitoring the state of the rail track [7].

4. **Methods for diagnostics of ballast and sub-grade.** In particular, this category refers to registration of deformability degree of under-rail and under-sleeper grounds during load tests, which are carried out by mobile diagnostic complexes [1]; to monitoring of the roadbed and track superstructure on the basis of a three-level control system [17]; to analysis of the ballast layer with undersurface radars [10]; to organization of permanent automated posts for mode observations of deformations of high railway slopes using deep groundwater frames based on inclinometers PIN [15].

5. **Methods of optical control,** that fix most clearly predominant trend towards the development of remote diagnostics of the railway track. In that case, the choice of technological combinations depends on methods of video recording of a controlled object and on capabilities of signal- transforming systems, as well as on equipment carriers, monitoring means. The examples are: a) use of the effect of polar-

ization during reflection of light in the visible range of the electromagnetic radiation from the surface of the rail head and further algorithmic processing of images, received from cameras [12, 4]; b) use of remotely piloted aircrafts (RPA) or other types of air vehicles (including helicopters [6]) to conduct surveillance in a flexible mode of diagnostic problems (in particular, we can cite an option of RPA with scanners, performing multispectral imagery in visible and infrared ranges of the electromagnetic spectrum; while devices of GPS / GLONASS system can be used as a surveying system, orienting to reflect on the map local objects and identifying marks on the track and in the right-of-way [13, 8]).

Research intensity in each case is provided, of course, by its own means and methodological approaches, but it is important to emphasize the desire to go beyond the usual technique, to denote approaching to the current level of practical requirements and technical process. From this point of view, in our opinion, the experience of participating in the development of two above mentioned types of optical control is illustrative.

APPROACHES TO THE METHOD IMPLEMENTATION

In a professional community of transport specialists each discussion on any scientific problem has a subtext of topics of risks, threats to safety on the roads. It is also always current for railways. Therefore, the development of improved technical means of diagnosis of the railway track, including those that allow installation on aircrafts, remains a need, first of all determined by this reason.

With regard to the same demand we consider, of course, a possibility of using fluorescent polarization effect of reflected light from the metal surface of the rail head for detecting traditional defects of rails, fasteners, sleepers, monitoring ballast layer condition. Justified by that basis, a non-contact method had passed through its own specific stages of development and experimental verification before it could qualify for some kind of continuation.

Upon reflection of the radiation of natural daylight, which is by its very nature non-polarized, from

the boundary between two media (air-metal) its partial polarization occurs, which depends on the one hand, on the viewing angle, and on the other hand – on the optical properties of the contacting media. The change of polarization characteristics of the reflected light carries information about the parameters of the surface. By tracking those changes, it is possible to determine the properties of the surface layer of metal. In our case, the objects of study are the rail heads, and as for normal operation they should have almost perfectly flat upper surface, all defects and foreign objects, different in polarization characteristics of the smooth track surface will show an increased contrast in the images after processing by the method described below. Due to significant loads generated during the passage of trains, various defects appear on the surface of the rail heads. Consequently, the rays reflected from the element areas, receive different polarization characteristics, thus allowing to detect local defects (chips, cracks, rail corrugation and so on).

In natural light variation of the electromagnetic field vector is chaotic, because it is a set of many incoherent components. In this case, all directions of the electric field are equally probable. Such light is called non-polarized. If any direction of the vector is preferred then such a wave is recognized partially polarized.

There are different methods used for description of polarized light (Poincare sphere, Stokes vector, Jones vector, the quantum mechanical image). We have chosen the Stokes vector, as it makes it easier to analyze the passage of rays of light through optical systems.

Stokes vector is a set of four values, called Stokes parameters that characterize intensity and polarization of light. Those parameters have the dimension of intensity; each of them corresponds not to the instantaneous intensity, but to the intensity, which is average in time required for measurement. Four parameters are the column vector

$$\begin{bmatrix} I \\ Q \\ U \\ V \end{bmatrix}$$

The first parameter I is intensity. Parameters Q , U and V are consequently parameter of preferential horizontal polarization, parameter of preferential polarization at the angle of 45° and parameter of preferential right-circular polarization. When a parameter has a negative value, it means that polarization of orthogonal shape is preferential.

The proposed method consists of recording the reflected light from the surface of the rails using photodetector equipped with a polarizing filter (like SLR camera). The railway track is processed fragment-wise, the size of each fragment is determined by the size of the matrix of the recording device, lens focal length and the distance from which the survey is conducted.

To establish relations between the polarization characteristics of the electromagnetic wave before and after the filter, Mueller method is used. It is a matrix description of the interaction of the light beam and of an optical device through which light passes, and helps to calculate the result of such a process.

Since the removal or installation of the filter could cause displacement of the camera and violate the framing, as well as to improve the accuracy of the measurements, an improved method proposed in [5] is used, according to which for each part of the track a series of shots was made using different orientation of the filter.

It should be noted, however, that any spatial variations in the values of any of the Stokes parameters indicate as far as problems of shooting in the area of rail track are concerned, the presence of a surface feature of the rail, which could potentially be a defect.

Simplified, see their technical essence, experiments at the site of October Railway at Krestovsky Bridge in Moscow have shown a promising way to visualize defects using the effect of polarization of the reflected light and optical control means.

ADVANTAGES OF AIR DIAGNOSTICS

The use of aerial reconnaissance methods to diagnose the state of railway tracks is not a new idea [see.

e.g., 6], although a restraining motive, which is present here, is quite understandable. Introduction of aerial photography on a regular basis is still very expensive in terms of conventional piloted aerial vehicles, airplanes and helicopters, their ties with airbases, maintenance, accounting for takeoffs and landings.

A possible alternative is a RPA, mentioned above within the fifth classification group (methods of optical control), which stands for remotely-piloted vehicle with scanners on board. Army prototypes (USA, Israel) have proven their effectiveness, and an increasing interest to them emerges in Russia, too.

The main advantages of RPA for diagnostics of railway tracks are:

- High efficiency of use, ability to achieve a given stretch of track in a relatively short time, because the speed of RPA on the route can reach 200-250 km/h or more;
- Relatively low cost of operation of RPA as compared to other types of aircrafts, helicopters and airplanes;
- Use of RPA does not require intervals in timetable of trains, which are inevitable when using track-measuring cars;
- Route of RPA may be adjusted in accordance with the information received during flight and that route can deviate from the axis of the track at a considerable distance;
- Control of RPA in flight if communication with them is conducted through satellite channels or specially designed fiber optic lines running along the track (it is possible to use another RPA as a booster converter) can be performed centrally from a single command post;
- Presence of infrared technology on board gives a possibility to monitor the state of electrified railways, identifying certain areas of high heating of electrical circuits due to bad contacts, as well as to remotely monitor transformer houses and other equipment;
- Infrared sensors allow monitoring twenty-four-hour a day without additional lighting;
- System based on RPA can be a supplement to existing and planned protection systems, including security systems switching on CCTV cameras.

The use of RPA will help to expand the search area and assess operational situation when alarm signals are received from other sources.

Note, however, that engineering of such an expensive system to solve specific tasks may not be appropriate. From this point of view other tasks should be anticipated, in addition to those, which regularly can be met on the railway. The first is the observation of a possible crash site of trains, damage assessment and management of operations aimed at liquidation of consequences; then there is a task of regular fly-by of railways to assess the track state in order to ensure safe traffic.

Many of those ideas were taken into account during implementation of the project, carried out with the support of Russian Foundation for Basic Research and JSC "Russian Railways" (grant №11-07-13112-ofi-m-2011-RR). It was called "The use of RPA to obtain images of railways and the right-of-way in order to ensure traffic safety and prevent acts of terrorism" and provided an ostensible rationale for the very possibility of inspection from the air by means of optical imaging sensors, including multi-zone ones. And the threat detection can be carried out automatically, using mathematical methods of pattern recognition, as well as in "live" mode by a human operator.

Demonstrated approach takes into account the need for the ability to see the heterogeneity of the environment (nature of the violations of the ground surface, the color of vegetation or snow, etc.), dynamics of weather conditions, illumination of controlled areas (especially in the presence of clouds, sunshine, provoking the formation of harsh shadows, contrasting backgrounds). Neutralization of some negative related phenomena, especially at dusk and at night, does not rule out the involvement of special electro-optical devices: TV cameras, capable of working in low illumination, and infrared devices.

Another possibility is the use of RPA using operational information for continuous observation of a designated section of the route in the loitering mode. Under this option it is possible to track an immediate moment of preparation of an act of unlawful interference into rail transport operation and to prevent the consequences of the derailment. To do this, images obtained in real time are to be forwarded to a central server, to be processed there, and at the moment of

detection of moving objects on the tracks immediate communication with the security agencies is provided to take measures to counter the threat.

To solve the problem, it is possible to optimally choose a type of sensor that records the image. In good light conditions, it is possible to use a video camera, a high-speed optical camera or scanner with a line of sensors. It should be borne in mind that a video camera allows to get more frames per second than a photo camera. However, the photo camera produces an image with better resolution; its matrix has more points. As for a linear matrix scanner for image storage, it will need significantly less memory, because in this case there will be no duplication, when the same fragment of the railroad tracks is present on multiple frames. Another situation is inevitable: the image quality depends on the speed of flight of the equipment carriers.

To conduct aerial photography of railway tracks in winter at the experimental ring in Scherbinka, Moscow region, a remotely piloted aircraft of a helicopter type of the video studio DT group was used. The selection of a helicopter-type RPA was justified by its better handling in tight spaces and by significantly lower operating costs.

Aircraft RPA, having a much greater range and flight time, requires a developed ground infrastructure (devices of takeoff and landing, maintenance facilities, etc.) and numerous personnel to operate them. This type of devices is available only to entities (public and private) with significant resources. In addition, in Russia there is now no legislative framework governing the operation and the permission of such aerial vehicles for flights.

Helicopter aerial vehicle of multi-rotor type – multicopter, used for shooting, allows to receive bird's eye panorama photos and videos of good quality. Aerial photography may relate to natural sites, monuments, documentary scenes, music videos, festive events, sporting events and many other things. The use of this type of shooting during the research work was, apparently, the first experience in the practice of DT group, as well as any other contractors of such orders.

Control of the movement of RPA was carried out through radio channel. To get images an aircraft was fitted with a camera Canon EOS 5D Mark II, which provides a remote control of the gate by a separate desk and simultaneous transmission of signals through radio channel. The camera was mounted on gimbal suspension, from where picture was continuously transmitted to the screen of the control unit. In that case, the operator could focus the camera at the subject.

Power supply of electric engines of helicopters was carried out by storage batteries. Depending on the load the device was able to continuously stay aloft for up to fifteen minutes and to gain a height of over 100 meters. Preparations for the shooting took less than 30 minutes.

The use of RPA of a helicopter type is a temporary measure. This type of device fully satisfies the requirements of experimental works as a technology demonstrator. For the monitoring system of railways RPA of an aircraft type are more preferable, as having much greater flying range and time of staying aloft.

ACCUMULATION OF ARGUMENTS AND FORECAST

A changing global environment, entry into the era of global electronic networks, nanotechnologies and nanomaterials, respectively change evaluation criteria of approaches, in force hitherto, to control of condition and safety of the railways. Risks, losses, economic benefits get a new price, and therefore the things that only recently seemed too expensive and low efficient, now emerge in a different coordinate system, have qualitatively different projections into the future. And it is from this angle that it is necessary to assess the prospects for use of remote diagnostics, suggesting their further development and reasonable claim to be promising ones.

It is important to emphasize, first of all, that certain priorities of remote (including air) diagnosis are not opposed to any traditional “terrestrial” methods of tracking of technical conditions of an operated railway lines and under-rail, under-sleeper grounds. In varying degrees, the collection of such information is equidirectional, is a controlling process, which

is complex in its aims, while none of the links can be taken out of the overall circuit. It is an axiom, which is clear for everybody.

The second fundamental point for the analyst: by isolating the interests of optical control and giving a special importance to them, it is impossible to be unaware of the need to build arguments for its priorities and, therefore, a critical interpretation of the results of experimental works, experimental check of ideas, offered by scientists and researchers, and of innovative solutions, should prevail. Designing of a trend is a considerable step in order to achieve at the end reliable, argued outcome.

In the context of existing materials we can confidently say that there is a rational and justifiable compatibility of not only contact and contactless diagnostics of the track, but already of long range diagnostics as well which is carried out at considerable distance from the earth's surface with the help of specially designed aircrafts and optical electronic monitoring devices.

Experimental data accumulated by our experts (in particular, at the facilities of October Railway, the experimental railway ring in Shcherbinka, Moscow region), as well as the views of numerous aerial photographs support this theses. Most often, pictures were taken in a densely populated area, which is typical for Western Europe and North America, and therefore it is certainly difficult to determine areas of risk or to assess the dynamics of accidents. However, there is an additional argument with regard to the Russian practice. After all, especially in the eastern part of the country railways are located mostly in uninhabited and inaccessible areas, and therefore, the use of RPA there is very productive and desirable considering many criteria, including purely economic ones.

CONCLUSION

Arguments, earlier put forward by researchers [8], and conclusions, summarized with their account enable to select multiple areas that could become a reference for RPA, tailored to remote diagnosis of the track and its safety.

It is necessary to use more purposefully the fact that operating costs of remotely piloted aircrafts are lower than costs of conventional aerial vehicles (airplanes, helicopters).

Railway-owned communication lines (they are laid along the rails) should be adapted for the needs of the flight control and receipt of information from RPA that will give additional savings for organization of monitoring control.

It is advisable to integrate aerial remote diagnostics to the relevant structures of railway companies, providing a certain cooperation (again, in order to reduce total costs) with the manufacturers and operators of RPA of this type.

In view of the emergence of optics, sensors, devices of a new generation, of increasingly sophisticated electronic means of communication and data processing there is a need for comprehensive approach to the design of models of remote monitoring of the technical condition of the railroad bed and safety of right-of-way, in view of achieving relevant goals and quality of diagnosis.

If high technologies will be fully in-demand at all levels of the system, being built in this way, its efficiency is not long in coming. In the meantime, the innovative research needs more coordination and joint efforts.

REFERENCES

- [1] Ashpiz, E.S., Zamuhovskiy, A. V. (2012). *Substantiation of deformability standards*, World of Transport and Transportation Journal, 43 (5): p. 112-119.
- [2] Bazulin, E.G. (2010). *SAFT imaging of flaws in the rail base blade with consideration of multiple reflections of an ultrasonic pulse from the boundaries of a test object*, Russian Journal of Nondestructive Testing, 46 (2): p.63-67.
- [3] Boronakhin, A.M., Gupalov, V.I., Mochalov, A.V. (2002). *The method of inertial measurement of track irregularities*, Patent of the Russian Federation №2242391 of 30.12.2002.
- [4] Bugaev, A. S. et al. (2012). *Contactless diagnostics of the rails: reflected light polarization effect*, World of Transport and Transportation Journal, 41(3): p. 82-88.
- [5] Cremer F., de Jong W., Schutte K. (2002). *Infrared polarization measurements and modeling applied to surface-laid antipersonnel landmines*, Optical Engineering, 41(5): 1021-1032.
- [6] Eyre-Walker R., Earp G. (2008). *Application of Aerial Photography to Obtain Ideal Data for Condition Based Risk Management of Rail Networks*, The **4th IET International Conference on Railway Condition Monitoring** 18–20 June **2008**, Conference Centre, Derby, UK.
- [7] Khodorkovsky, Ya. I. et al. (1998). *The method and device for monitoring of a rail track condition*, Patent of the Russian Federation №2123445 of 20.12.1998.
- [8] Lievin, B.A. et al. (2013). *Distantly piloted aircrafts and the track security*, World of Transport and Transportation Journal, 46(2): p. 152-157.
- [9] Manual for ultrasonic testing of rails and welds (2006). Government of India, Ministry of Railways, Research Designs & Standards Organisation Lucknow- 226011. <http://www.ecr.indianrailways.gov.in/uploads/files/1357555682170-usfd.pdf>.
- [10] Olhoeft G., Selig E. (2002). *Ground Penetrating Radar Evaluation of Railway Track Substructure Conditions*, Proceedings of SPIE, 4758: p.48.
- [11] Podgornaya, L.N. (2010). *Development and research of system of track diagnostics on micromechanical sensor elements*. Abstract from PhD (Tech.) Thesis, St.Petersburg.
- [12] Razevig, V.V. et al. (2012). *Using the effect of polarization of the reflected light for contactless diagnostics of rails, Intelligent transportation systems*: Proceedings of the II International scientific-practical conference “IntellectTrans 2012”, p. 379-386, St.Petersburg, Petersburg State Transport University.
- [13] Razevig, V.V. et al. (2012). *The use of RPAV to obtain images of railways and the right-of-way in order to ensure safety and prevent terrorist attacks, Intelligent transportation systems*: Proceedings of the II International scientific-practical conference “IntellectTrans 2012”, p. 370-379, St. Petersburg, Petersburg State Transport University.
- [14] Satov, M.D., Kvashnin, M. Ya., Kvashnin, N.M. (2010). *Monitoring of the railway track*, Industry of Kazakhstan, 62(5): p. 58-60.
- [15] Savin, A. N. (2012). *Automated posts to observe deformation of embankments*, World of Transport and Transportation Journal, 44(6): p. 160-163.
- [16] Shulman, Z. A. (2014). *Continuous measurements of vertical forces of track and rolling stock interaction*, World of Transport and Transportation Journal, 55(6): p.68-77.
- [17] Zagirov, E.D., Igonkin, S.N. (2012). *Monitoring of the permanent way and of the subgrade*, World of Transport and Transportation Journal, 43(5): p. 124-128.
- [18] Zamukhovskiy, A. V., Kvashnin, N. M., Zhangabylova, A. M. (2014). *Control of vehicle's dynamic impact on a track*, World of Transport and Transportation Journal, 54(5): p. 72-81.

Submitted: April 30, 2015.

Accepted: May 8, 2015.

INSTRUCTIONS FOR AUTHORS

The *Journal of Information Technology and Application (JITA)* publishes quality, original papers that contribute to the methodology of IT research as well as good examples of practical applications.

Authors are advised that adherence to the Instructions to Authors will help speed up the refereeing and production stages for most papers.

- Language and presentation
- Length of submissions
- Submission
- Contact details/biographies
- Title of the paper
- Abstract and keywords
- Figures and tables
- Sections
- Footnotes
- Special characters
- Spelling
- References
- Proofs
- PDF offprint
- Copyright and permissions
- Final material
- Correspondence
- Publication ethics

LANGUAGE AND PRESENTATION

Manuscripts should be written in English. All authors should obtain assistance in the editing of their papers for correct spelling and use of English grammar. Manuscripts should have double spacing, with ample margins and pages should be numbered consecutively. The Editors reserve the right to make changes that may clarify or condense papers where this is considered desirable.

LENGTH OF SUBMISSIONS

Papers should not normally exceed 12 Journal pages (about 8000 words). However, in certain circumstances (e.g., review papers) longer papers will be published.

SUBMISSION

Manuscripts must be submitted through the JITA online submission system.

Please read the instructions carefully before submitting your manuscript and ensure the main article files do not contain any author identifiable information.

Although PDF is acceptable for initial submission original source (i.e. MS Word) files will be required for typesetting etc.

CONTACT DETAILS/BIOGRAPHIES

A separate file containing the names and addresses of the authors, and the name and full contact details (full postal address, telephone, fax and e-mail) of the author to whom correspondence is to be directed should be uploaded at the time of submission (you should select Contact details/Biographies as the file type). This file is not shown to reviewers. This file should also contain short biographies for each author (50 words maximum each) which will appear at the end of their paper.

The authors' names and addresses must not appear in the body of the manuscript, to preserve anonymity. Manuscripts containing author details of any kind will be returned for correction.

TITLE OF THE PAPER

The title of the paper should not be longer than 16 words.

ABSTRACT AND KEYWORDS

The first page of the manuscript should contain a summary of not more than 200 words. This should be self-contained and understandable by the general reader outside the context of the full paper. You should also add 3 to 6 keywords.

FIGURES AND TABLES

Figures which contain only textual rather than diagrammatic information should be designated Tables. Figures and tables should be numbered consecutively as they appear in the text. All figures and tables should have a caption.

SECTIONS

Sections and subsections should be clearly differentiated but should not be numbered.

FOOTNOTES

Papers must be written without the use of footnotes.

SPECIAL CHARACTERS

Mathematical expressions and Greek or other symbols should be written clearly with ample spacing. Any unusual characters should be indicated on a separate sheet.

SPELLING

Spelling must be consistent with the Concise Oxford Dictionary.

REFERENCES

References in the text are indicated by the number in square brackets. If a referenced paper has three or more authors the reference should always appear as the first author followed by et al. References are listed alphabetically. All document types, both printed and electronic, are in the same list. References to the same author are listed chronologically, with the oldest on top. Journal titles should not be abbreviated.

Journal

Avramović ZŽ (1995) Method for evaluating the strength of retarding steps on a marshalling yard hump. *European Journal of Operational Research*, 85(1), 504–514.

Book

Walsham G (1993) *Interpreting Information Systems in Organizations*. Wiley, Chichester.

Contributed volume

Huberman AM and Miles MB (1994) Data Management and analysis methods. In *Handbook of Qualitative Research* (Denzin NK and Lincoln YS, Eds), pp 428–444, Sage, Thousand Oaks, California.

Conference Paper

Huberman AM and Miles MB (1994) Data Management and analysis methods. In *Handbook of Qualitative Research* (Denzin NK and Lincoln YS, Eds), pp 428–444, Sage, Thousand Oaks, California.

Unpublished reports/theses

Nandhakumar JJ (1993) The practice of executive information systems development: and in-depth case study. PhD Thesis, Department of Engineering, University of Cambridge.

PROOFS

Proofs of papers will be sent to authors for checking. Alterations to diagrams should be avoided where possible. It will not be possible to accept major textual changes at this stage. Proofs must be returned to the publishers within 48 hours of receipt by fax, first-class post, airmail or courier. Failure to return the proof will result in the paper being delayed.

PDF OFFPRINT

Corresponding authors will receive a PDF of their article. This PDF offprint is provided for personal use. It is the responsibility of the corresponding author to pass the PDF offprint onto co-authors (if relevant) and ensure that they are aware of the conditions pertaining to its use.

The PDF must not be placed on a publicly-available website for general viewing, or otherwise distributed without seeking our permission, as this would contravene our copyright policy and potentially damage the journal's circulation. Please visit http://www.apeiron-journals.com/JITA/authors/rights_and_permissions.html to see our latest copyright policy.

COPYRIGHT AND PERMISSIONS

The copyright of all material published in the Journal is held by Paneuropean University APEIRON. The author must complete and return the copyright form enclosed with the proofs.

Authors may submit papers which have been published elsewhere in a foreign language, provided permission has been obtained from the original publisher before submission.

Authors wishing to use material previously published in JITA should consult the publisher.

FINAL MATERIAL

All final material must be submitted electronically in its original application format (MS Word is preferred). The file must correspond exactly to the final version of the manuscript.

CORRESPONDENCE

Business correspondence and enquiries relating to advertising, subscriptions, back numbers or reprints should be addressed to the relevant person at:

Paneuropean University APEIRON
Journal JITA
Pere Krece 13, P.O.Box 51
78102 Banja Luka
Bosnia and Hercegovina / RS

PUBLICATION ETHICS

We take an active interest in issues and developments relating to publication ethics, such as plagiarism, falsification of data, fabrication of results and other areas of ethical misconduct. Please note that submitted manuscripts may be subject to checks using the corresponding service, in order to detect instances of overlapping and similar text.

JITA

PUBLISHER

Paneuropean University APEIRON,
College of Information Technology
Banja Luka, Republic of Srpska, B&H
www.apeiron-uni.eu

Darko Uremović, Person Responsible for the Publisher
Aleksandra Vidović, Editor of University Publications

EDITORS

Gordana Radić, PhD, Editor-in-Chief (B&H)
Zoran Ž. Avramović, PhD, (B&H)
Dušan Starčević, PhD, (B&H)

EDITORIAL BOARD

Zdenka Babić, PhD, (B&H)
Leonid Avramović Baranov, PhD, (Russia)
Patricio Bulić, PhD, (Slovenia)
Valery Timofeevič Domansky, PhD, (Ukraine)
Hristo Hristov, PhD, (Bulgaria)
Emil Jovanov, PhD, (USA)
Petar Marić, PhD, (B&H)
Vojislav Mišić, PhD, (Canada)
Boško Nikolić, PhD, (Serbia)
Dragica Radosav, PhD, (Serbia)
Gjorgji Jovanchevski, PhD, (Macedonia)
Branko Latinović, PhD (B&H)
Vladimir Nikolajevič Mališ, PhD (Russia)
Goran Đukanović, PhD (B&H)
Yidong Li, PhD (China)

EDITORIAL COUNCIL

Siniša Aleksić, APEIRON University, Director
Esad Jakupović, APEIRON University, Rector

TECHNICAL STAFF

Stojanka Radić, Lector

EDITOR ASSISTANTS

Sretko Bojić, APEIRON University
Gordan Ružić, ETF University of Belgrade

ISSN 2232-9625



9 772232 962005